

DELFT UNIVERSITY OF TECHNOLOGY

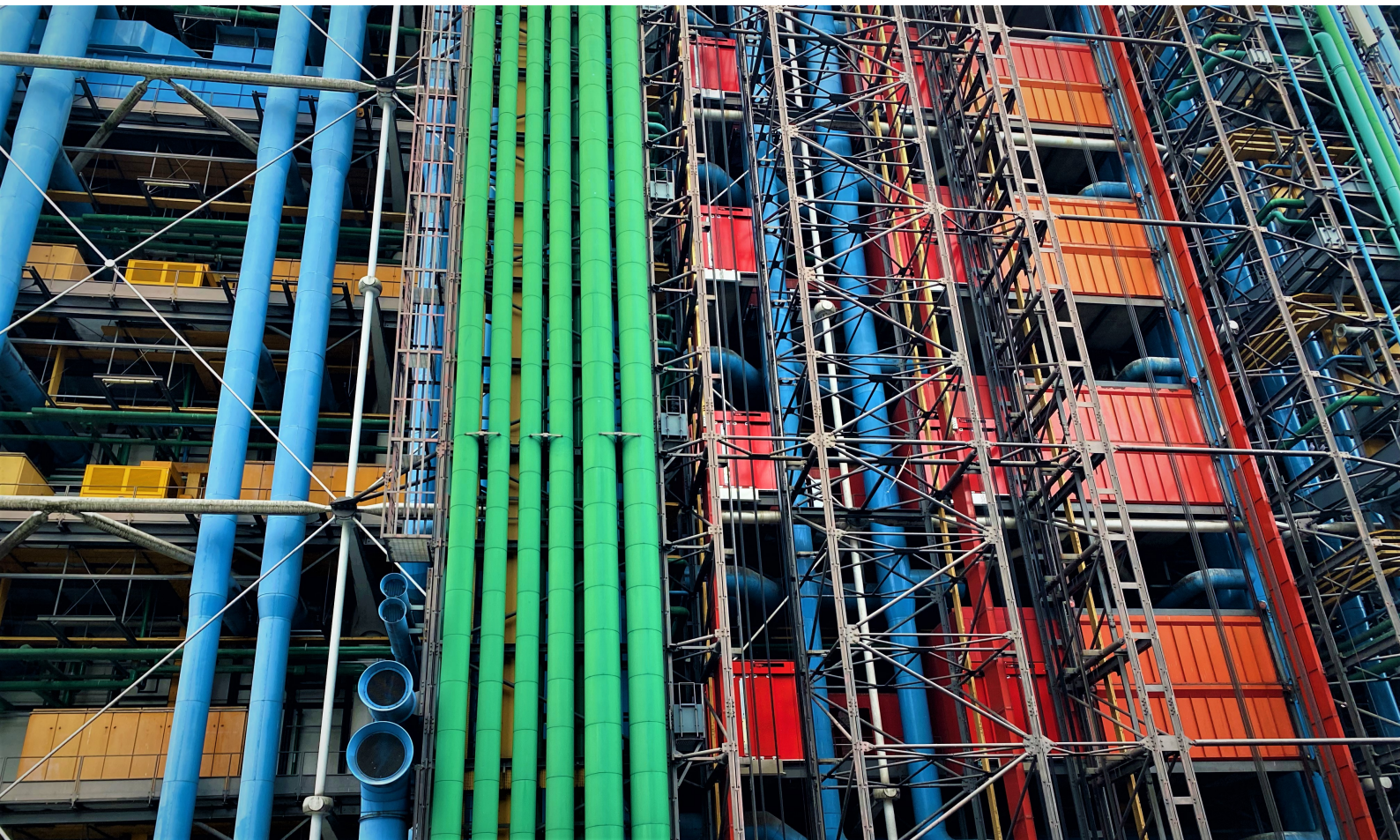
---

An improved approach for on-board  
distribution system robustness estimation in  
early-stage ship design

---

Evelien Scheffers

November, 2021





# An improved approach for on-board distribution system robustness estimation in early-stage ship design

by

Evelien Scheffers

to obtain the degree of Master of Science in Marine Technology  
at the Delft University of Technology,  
to be defended publicly on Monday November 15, 2021 at 14:30.

Report number: MT.21.006.m  
Student number: 4293592  
Specialisation: Marine Engineering  
Project duration: November 16, 2020 – November 15, 2021

Thesis committee: Ir. K. Visser, TU Delft, chair  
Dr. Ir. P. de Vos, TU Delft, supervisor  
Dr. Ir. A. A. Kana, TU Delft  
Dr. Ir. A. C. Habben Jansen, DMO

An electronic version of this thesis is available at <http://repository.tudelft.nl/>.

---

The figure on the front is a photograph (June, 2021) of the east side of *Centre national d'art et de culture Georges-Pompidou* in Paris. This building is an example of an *inside-out* building, with systems, e.g. HVAC, energy distribution and plumbing, exposed on the exterior of the building. The figure is chosen to show to amount, complexity and beauty of systems present in large structures.

# Preface

*L.S.*

The document before you is my master thesis on "*An improved approach for on-board distribution system robustness estimation in early-stage ship design*" to obtain the degree of Master of Science in Marine Technology. Marine Technology was, unconsciously, the first study I considered doing: the first thing I wanted to be as a child was to saviour people who had sunk. I would grow my hair long enough to use it as a rope for the sunken people to climb to the surface of the water. Later, I wanted to become a farmer, veterinarian, writer and neurologist. However, the image of a little girl saving people at sea never left my mind and resurfaced when I had to choose a study. With this thesis, I conclude my time as a student of the master Marine Technology at the Delft University of Technology.

During my internship at a shipyard for sailing yachts, I discovered my interest in systems on-board ships. The complexity of the combined system and the endless possible topologies make this a challenging and fascinating part of ship design. Moreover, the crucial implementation of sustainable technologies takes place within the context of marine engineering. Therefore, I am grateful to the TU Delft and Peter de Vos for providing me with the opportunity to graduate on this important and exciting topic.

Thank you, Peter, for guiding me in starting, improving and finishing my own research. Your open and honest approach helped me, personally, in understanding my pitfalls and, academically, in keeping my scope under control. Second, I would like to thank my other thesis committee members Agnieta, Austin and Klaas, for our fruitful discussions over the past year. Your different perspectives helped me direct my study and maintain the maritime perspective on this mathematical research. Moreover, I want to thank professor Piet Van Mieghem, who helped me understand his robustness approach, among other graph theory and normalisation concepts.

On a more personal note, I would like to thank my friends and housemates, who joined me for hockey, walks and coffee when all other distractions were cancelled. Thank you to my parents and sisters, who have raised me well and provided me with a pied-à-terre in the most beautiful forests. And finally, thank you, Joris, for understanding my brain sometimes better than I do and, above all, for making me happy.

Evelien Scheffers

Delft, November 2021

# Summary

Robust systems are crucial in ensuring safe sailing, e.g. for autonomous vessels, naval vessels, cruise ships and ships with unconventional sustainable propulsion systems. However, during early-stage ship design, there is a lack of knowledge on determining the robustness of distribution systems. This hinders making a substantiated trade-off between different properties of systems on-board ships. Therefore, there is a need to better estimate the robustness of distribution systems in early-stage ship design. This study aims to provide an improved system robustness estimation in early-stage ship design through comparing and verifying the robustness approach by [de Vos \(2018\)](#) using the robustness approach by [Van Mieghem, Doerr, et al. \(2010\)](#).

Distribution systems on-board ships are defined as a number of connected components together transporting a flow from a source component via hub components to a user component. Graphs are used to model the distribution systems, with nodes and links representing components and connections. According to maritime design rules or rules of thumb, a robust system has three properties: independent subsystems, redundancy and reconfigurability. The first studied robustness approach ([de Vos, 2018](#)) reduces system robustness to system reconfigurability, measured using the maximum flow between hub nodes. The R-value indicates robustness for the second approach ([Van Mieghem, Doerr, et al., 2010](#)). This approach provides a framework for computing topological network robustness, applicable to most or all networks. The R-value is calculated using a topology and weight vector, consisting of normalised graph measures and their respective weight.

First, the robustness of a set of graphs within five verification sets is analysed. The five sets all contain undirected graphs with a varying number of supplier nodes, hub nodes, user nodes and links. According to the design rules, the graphs within a set show an increase in robustness. However, the analysis shows that the normalised R-values do not follow the increasing trend, except for the verification set with a constant number of supplier nodes, hub nodes and user nodes. This result is in line with the system reconfigurability; therefore, the verification set in which only the number and location of links is varied forms the basis for the case study.

The case study consists of a system containing five subsystems, differentiated by flow type. The subsystems are individually analysed on system reconfigurability and R-value; constant minimum and maximum connected graphs are used for the normalisation of the latter. The summation of the values for the subsystems is done using superposition; the interaction between subsystems is not part of the scope. Again, this study shows that the system reconfigurability can be verified using the R-value.

To conclude, this study provides an improved approach to system robustness estimation in early-stage ship design. Not only system reconfigurability is included in the robustness measure, the robustness properties *independent subsystem* and *redundancy* are now part of the measure as well. Moreover, systems without hub nodes can be analysed because the measure is not solely dependent on the presence of hub nodes. The measure is also applicable to data distribution systems because of the general robustness approach of the R-value. The main shortcomings are in the selection of the graph measures and the absence of values within the weight vector. Finally, the applicability of the measure on distribution systems onboard ships remains limited as long as the number of supplier nodes, hub nodes and user nodes must remain constant.

# Contents

<b>List of Figures</b>	<b>vi</b>
<b>List of Tables</b>	<b>vii</b>
<b>1 Introduction</b>	<b>1</b>
1.1 Motivation	1
1.2 Project Description	2
1.2.1 Brief Introduction Robustness Approach de Vos (2018)	2
1.2.2 Brief Introduction Robustness Approach Van Mieghem, Doerr, et al. (2010)	3
1.2.3 Academic Knowledge Gap	3
1.2.4 Problem Statement	4
1.2.5 Ethical Considerations	4
1.2.6 Research Approach	5
1.3 Report Introduction	5
1.3.1 Report Objectives	5
1.3.2 Report Outline	5
1.3.3 Reading Guide	6
<b>Part I: Literature Review</b>	<b>7</b>
<b>2 Distribution Systems Onboard Ships</b>	<b>8</b>
2.1 Ship Design	8
2.1.1 Early-Stage Ship Design	9
2.1.2 Early-Stage Design Challenges	10
2.2 Overview Distribution Systems	10
2.2.1 System Categorisation	10
2.2.2 Distribution System and Distributed System	10
2.2.3 Marine Distribution Systems	11
2.3 Distribution Systems Architecture	11
2.3.1 An architectural framework for distributed systems (Brefort et al., 2018)	12
2.3.2 Two-layer network model (Van Mieghem, Doerr, et al., 2010)	13
2.3.3 OSI-Model	14
2.3.4 Architectural Framework Comparison	15
2.4 Reliability Distribution Systems	16
2.4.1 Attributes of Network Robustness	16
2.4.2 Network Performance	16
2.4.3 Network Robustness Design Rules	16
2.5 Conclusion	17
<b>3 Automatic Topology generation Tool (ATG Tool)</b>	<b>18</b>
3.1 Reliability and Survivability	18
3.2 Network Properties	19
3.2.1 Network Boundary Conditions	20
3.2.2 Benchmark System & Subsystems	20
3.3 Topology Generation	21

3.3.1	Design Space Exploration: Theoretical Background . . . . .	21
3.3.2	Design Space Exploration: Application in ATG Tool . . . . .	21
3.3.3	Automatic Topology Generation Tool . . . . .	22
3.4	Objective Function I: System Claim . . . . .	22
3.5	Objective Function II: System Robustness . . . . .	23
3.5.1	Design for maximum robustness . . . . .	24
3.5.2	Design for maximum reconfigurability . . . . .	24
3.5.3	Design for minimum vulnerability . . . . .	25
3.6	Case Study and Verification Study . . . . .	25
3.7	Conclusion . . . . .	25
<b>4</b>	<b>Framework for Computing Topological Network Robustness</b> . . . . .	<b>26</b>
4.1	Network Properties . . . . .	26
4.2	R-Value . . . . .	26
4.2.1	Computation . . . . .	27
4.2.2	Normalisation . . . . .	28
4.3	Temporal Aspects . . . . .	28
4.3.1	Elementary Change . . . . .	28
4.3.2	Recoverability . . . . .	28
4.3.3	Scope Concerning Time-Related Concepts . . . . .	30
4.4	Graph Measures . . . . .	30
4.4.1	Degree . . . . .	30
4.4.2	Connectivity . . . . .	30
4.4.3	Modularity . . . . .	31
4.4.4	Eccentricity . . . . .	31
4.4.5	Cycle Basis . . . . .	32
4.4.6	Effective Resistance . . . . .	32
4.5	Conclusion . . . . .	33
<b>Part II:</b>	<b>Network Analysis</b> . . . . .	<b>34</b>
<b>5</b>	<b>Network Set Introduction</b> . . . . .	<b>35</b>
5.1	Verification Set in Literature . . . . .	35
5.2	Development Verification Sets . . . . .	39
5.2.1	Verification Set I: <i>NU10</i> . . . . .	40
5.2.2	Verification Set II: <i>NN24</i> . . . . .	41
5.2.3	Verification Set III: <i>NN24NS6</i> . . . . .	42
5.2.4	Verification Set IV: <i>NU18NS6</i> . . . . .	43
5.2.5	Verification Set V: <i>NH8NS8</i> . . . . .	44
5.2.6	Overview Verification Sets . . . . .	44
5.2.7	Minimum and Maximum Values . . . . .	45
5.3	Selection Sample Set . . . . .	46
5.3.1	Total System to Separate Subsystems . . . . .	48
5.4	Network Set Conclusion . . . . .	50
<b>6</b>	<b>Verification Set Network Analysis</b> . . . . .	<b>51</b>
6.1	R-calculation . . . . .	51
6.1.1	Step 1: Input . . . . .	52
6.1.2	Step 2: Graph Measure Calculation . . . . .	53
6.1.3	Step 3: Graph Measure Normalisation . . . . .	54
6.1.4	Step 4: R-value Calculation . . . . .	55
6.2	Graph Measure Analysis . . . . .	55
6.2.1	Clean Increasing Trend for <i>NH8NS6</i> . . . . .	56
6.2.2	Clean Decreasing Trend for <i>NH8NS6</i> . . . . .	56
6.2.3	Variable Results . . . . .	57
6.2.4	Independent Modularity Normalisation . . . . .	58
6.2.5	Graph Measure Noteworthy Plots . . . . .	59
6.3	Alternative Normalisation . . . . .	61

6.3.1	Un-normalised Graph Measures . . . . .	61
6.3.2	Graph Measures Normalised per Set . . . . .	61
6.3.3	Graph Measures Normalised per Graph Measure . . . . .	62
6.4	Objective Function Analysis . . . . .	63
6.5	Robustness Measure Comparison . . . . .	65
6.5.1	Verification Study Conclusion . . . . .	67
<b>7</b>	<b>Case Study Network Analysis</b>	<b>68</b>
7.1	Case Study Approach . . . . .	68
7.2	Minimum and Maximum Connected Graph . . . . .	69
7.2.1	Constant Topology Generation . . . . .	69
7.2.2	Constant Maximum/Minimum Topology . . . . .	70
7.3	Subsystem R-Calculation . . . . .	72
7.4	Combining the R-Values . . . . .	74
7.4.1	Subsystem Coupling . . . . .	76
7.5	Robustness Comparison . . . . .	76
7.5.1	Application . . . . .	76
7.5.2	Case Study Conclusion . . . . .	77
<b>8</b>	<b>Conclusion, Discussion and Reflection</b>	<b>78</b>
8.1	Conclusions . . . . .	78
8.1.1	Marine Assumptions . . . . .	78
8.1.2	Robustness Approach Verification . . . . .	79
8.2	Discussion and Recommendations . . . . .	80
8.2.1	R-Value Calculation . . . . .	80
8.2.2	Limitation . . . . .	80
8.2.3	Implementation . . . . .	80
8.3	Reflection . . . . .	81
	<b>Appendices</b>	<b>85</b>
<b>A</b>	<b>Robustness Related Definitions</b>	<b>87</b>
<b>B</b>	<b>Verification Set: Robustness and Graph Measure</b>	<b>89</b>
<b>C</b>	<b>Case Study Sample Set: Robustness and Graph Measures</b>	<b>93</b>
<b>D</b>	<b>Schematic Representation MATLAB</b>	<b>97</b>
<b>E</b>	<b>Verification Set I-V</b>	<b>100</b>
<b>F</b>	<b>Case Study Sample Set</b>	<b>102</b>

# List of Figures

1.1	Knowledge Gap . . . . .	4
1.2	Report Overview . . . . .	6
2.1	Early-Stage (Ship) Design . . . . .	9
2.2	Design Process . . . . .	10
2.3	Onboard Distribution Systems . . . . .	11
2.4	Architectural Framework . . . . .	12
2.5	Architectural Framework Applied . . . . .	13
2.6	Two-Layer Network Model . . . . .	14
2.7	OSI-Model . . . . .	15
3.1	Disruption Response Curve . . . . .	19
3.2	Benchmark System of Case Study I . . . . .	21
3.3	Pareto Front . . . . .	22
3.4	ATG Tool Design Space Exploration . . . . .	23
3.5	Maximum Flow . . . . .	24
4.1	R-Value Envelope . . . . .	27
4.2	Probability density of energy ratio's of different communication networks (He, 2020) . . . . .	29
4.3	Ring Distribution (NU18NS6) . . . . .	31
4.4	Cycle Basis (NU10) . . . . .	32
5.1	Radial Distribution (Star Network) . . . . .	36
5.2	Single (Zonal) Distribution . . . . .	37
5.3	Double (Vital) Distribution . . . . .	38
5.4	Ring and Zonal Distribution . . . . .	39
5.5	Verification Set I (NU10) . . . . .	40
5.6	Verification Set II (NN24) . . . . .	41
5.7	Verification Set III (NN24NS6) . . . . .	42
5.8	Verification Set IV (NU18NS6) . . . . .	43
5.9	Verification Set V (NH8NS6) . . . . .	44
5.10	Complete (Ring) Graph (NU18NS6) . . . . .	45
5.11	Minimum/Maximum Connected (NU18NS6) . . . . .	46
5.12	ATG Tool Selected Topologies . . . . .	47
5.13	Selected Topologies: System Claim and System Robustness . . . . .	48
5.14	Total System (NN36 Graph 2) . . . . .	49
5.15	Five Subsystems (NN36 Graph 2) . . . . .	49
6.1	R-Value Calculation . . . . .	51
6.2	Minimum/Maximum Connected (NN24NS6) . . . . .	52
6.3	Mean Hub-Hub Degree (NN24NS6) . . . . .	53
6.4	Normalised Mean Hub-Hub Degree (NN24NS6) . . . . .	54
6.5	Robustness and Normalised Mean Hub-Hub Degree (NN24NS6) . . . . .	55
6.6	Mean Hub-Hub Degree (NH8NS6) . . . . .	56
6.7	Mean Node Eccentricity (NH8NS6) . . . . .	57
6.8	Mean Node Eccentricity (NU18NS6) . . . . .	58
6.9	Normalised Modularity . . . . .	59

6.10	Cycle Basis (NN24NS6)	60
6.11	Mean Hub-Edge Connectivity (NN24NS6)	60
6.12	Robustness Unnormalised (NN24NS6)	61
6.13	Robustness Set Normalised (NN24)	62
6.14	Robustness Normalised Graph Measures	63
6.15	System Claim and System Robustness (NU18NS6)	64
6.16	System Claim and System Robustness (NH8NS6)	64
6.17	R-Value and F2 System Robustness (NN24NS6)	65
6.18	R-Value and F2 System Robustness (NH8NS6)	66
6.19	Robustness Normalised Graph Measures and R-Value (NH8NS6)	66
7.1	Case Study Approach	68
7.2	Variable Minimum/Maximum Connected (NN36 Subgraph 1)	69
7.3	Mean Node Eccentricity Variable Minimum/Maximum (NN36 Subgraph 1)	70
7.4	Constant Minimum/Maximum Connected (NN36 Subgraph 1)	71
7.5	Mean Node Eccentricity Constant Minimum/Maximum (NN36 Subgraph 1)	71
7.6	Effective Resistance (NN36 Subgraph 3)	72
7.7	R-Value (NN36 Subgraph 5)	73
7.8	R-Value (NN36 Subgraph 2)	73
7.9	R-Value Combined and Original (NN36)	74
7.10	R-Value (NN36)	75
7.11	Robustness Normalised Graph Measures (NN36)	75
7.12	R-Value and F2 System Robustness (NN36)	76
7.13	System Claim and Robustness per System Claim (NN36)	77
A.1	Overview of Robustness Related Definitions by Bondavilli et al. (2016)	87
A.2	Overview of Robustness Related Definitions in Literature	88
B.1	Verification Study Mean Hub-Hub Degree	89
B.2	Verification Study Number of Cycles	90
B.3	Verification Study Mean Node Eccentricity	90
B.4	Verification Study Modularity	91
B.5	Verification Study Effective Resistance	91
B.6	Verification Study Mean Connectivity	92
B.7	Verification Study R-Value	92
C.1	Case Study Mean Hub-Hub Degree	93
C.2	Case Study Number of Cycles	94
C.3	Case Study Mean Node Eccentricity	94
C.4	Case Study Effective Resistance	95
C.5	Case Study Mean Connectivity	95
C.6	Case Study R-Value	96
D.1	Schematic Representation MATLAB Input	98
D.2	Schematic Representation MATLAB R-Calculation	99

# List of Tables

1.1	System, Network and Graph Terms . . . . .	2
5.1	Overview node and edge properties verification sets . . . . .	45
5.2	Overview system properties sample sets for case study . . . . .	48
5.3	Overview node and edge properties sample sets for case study . . . . .	48

# Chapter 1

## Introduction

This chapter provides context and knowledge on the research topic, introduces the research and its plan of approach, and ensures that the report is read and understood according to its intended purpose. This introductory chapter can be split into two parts: a *research introduction* and a *report introduction*. First, the research background and motivation can be found in [section 1.1](#). The background provided in this section functions as a context for [section 1.2](#) and [subsection 1.2.6](#). [section 1.2](#) describes the problem definition, followed by the academic knowledge gap and concluding with the research statement and goal. This section also contains the ethical considerations made regarding this study. The research approach describes the applied research method and the deliverables defined for this study and can be found in [subsection 1.2.6](#). The reader is guided through the report aided by the final section of this chapter, [section 1.3](#). The report introduction forms the second part of the introduction and contains the report's objective, an outline and a reading guide.

### 1.1 Motivation

It is generally accepted that ships can be regarded as complex systems ([Gaspar et al., 2012](#)). According to [Rhodes & Ross \(2010\)](#), there are five distinct aspects when engineering complex systems: structural, behavioural, contextual, temporal and perceptual aspects. The structural aspects are the focus of this study and are related to system components and their interrelationships. Subsystems such as on-board distribution systems need to be improved to improve the structural aspects. In this case, *improving* means making the ship, therefore its systems and components, more robust. The reasons for isolating the robustness element from the total ship improvement is explained using three arguments below.

The concept of *robustness* can have many different meanings, depending on the subject. For example, robust red wine is intense and full-bodied, whereas, in biology, a robust person is strong and has a heavy build. Within this report, the term robustness is applied to general systems and distribution systems on-board ships. Furthermore, the concept of robustness is often linked to solid structures or systems, directly related to increased financial and time-investments during the design and building process. The meaning of robustness in this report is explained in [section 2.4](#).

Hence the question arises: why would one invest in designing and building a more robust ship? To answer this question, there are three overarching arguments to make a ship more robust: autonomous shipping, sustainability and operational profiles.

First, significant steps are expected in the development of autonomous surface vessels (ASV) during the next five to ten years ([Cerulli et al., 2018](#)). Remote-controlled vessels with reduced crews are considered the first step on the track to fully autonomous vessels. It is generally assumed that autonomous vessels improve safety, increase efficiency and provide greener ship traffic ([Haugen et al., 2018](#)). However, [Haugen et al. \(2018\)](#) states that, despite the decrease in accidents caused by human error, new forms of error might occur. Some of those risks are currently averted by the crew, which is complex with a higher grade of autonomy, i.e. fewer crew members. To minimise this type of error, an improvement in the robustness of on-board systems is required to ensure crew- and public safety.

Sustainability is a second argument for implementing robustness optimisation in the design process. The selection of system components, especially in the propulsion system, provides a possibility to enhance

the sustainability. Han (2010) states that pollution emissions from international ocean-going vessels significantly impact air quality and public health. Technology strategies such as replacing or upgrading older engines or improving fuel qualities can be implemented in current and future marine vessels to improve environmental performance. According to Nguyen et al. (2020), objective measures can be applied to compare conventional and advanced propulsion systems. One of these measures could be the robustness of the system.

The last argument for improving system robustness can be found for ships with specific operational profiles such as naval vessels, sailing yachts and cruise ships. In 2019, a cruise ship experienced engine problems, endangering the life of passengers due to drifting towards rocks (BBC, 2019). Extensive research on improving the robustness of naval vessels has been conducted to improve the vessel's survivability during a hostile attack (Habben Jansen, 2020; de Vos, 2018). Some weapons require multiple distribution systems to function (de Vos, 2018). Therefore, these distribution systems must stay operational despite experiencing failures of system parts caused by an attack. The risk of a distribution losing its complete function decreases with increased system robustness.

To conclude, an improved estimation of the robustness of distribution systems offers a more substantiated trade-off between robustness and other system properties during ship design. It is essential to include robustness explicitly within this trade-off to ensure crew-, passenger- and environmental safety, to increase the possibilities in autonomous shipping and to provide for the integration of sustainable components in the propulsion system. The analysis and prediction of system robustness of distribution systems on-board ships form the basis of this study.

## 1.2 Project Description

As described in the previous section, the research motivation provides a ground for a broad range of research topics. Research concerning the improvement of system analyses during early-stage design can be done on process level (Gaspar et al., 2012), system-level (Brefort et al., 2018) or from a mathematical perspective He (2020). The selected scope, further explained in subsection 1.2.6, holds between the system perspective and mathematical perspective. At this level of abstraction, two robustness approaches are examined, which are first briefly introduced below before continuing with the explanation of this research. The selection of these approaches is based on access to background information to both methods, combined with an academic interest in combining the approaches. In line with the recommendations by de Vos (2018), applying the more fundamental network theory concepts on system robustness estimation could prove to be an interesting topic of research. A more extensive explanation of the robustness approach by de Vos (2018) and Van Mieghem, Doerr, et al. (2010) can be found in respectively chapter 3 and chapter 4. First, distribution systems are defined as a number of connected components, together transporting a flow (e.a. cooling water, lubrication oil, electricity or data) from a source component via other components to a certain user component (section 2.2). These components are called nodes in a graph representation of the network system; the connections are links or edges within this representation. Table 1.1 provides an overview of the different terms used within literature and this research. A system is a physical entity, a network is a model of such an entity, and a graph is a mathematical representation of a network; Table 1.1 provides an overview of different concepts within different research fields.

<b>System</b>	Component	Connection
<b>Network</b>	Node	Link
<b>Graph</b>	Vertex	Edge

Table 1.1: System, Network and Graph Terms

### 1.2.1 Brief Introduction Robustness Approach de Vos (2018)

During early-stage ship design (subsection 2.1.1), most choices are made based on design rules or rules of thumb. To make this process more reproducible and reliable, de Vos & Stapersma (2018)<sup>1</sup> has developed a tool (subsection 3.3.3) used to automate design space exploration and to generate onboard distribution system topologies. The "goodness" of these topologies is measured using two objective functions: system claim (section 3.4) and system robustness (section 3.5); here, robustness is reduced to system reconfigurability. While the first function essentially calculates the number of nodes and edges

<sup>1</sup>This section is based on chapter 3; the primary source is de Vos (2018) unless explicitly stated differently

within a network, the second function uses a specific network property defined by [de Vos \(2018\)](#): *hub nodes*.

**Graph, nodes and edges** A graph  $G$  is an ordered pair of disjoint sets  $(V, E)$ , in the standard case of a finite graph  $G$ , these two finite sets are defined as vertices  $V = V(G)$  and edges  $E = E(G)$  ([Bollobás, 1998](#)). In network theory, the same concepts are called differently, respectively nodes and links or connections. Since this research is written in the context of the maritime industry, the terms *nodes* and *edges or connections* are used in this report, in line with the research by [Habben Jansen \(2020\)](#); [de Vos \(2018\)](#).

All nodes are labelled either supplier nodes, hub nodes or user nodes; the first and last categories are flow converters connected to subsystems distributing a different flow type. The second objective function, system reconfigurability, is determined by calculating the maximum flow between hub nodes, normalised per subsystem. Next to this *node differentiation*, *edge differentiation* is used to distinguish subsystems. The total system has a fixed number of nodes with predetermined functions and undirected edges.

### 1.2.2 Brief Introduction Robustness Approach [Van Mieghem, Doerr, et al. \(2010\)](#)

Several frameworks to improve network robustness have been developed over the last 50 years. The reliability studies focus on the probability of remaining functionality after network component failures, while performance studies focus on higher levels of abstraction to calculate performability. [Van Mieghem, Doerr, et al. \(2010\)](#)<sup>2</sup> has developed a framework to calculate network robustness applicable to most network types. The network is defined as a two-layered structure, combining a network topology layer and a service layer, defining the undirected relations between network components and the functions performed by the network ([subsection 2.3.2](#)).

The "goodness" measure or network robustness (*R-value*) is calculated using graph measures combined in a topology vector ([section 4.2](#)). The normalised graph measures, such as degree and connectivity, focus exclusively on the network topology and are no service metrics. The selection and weight of the measures is made based on a specific network service; a network providing more than one service has an *R-value* in which the values per service are combined.

The scope of this framework reaches from physical networks such as power distribution grids and pipelines to digital networks like the internet. Therefore, the network is defined in a general and mathematical way. As a result, the networks compared are undirected and only affected by a discrete-time approach. Moreover, when part of a single comparison, the networks have an equal number of nodes without specified functionality. Comparing graphs of equal size is considered good practice within the field of graph theory.

### 1.2.3 Academic Knowledge Gap

The approaches by [de Vos \(2018\)](#) and [Van Mieghem, Doerr, et al. \(2010\)](#) aim to define and analyse network robustness and therefore have a common goal. However, as can be read in the brief introductions in the previous sections, the robustness approaches differ significantly. The two approaches differ in applied scope, network definition and robustness definition. The concept of these differences is grasped within the academic knowledge gap, based on the literature review as described in Part I. [Figure 1.1](#) shows a diagram with the knowledge gap in between the two studied robustness approaches. This gap has two components, formulated as questions:

- If the robustness approach by [Van Mieghem, Doerr, et al. \(2010\)](#) is currently not applicable to on-board distribution systems, what assumptions must be made to transform this approach to a robustness approach that can be applied to distribution systems on-board ships?
- To what extent can the specific robustness approach by [de Vos \(2018\)](#) for on-board distribution systems be verified using a general robustness approach such as the approach by [Van Mieghem, Doerr, et al. \(2010\)](#)?

---

<sup>2</sup>This section is based on [chapter 4](#); the primary source is [Van Mieghem, Doerr, et al. \(2010\)](#) unless explicitly stated differently

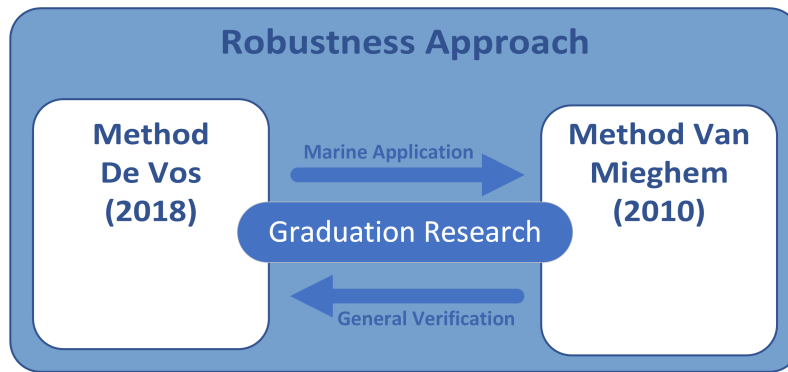


Figure 1.1: Knowledge Gap Robustness Approach de Vos (2018) and Van Mieghem, Doerr, et al. (2010)

#### 1.2.4 Problem Statement

The statement follows directly from the definition of the knowledge gap:

*The robustness approach by de Vos (2018) is not verified using a general robustness approach. At the moment, it is unknown whether or to what extent the robustness approach by Van Mieghem, Doerr, et al. (2010) verifies the robustness approach by de Vos (2018), nor is it known what assumptions are required for the robustness approach by Van Mieghem, Doerr, et al. (2010) to apply to distribution systems on-board ships.*

The scope and deliverables of this study are based on the following research goal:

*An improved approach for on-board distribution system robustness estimation in early-stage ship design, through comparing and verifying the robustness approach by de Vos (2018) using the robustness approach by Van Mieghem, Doerr, et al. (2010).*

#### Scope

The *scope* of this study mainly contains the two robustness approaches as described above and in [chapter 3](#) and [chapter 4](#). Even though many other approaches to system robustness exist, no third approach is included in this research project. Limiting the scope in this way ensures sufficient level of detail for the comparison and verification study. Only if there is an undeniable reason for a more extensive study of an assumption, this study to other robustness approaches is carried out. This study aims not to generate new system topologies; the goal is to analyse and compare existing ones.

#### 1.2.5 Ethical Considerations

The ethical behaviour of ship designers or maritime engineers directly influences public and crew safety, the environment, and resources. One way of approaching the challenges that maritime engineers face is by simply following the *code of ethics* by, e.g. SNAME.

This code of ethics is broadly applicable on engineering related topics; most of them not directly matters of life and death. However, a little more sensitivity is needed on this subject, as a significant portion of the literature originates from the Dutch or US navy; military information sources. These information sources have, more or less, a relation to warfare, meaning that the loss of life is not just a hypothetical situation. Moreover, most applications of contemporary ship robustness research are in or related to navy ships.

One could reason that increasing the robustness of such ships is part of the defensive part of the ship design process. After all, more robust systems increase the survivability of the ship and its crew. On the other hand, the functioning of the distribution systems is a precondition for the functioning of certain weapons. Therefore, more robust systems increase the operational capabilities of those weapons, which means robustness becomes part of the offensive part of the ship design process. The question remains whether a maritime engineer should contribute to military operations, either directly or indirectly.

A second element within this research topic is sustainability, which is also subject to ethical considerations. In general, a more robust system can be considered more sustainable. However, this statement is only valid if the system claim is kept constant or has decreased; otherwise, the carbon footprint based on the used materials does not decrease. Fewer failures within the system is sustainable development

in itself because it leads to fewer component replacements. The relation between the system efficiency and system robustness in maritime context is not yet researched; it is difficult to say how the robustness influences the system efficiency in general.

More robust systems most likely lead to a higher overall safety on-board ships because the probability of dangerous failures is decreased. If an uncrewed vessel or a vessel sailing with less crew, the job safety for specific jobs on-board ships possibly decreases.

### 1.2.6 Research Approach

The improvement of robustness calculations for distribution systems on-board ships is approached by dividing the challenge in multiple steps. First, concepts used in the research goal are defined: early-stage (ship) design, on-board distribution systems and robustness. Second, the verification study as performed by [de Vos \(2018\)](#) in section 6.3 of the dissertation is redefined to be in line with the generally accepted graph theory rules and with the case study. Third, the newly developed verification sets are used to analyse the different robustness measures: the objective function system robustness by [de Vos \(2018\)](#) and the  $R$ -value as defined by [Van Mieghem, Doerr, et al. \(2010\)](#). The practical applicability of the robustness measures on on-board distribution systems is analysed using a case study. This case study is based on a sample set of the first case study by [de Vos \(2018\)](#).

#### Deliverables

The research is considered to be finished when the following *deliverables* have been completed:

- An overview of assumptions required to apply the robustness approach by [Van Mieghem, Doerr, et al. \(2010\)](#) on simplified networks of distribution systems on-board ships.
- A comparison between the resulting robustness measure of both approaches of the graphs in section 6.3 in [de Vos \(2018\)](#), including the assumptions made for both approaches.
- A modified MATLAB script in which the robustness approach by [Van Mieghem, Doerr, et al. \(2010\)](#) is implemented in the robustness approach by [de Vos \(2018\)](#).
- A comparison between the results returned by the modified and original robustness MATLAB script, including the assumptions made for both approaches.
- A conclusion, stating whether or not the robustness approach by [Van Mieghem, Doerr, et al. \(2010\)](#) improves the robustness approach by [de Vos \(2018\)](#): to what extent and in what way does the first approach verify the second robustness approach?

## 1.3 Report Introduction

The aim of this final introductory section is for the reader to understand the structure of this study report properly. Therefore, the section titles speak for themselves, containing the report objective, the report outline and a reading guide for this report.

### 1.3.1 Report Objectives

The main goal of the first part of this report is to provide a clear and well-structured insight into two robustness approaches, their context, assumptions, differences and application. For the second part, the objective is to explain the analyses performed on the two approaches. This explanation contains the initial assumptions, the tools used for the verification, the analysis itself and, finally, a conclusion based on the results. This conclusion should cover the knowledge gap defined before.

### 1.3.2 Report Outline

The report structure is provided in [Figure 1.2](#). This figure shows the two main parts of this report: the literature review and the network analysis. The first part is based on a separate literature study ([Scheffers, 2021](#)); however, both the content and the structure of this study have been adjusted significantly. The "new" literature review starts with [Distribution Systems Onboard Ships](#), a combined chapter including a brief introduction to shipbuilding and on-board distribution systems. Moreover, the chapter contains different approaches to describe network systems and state of the art concerning system reliability research. Within this chapter, three key concepts are discussed and defined: early-stage (ship) design, on-board distribution systems and robustness approaches now typically applied in the marine industry. The subsequent two chapters [Automatic Topology generation Tool \(ATG Tool\)](#) and [Framework for Computing Topological Network Robustness](#) explain the two robustness approaches introduced earlier in this chapter in [section 1.2](#) in more detail. The three chapters together form part I of this report and provide the context for the second part.

The conclusion is supported by the three chapters in Part II: [chapter 5](#), [chapter 6](#) and [chapter 7](#). These chapters contain the research method, the results and the analysis of these results. First, [Network Set Introduction](#) introduces and compares the possible approaches to verifying the results of the two robustness approaches. These approaches are presented in the form of verification sets containing simplified distribution networks. In [Verification Set Network Analysis](#), the verification sets are used to compare different graph measures, originating in the two robustness approaches. [Case Study Network Analysis](#) provides a case study, which is included to improve the applicability of the abstract study within the maritime industry. The [Conclusion, Discussion and Reflection](#) is the last chapter of this report and contains the conclusions based on the research goal and addresses the knowledge gap.

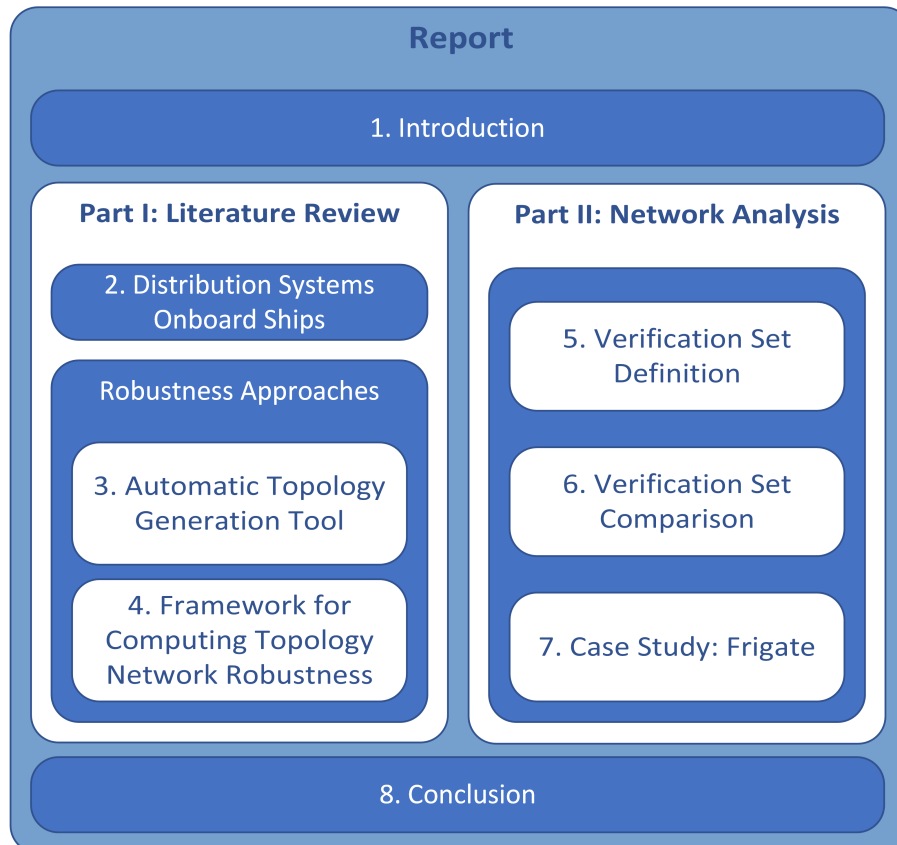


Figure 1.2: Graphic Overview of Report Content

Apart from the eight chapters, this report also contains two separate inserts. These inserts, officially defined as [Appendix E](#) and [Appendix F](#), contain an overview of the five verification sets and the case study sample set as introduced in [chapter 5](#). In [chapter 4](#), [chapter 6](#) and [chapter 7](#), there are frequent references to these sets. Therefore, the overview is provided separately from the report itself to provide for more comfortable reading.

### 1.3.3 Reading Guide

Various formatting styles support the structure and accessibility of this report. The report contains parts, chapters, sections and subsections, of which the first three categories are included in the table of contents. *Some words or word combinations* are written in italics to emphasise them.

**Graph Theory Concept** At given places through this report, such as the brief introduction of the first robustness approach, boxes like this text box can be found. These boxes contain information on a specific concept in graph/network theory. Some readers might be unfamiliar with these concepts; these boxes provide additional information to those who require this but can otherwise be ignored.

To conclude, this page is page [6](#). The digital version of this report uses hyperlinks as cross-references for chapters, sections, references and figures; Do not click on [Figure 5.9](#) unless you want to jump through the report to a completely different page (...)

# Part I: Literature Review

## Chapter 2

# Distribution Systems Onboard Ships

This chapter, the first chapter of Part I, provides the context for the following chapters: the two robustness approaches. This chapter defines three key concepts used in the research goal: early-stage (ship) design, onboard distribution systems and robustness. First, the ship design process is introduced in [section 2.1](#). The focus of this section mirrors the focus of the study: the first design stages, also called early-stage ship design. Second, with the design timeline defined, an overview of distribution systems onboard ships can be found in [section 2.2](#). Here, some frequently used systems are presented, together with a couple of general properties of distribution systems.

The second part of this chapter approaches distribution systems from a more theoretical point of view. The overview of distribution systems is followed by different approaches used to describe a system in [section 2.3](#). Finally, some applied theories on improving the reliability of distribution systems are described in [section 2.4](#), followed by a general conclusion in [section 2.5](#).

### 2.1 Ship Design

In between a concept mission profile by the shipowner and the actual shipbuilding at a shipyard, there is ship design. According to [Hornby & Turnbull \(2010\)](#), design is "... the art or process of deciding how something will look, work, etc. by drawing plans, making computer models, etc.". From this interpretation of design, the definition of ship design can easily be derived by replacing *something* with *a ship*. The process of ship design can be divided into multiple phases or stages, ranging between two stages ([Habben Jansen et al., 2020](#)) and six stages ([Lamb & Thomas, 2003](#)). This division is based on certain documents or drawings that must be delivered before or at the conclusion of said design stage; these moments are called milestones. According to [Lamb & Thomas \(2003\)](#), the following design phases can be identified:

- Concept Design
- Preliminary Design
- Contract Design
- Functional Design
- Transition Design
- Workstation/Zone Information Preparation

The six phases can be combined or divided to form a different division of the design process ([Chalfant, 2015](#); [Habben Jansen et al., 2020](#)). The distribution systems within this study are defined and analysed within the context of the first part of the design process: the *early-stage ship design*.

This report focuses on the first two phases: concept design and preliminary design, together called the *early-stage ship design*. This focus is chosen because of the design challenges ([subsection 2.1.2](#)) faced by ship designers during this design stage. The so-called single line diagram, one of the preliminary design deliverables, is analysed more in-depth throughout this research. However, to understand the function and the importance of the first two phases, some basic understanding of the complete ship design process is required. The six phases as identified by [Lamb & Thomas \(2003\)](#) are explained below.

### 2.1.1 Early-Stage Ship Design

"One of the truisms of ship design is that the decisions of greatest impact are made in the early stages of design when the least information and the greatest uncertainty are present."  
 — Julie Chalfant

Early-stage ship design includes the first design stages of the ship design process. The first two design stages, concept design and preliminary design (Lamb & Thomas, 2003), form the early design stages (de Vos, 2018). The so-called deliverables and main activities within the two phases are provided in the paragraphs below. A different approach to defining early-stage design is made by Habben Jansen (2020), through splitting the concept design process in concept exploration and concept definition. Concept exploration is the process of establishing requirements by means of the analysis of multiple possible concept solutions. The mission of the ship provides the initial information to define these preliminary concepts. In Figure 2.1, some possible layouts of the design process are shown. The light blue box shows the phases that are usually considered early-stage design.

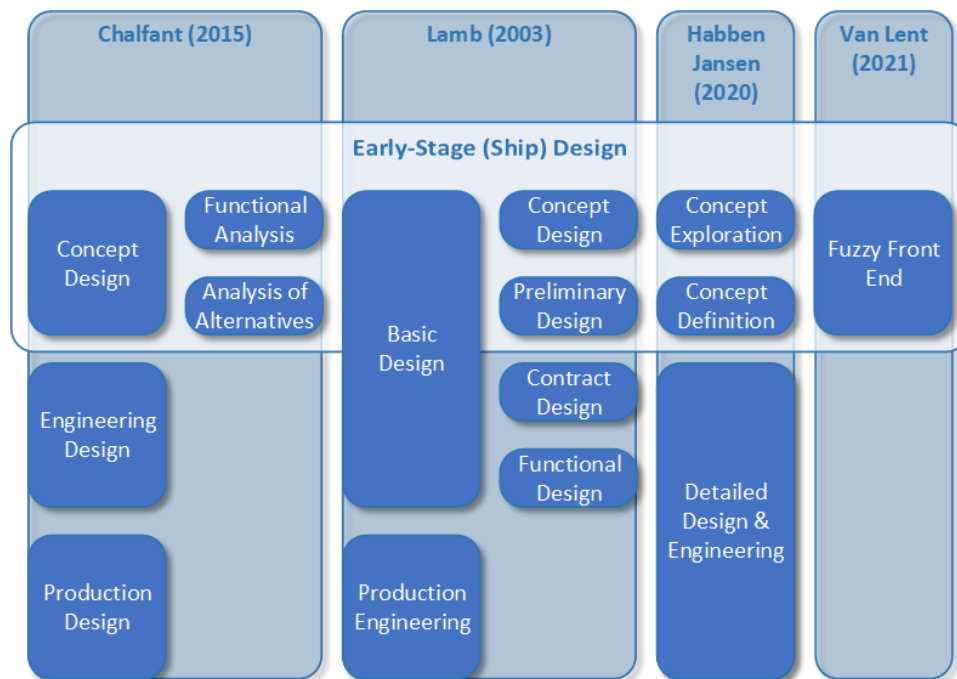


Figure 2.1: Design Stage Definitions with Early-Stage (Ship) Design Emphasised

#### Concept Design

This phase is also called the cost and feasibility study phase. This phase's primary goal is to understand the client's actual requirements: the combination of the ship's mission and the principal performance attributes. The deliverables of this phase are, amongst others, a clear mission statement and a concept design that meets the owner's overall requirements. Since not all requirements are financially and technically feasible, a cost estimate and a risk assessment are made in this phase as well. The main trade-off is cost and building time and the required ship capabilities, on the other hand. In general, the capacity of the main components on board is determined at the end of this phase. For example, the required propulsion and an estimate of the total energy consumption are calculated.

#### Preliminary Design

The costs and performance of the ship are determined in this phase. During this phase, major design decisions are taken using trade-off studies. Decisions in this category have a significant impact on the dimensions, the overall configuration, the performance, the costs, and the ship's risks. Studies with a minor impact are conducted in a later design stage.

The following ship components are determined during this phase: the hull size and shape, the general arrangement (GA), the crew size, the mission-critical payload features and, in case this has not been determined in the first phase, the propulsion plant. The deliverables include a description of the principal

ship systems and features, a propulsion system drawing, an electric load analysis, an HVAC load analysis and the single line diagrams. This list is far from complete; the deliverables mentioned here are expected to relate to the distribution systems.

### 2.1.2 Early-Stage Design Challenges

Figure 2.2a and Figure 2.2b show different representations of a general design process. While the cost and information/problem knowledge graphs show different increasing trends, a rapidly decreasing graph represents the design freedom/influence graph. This means that, for these design process models, the design space for a certain problem decreases rapidly during the early design stage. The challenge lies in the second graph line, the information graph. The known information on the problem and its possible solutions is limited during the early stages; therefore, the most important decisions concerning design direction are to be made with minimal access to information.

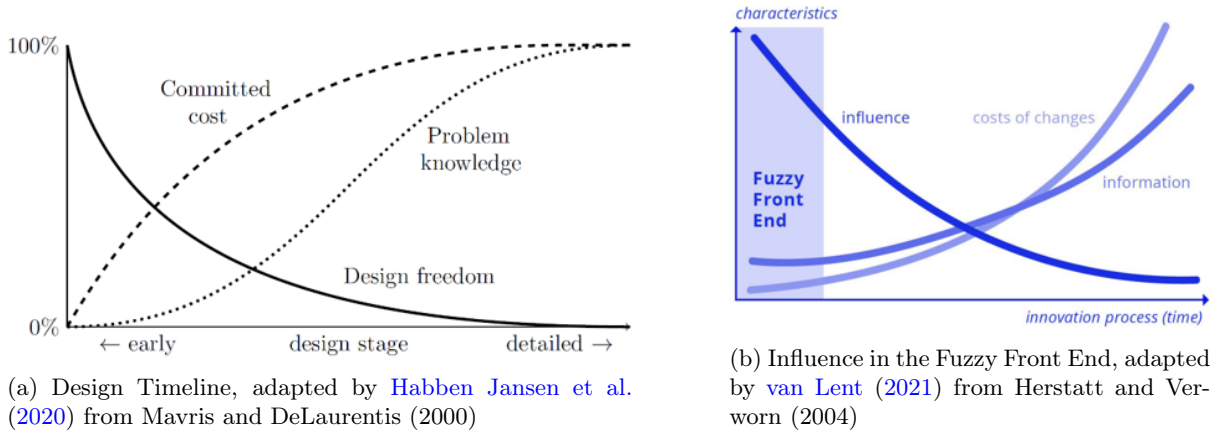


Figure 2.2: Two Design Process Representations

## 2.2 Overview Distribution Systems

Several systems can be found onboard ships, including a propulsion system, a power generation and distribution system, water distribution systems and a heat, ventilation, and air-conditioning (HVAC) system<sup>1</sup>. These systems provide a function, and with that, assist in the main functions, operational functions, or supports the main functions, provides general support.

### 2.2.1 System Categorisation

"Marine engineering is the art of integrating the components into systems to perform a specific set of functions." The systems onboard can be categorised based on their multiple properties; here, they are categorised based on their functions as defined by Klein Woud & Stapersma (2016). The first category is *platform systems*, the functions included in this category are protection against the environment, mobility and survivability. The firefighting (Fifi) system is a system in this category. The *hotel systems* form the second category and provide comfort and entertainment to the crew and guests. The catering system and sanitary system are part of the hotel systems category. Other system categories are the support systems and the operational systems. The classification of systems based on their function is mainly used to determine which systems need to be installed to create a functional ship. This research focuses on the distribution systems, a subgroup present in most functional system categories.

### 2.2.2 Distribution System and Distributed System

According to the Oxford Dictionary, a distribution system is "the way that something is spread or exists over a particular area or among a particular group of people" (Hornby & Turnbull, 2010). A distribution system is not to be confused with a distributed system, in which distributed means "to spread something, or different parts of something, over an area" (Hornby & Turnbull, 2010). The difference between a distribution system and a distributed system is what gets distributed; a distribution system distributes a substance (flow, energy, information) over its operational area, while for a distributed system, the components of the system are distributed over its operational area. Habben Jansen et al. (2020) defines distributed systems as systems distributed throughout the ship, where distribution systems

<sup>1</sup>The primary source of section 2.2 is Klein Woud & Stapersma (2016) unless explicitly stated differently

are systems that distribute vital commodities throughout the ship. [de Vos \(2018\)](#) and [Leeuwen \(2017\)](#) do not explicitly define distribution systems and distributed systems; however, they use the same definitions as [Habben Jansen et al. \(2020\)](#).

There can be a discussion about the overlap between a distribution system and a distributed system. [Habben Jansen et al. \(2020\)](#) states that terms can be used interchangeably since most systems cover both characteristics. One could argue that most distributed systems contain a distribution system; for example, data is distributed through the system to create system interaction instead of fully independent components. However, if a distributed system’s primary function is not to distribute a particular flow type, this system might not be called a distribution system. Conversely, not all distribution systems can be considered as distributed systems. For example, certain coolants are not distributed over a ship but are contained within one component; the flow is limited to a distribution system within a chilled water plant (CWP).

### 2.2.3 Marine Distribution Systems

A distribution system onboard ships can be described using the following generic properties defined by [Klein Woud & Stapersma \(2016\)](#):

- The system contains one or more supply components, such as generators and pumps. In addition, a supplier can be connected to another system with a different type of flow.
- The system moves a particular flow from the suppliers through the system, which happens due to an effort like pressure or voltage. Thus, the system can be modelled like a network in which the flow is distributed.
- The system can contain components in which the flow gets temporarily stored. For example, this can be a tank for fluid systems, while the storage can be batteries in an electric distribution system.
- The system contains users that convert the flow and can be connected to a different distribution system for a particular flow type. The flow can leave the system at the user, or it can be redirected to the supplier side of the system.

In [Figure 2.3](#), an overview is given of the distribution systems onboard ships. Some system users or systems require different flow types; therefore, they are connected to multiple distribution systems.

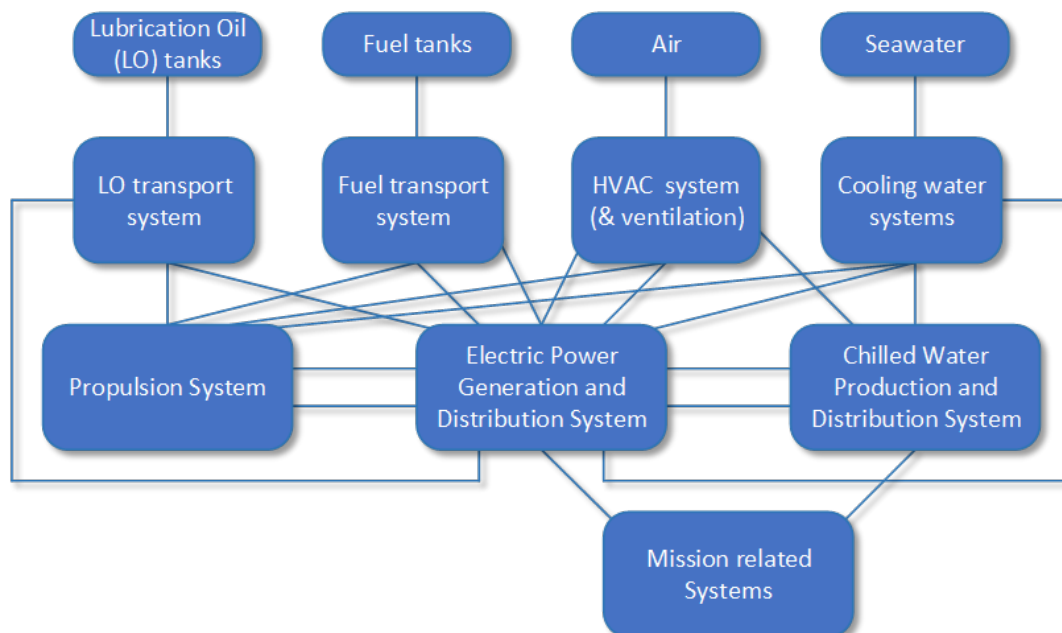


Figure 2.3: Distribution Systems On-Board of Ships and Their Interdependencies ([de Vos, 2018](#))

## 2.3 Distribution Systems Architecture

The distribution systems mentioned in [section 2.2](#) can be described and analysed using different viewpoints. These viewpoints or perspectives are ways to model the distribution system, with a specific point

of focus for each type of model. Therefore, the different perspectives provide information on the system within a certain scope. Three types of architectural frameworks are described below: an information framework by [Brefort et al. \(2018\)](#), the OSI-Model by International Organization for Standardization (ISO) and the two-layer representation by [Van Mieghem, Doerr, et al. \(2010\)](#).

### 2.3.1 An architectural framework for distributed systems ([Brefort et al., 2018](#))

The main goal of this framework is to provide "a conceptual method of capturing the key attributes of a distributed ship system ... to describe such a system, ensuring all important aspects are covered ..." ([Brefort et al., 2018](#)). It is aimed to be a tool in analysing and designing distributed ship systems by increasing the opacity of the interrelations and therefore preventing latent errors. This framework is not limited to distribution systems but to distributed systems, defined as specific types of systems disbursed throughout the vessel. [Figure 2.4](#) provides a qualitative representation of the different viewpoints used to analyse the distributed system. This framework is applied to a single distributed system; however, different flows can coexist within this specific system. Subsystems and systems-of-systems have not been included in the framework, nor have relations between different systems.

The *physical architecture* consists of two elements: the constraining architecture and the physical attributes of the components within a distributed system. This view combines the physical attributes of the ship with the physical attributes of the system components, i.e. what is the ship configuration of spaces and their relationships and where do the system components fit physically. The overall layout can be done in multiple ways; the bounds of these layouts are provided with the physical architecture. To model a system using this architecture, information on the overall ship configuration and the physical attributes of the main components within the system is required.

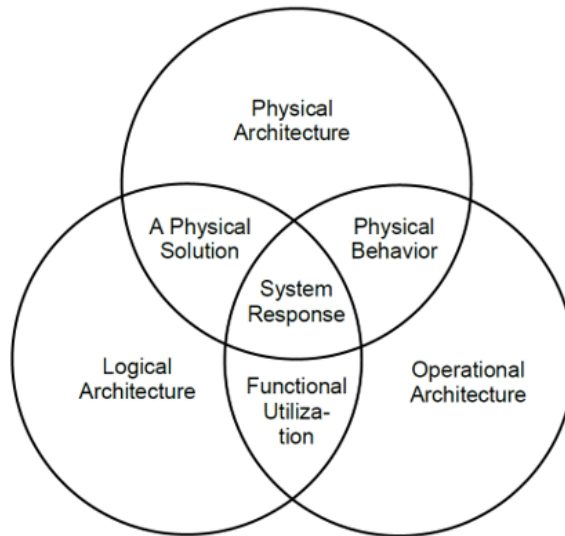


Figure 2.4: Architectural framework for naval distributed systems ([Brefort et al., 2018](#))

The second architecture, the *operational architecture*, defines what is required to happen through time to accomplish a given mission. It defines the input and output of the system, including the order in which the system is used and what functions the system is required to fulfil. The human-machine interaction is part of this architecture since it includes the kind and order of the decisions made over time. The temporal operational profile, the functions and requirements through time, must be known to develop this architecture.

The connections or links between components within a system are described within the *logical architecture*. The way the components are connected provides information on the specific service or function a system can fulfil. A system with a number of components can be simultaneously connected in different ways through a specific flow within each subsystem. The (main) components and the connections between these components are required as input for this architecture to be constructed.

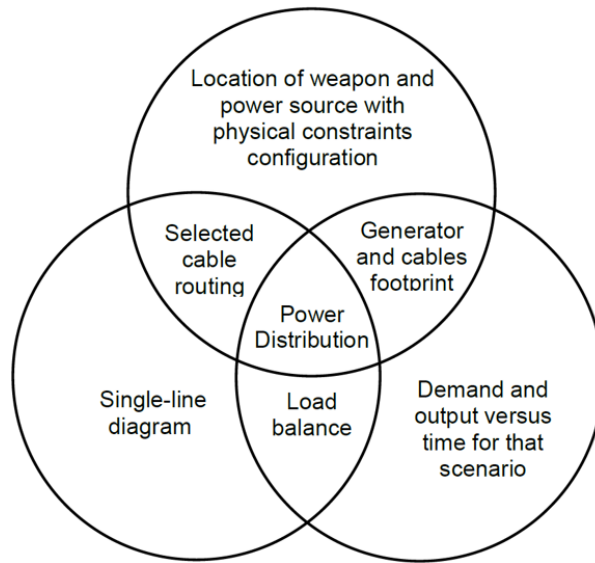


Figure 2.5: Architectural framework applied on a simple system used to power a high energy weapon (Brefort et al., 2018)

In Figure 2.5, an example (the powering of a high energy weapon) can be found of the applied architectural framework as shown in Figure 2.4. The architectures are represented by some means of presenting that architecture. Similarly, the overlap show what information can be analysed within that specific area of the framework. The interrelations *provide* an information base that can be analysed. The information required to construct the overlap originates in input from the two or three combined architectures and can be used in better understanding a potential design solution.

### 2.3.2 Two-layer network model (Van Mieghem, Doerr, et al., 2010)

According to Van Mieghem, Doerr, et al. (2010), any network contains at least two crucial *features* or, in other words, architectures: "the network topology or infrastructure and the service for which the network is designed or created." A service uses the network infrastructure to transport items between two or more nodes. The service can be subject to constraints. Sometimes, the services themselves, such as security services like anti-virus spread, can be regarded as constraints since they cannot be considered the network's primary goal. An example of a network providing different services is the internet; this network provides communication services such as email and web services.

Together with the network topology, the network service makes up the network. The network topology defines how the nodes are interconnected by links and can be represented by a graph with several links and nodes. Those two network layers can be visualised, as shown in the red box in Figure 2.6. The figure also includes the *R*-value; a robustness representation explained in section 4.2. Furthermore, this figure provides a flow chart that shows one of the two main goals of clear and computable network robustness: improving a network to achieve a desirable level of robustness. The second main goal is being able to compare two different networks on robustness. This framework aims to apply to all kinds of networks, therefore implicitly including distribution systems onboard ships.

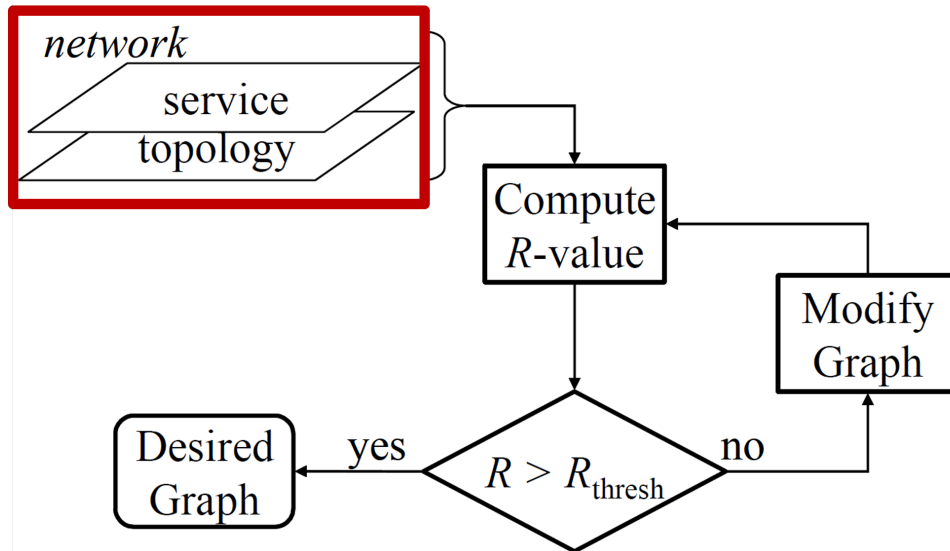


Figure 2.6: The organigram or flow chart of the high level goal to achieve network robustness. The network is defined by two network layers: network service and network topology, adapted from (Van Mieghem, Doerr, et al., 2010)

### 2.3.3 OSI-Model

The Open System Interconnection (OSI) model is a standard idealised heterogeneous computer network model developed by the International Organization for Standardization (ISO) (Saxena, n.d.). The main goal of this architecture is to function as a framework for the definition of standard protocols. Despite that no particular systems are implemented in this system, its scope is primarily concerned with systems comprising terminals, computers and associated devices (ISO/IEC 7498-1 : 1994, n.d.). Handel & Sandford (1996) emphasises that the OSI model represents an idealised network, comprised of seven layers that each provides specific functionality or service to the adjacent layer. Some technologies do not fit within the functionalities described in a specific layer but run on none or more layers simultaneously (Sequeira, 2018). The first of the seven layers is the physical layer.

The physical layer contains the hardware necessary to transmit bits through the network's communication channels (Handel & Sandford, 1996). This layer defines the physical network structures, the mechanical and electrical specifications and the hubs or switches. These elements include the physical topology (examples of topology mentioned are a mesh, a star, a ring or bus topologies) of the network; therefore, this layer mirrors the network topology layer by Van Mieghem, Doerr, et al. (2010) or the logical architecture layer by Brefort et al. (2018).

Contrary to the network topology layer (Van Mieghem, Doerr, et al., 2010), the physical layer includes directed edges between nodes as defined by the data transmission function, in the form of the simplex mode, the half-duplex mode and the full-duplex mode (Saxena, n.d.). Simplex mode represents unidirectional communication such as keyboards; a device can either receive or transmit data but not both. With a half-duplex connection, stations can transmit and receive but not simultaneously, such as walkie-talkies. A full-duplex connection provides for simultaneous communication like telephones, respectively (GeeksforGeeks, 2021). Since this model mainly focuses on computer networks, the physical architecture, as defined by Brefort et al. (2018), is not emphasised in this model.

The different layers and the flow transported can be found in Figure 2.7; the key functionality of all seven layers is (Sequeira, 2018):

1. **Physical Layer** Defines the *physical topology*: the way components are physically interconnected. Includes the bandwidth usage and multiplexing strategy too (data transmission function).
2. **Data Link Layer** Contains the *logical topology*: the actual traffic flow. Handling flow control and performing error detection and correction
3. **Network Layer** Forwarding data based on logical addresses (like Internet Protocol addressing) and route discovery and selection.
4. **Transport Layer** Division between upper layers (layers 5-7) and lower layers (layers 1-3).

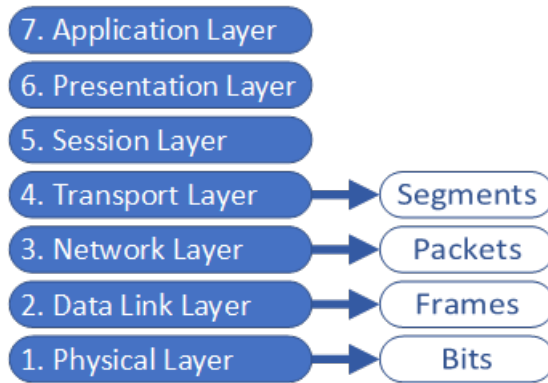


Figure 2.7: The seven layers of the OSI model including type of data distributed over the system through a specific layer, adapted from [Sequeira \(2018\)](#)

5. **Session Layer** Setting up, maintaining and tearing down a session: a conversation in which the intermingling of data from other conversations must be avoided.
6. **Presentation Layer** Data formatting and encryption.
7. **Application Layer** Supports services used by end-user applications and service advertisement such as the availability of networked printers

In summary, according to [Lowe \(2020\)](#), the lower three layers deal with *the mechanics of how information is sent from one computer to another over a network*. The final use of the data is not relevant within these layers; the layers manage the timing, the amount and the direction of the data transported over the system. The upper layers deal with applications through application programming interfaces.

### 2.3.4 Architectural Framework Comparison

An analogy can be found between the architecture definitions by [Brefort et al. \(2018\)](#) and [Van Mieghem, Doerr, et al. \(2010\)](#): the logical architecture by [Brefort et al. \(2018\)](#) mirrors the functions of the network topology by [Van Mieghem, Doerr, et al. \(2010\)](#) and the operational architecture by [Brefort et al. \(2018\)](#) can be considered similar to the network service layer by [Van Mieghem, Doerr, et al. \(2010\)](#). However, significant differences between the methods are apparent.

First, a network as defined by [Van Mieghem, Doerr, et al. \(2010\)](#) does not contain a physical or spatial architecture. While [Brefort et al. \(2018\)](#) model focuses explicitly on *distributed naval ship systems*, the aim of the framework by [Van Mieghem, Doerr, et al. \(2010\)](#) is to be applicable for all kinds of networks. Therefore, networks without an apparent spatial architecture, such as computer network models like the internet, need to be included as well.

Second, [Brefort et al. \(2018\)](#) includes temporal behaviour of the system only in the operational architecture; the physical and logical architectures are considered time-independent. [Van Mieghem, Doerr, et al. \(2010\)](#) aims to analyse the robustness of a network based on a changing topology, with a series of removal of single links or nodes. These perturbations or challenges, such as failures or external attacks, lead to a time-discreet topology analysis. One could argue that this analysis occurs in the overlap between logical and operational architecture since human intervention (attacks) and machine response to these interventions is included. However, [Van Mieghem, Doerr, et al. \(2010\)](#) only includes topology metrics in his scope, leaving service metrics out due to their fuzzy measurability.

Within this comparison, the OSI model is not included because its application does not overlap with the application of [Brefort et al. \(2018\)](#) network architecture model. Most layers within the OSI model provide services that cannot be applied to physical distribution systems. However, the OSI model makes one relevant distinction: the difference between the physical and logical topology. This distinction, combined with the data transmission function, might prove helpful in later research concerning the influence of directionality on the network robustness.

To finish this comparison, the main conclusion is that any network can be described from multiple perspectives. For a particular network analysis, one should determine which perspective or architecture provides the required information structure. An example of these requirements can be found in [Alshattnawi \(2017\)](#).

## 2.4 Reliability Distribution Systems

In 1980, a joint committee on *Fundamental Concepts and Terminology* was formed "... with the intent of merging the distinct but convergent paths of dependability and security communities ..." (Bondavilli et al., 2016). The definitions provided by this committee can historically be considered as the reference taxonomy of the basic concepts of dependability. Bondavilli et al. (2016) defines dependability as *the ability to avoid failures that are more frequent and more severe than is acceptable*. Several attributes can be assigned to dependability, which can be divided into two categories: primary and secondary attributes. The primary attributes, availability, reliability, maintainability, safety and integrity, are comprised within dependability. The secondary attributes, however, can be used to define dependability in specific circumstances. For example, system robustness is defined as *the dependability concerning external faults (including malicious external actions)*. The block diagrams in Appendix A provide an overview of the multiple robustness related definitions used in this chapter; Figure A.1 shows the definitions used by Bondavilli et al. (2016) and Figure A.2 shows a broad selection of robustness-related definitions found in literature. The yellow box implies that those definitions are applied to ships.

### 2.4.1 Attributes of Network Robustness

One of the most narrow definitions of network robustness is given by Cuadra et al. (2015): "robustness is the degree to which a network can withstand an unexpected event without degradation in performance. It quantifies how much damage occurs as a consequence of such unexpected perturbation". While other definitions include the element of unexpectedness within the definition (Koç et al., 2016; Çetinay et al., 2019) as well; this is not a necessity in most definitions. Another point in which definitions differ is in the description of the residual functionality after a challenge. Ellens & Kooij (2013) defines this as *the ability to continue performing well*, Trajanovski et al. (2013) as *the maintenance of function (measured by a graph metric)* and Cats et al. (2017) as *the capacity to absorb disturbances with a minimal impact on network performance*. It can be concluded that no uniform definition of robustness is currently available and used in different research areas.

### 2.4.2 Network Performance

Within the definition of robustness provided by Cats et al. (2017), the concept of network performance is mentioned. This network performance is defined by He (2020) as *the interplay of the structure of the network and the dynamic process that runs on top of the network*. The metrics to quantify this network performance can broadly be divided into two categories: network efficiency and network robustness. The author defines efficiency as *the ability to avoid wasting materials, energy, money, and time in producing the desired output or providing the desired service*. Apart from this definition, the focus is from now on in the second category: the network robustness. He (2020) uses the same definition for robustness as Trajanovski et al. (2013); however, the calculations of this robustness are based on the definition by Van Mieghem, Doerr, et al. (2010).

In subsection 4.4.4, Ellens & Kooij (2013) states that a higher efficiency value means higher graph robustness when introducing efficiency as a graph measure. The apparent contradiction stated by He (2020) above is nullified with this alternative definition of efficiency. An unambiguous definition of robustness as well as efficiency is needed to resolve this paradox.

### 2.4.3 Network Robustness Design Rules

In chapter 1, a motivation based on three maritime developments is provided to make a ship more reliable and, to achieve this increased reliability, more robust. The ship's reliability can be improved by improving the reliability of the onboard systems; this improvement can be tackled from different approaches (Woud & Stapersma, 2003), applied as *design rules*. Spruit et al. (2009) has distilled ten design rules (rules of thumb) that can be used to improve distribution system survivability:

1. Avoid central distribution systems
2. Separate redundant sources
3. Apply protection if sources must be in each other's vicinity
4. Separate redundant paths
5. Apply protection where redundant paths have to be close together
6. Arrange feed and return lines for closed-loop systems next to each other
7. Avoid single points of failure
8. Implement a cross-over near the system's essential users
9. Implement a cross-over near the systems' sources

## 10. Combine paths of distribution systems for essential capabilities

These ten design rules can be reduced to three key concepts in improving system robustness: *independent subsystems*, *redundancy* and *reconfigurability*. First, *independent subsystems* can be designed within a system, covering design rule 1. If a node or edge of a particular subsystem fails, this does not influence the other subsystems.

The second way of making a system more reliable is including a degree of redundancy in the system, which includes design rules 2 and 4. *Redundancy* is the duplication of specific components or connections, in graph theory called nodes and edges, respectively. The top-level redundancy is full-backup redundancy; the complete functionality of the system stays intact when a component or connection is removed from the system. A system has a lower level of redundancy if it has some functionality loss but does not entirely shut down. *Spatial Redundancy* is contrary to *functional redundancy*, based on the location of the components and connections throughout the ship. If a system is spatially redundant, it remains complete or partially functional when a particular area in the ship suffers damage. For systems, a trade-off has to be made between spatial and functional redundancy and system claim, on the other hand. The system claim, i.e. the system costs, weight and volume, increase with a higher level of redundancy.

Redundancy is only helpful if the duplicated components or connections can be reconnected to the system. The capacity of a system to connect components or connections in different ways is called *reconfigurability* and represents design rules 7, 8 and 9. Reconfigurability is the third way of making a system more reliable and depends on the topology of the distribution system.

## 2.5 Conclusion

In this chapter, three key concepts are defined: early-stage (ship) design, onboard distribution systems, and robustness. First, early-stage design is the design stage at the start of the ship design process, during which the knowledge-investment gap plays a dominant part. Important decisions that significantly influence the design need to be made without the required knowledge to make these decisions. The general aim of this study is to improve a theoretical robustness approach that provides information while requiring little input.

The second concept, the distribution system onboard ships, is defined as a number of connected components transporting a flow (e.a. cooling water, lubrication oil, electricity or data) from a source component via other components to a certain user component. The way the network is described is dependent on the applied network analysis, for example, with a focus on the system topology. Therefore, the focus of this study is on the *logical architecture* (Brefort et al., 2018) or the *network topology layer* (Van Mieghem, Doerr, et al., 2010). Within this research scope, a set of simplified onboard distribution system networks is analysed.

To design a reliable distribution system, the system must not only have a degree of redundancy; it must have a certain degree of reconfigurability as well. Spare or redundant components become functional only after they have been connected to the system. Measuring service or functionality is challenging, especially at a design stage where little information is known compared to the weight of the design choices to be made. Within this study, the third key concept, robustness, is defined as the combination of independent subsystems, redundancy and reconfigurability.

## Chapter 3

# Automatic Topology generation Tool (ATG Tool)

This chapter aims to provide an overview of a robustness approach by [de Vos \(2018\)](#). Some major elements of this approach are used as input and further analysed in Part II of this report. Most importantly, the second objective function, system robustness, is verified in [chapter 6](#) and [chapter 7](#). [chapter 6](#) also applies F2 to the verification study mentioned in [section 3.6](#). The case study, also introduced in [section 3.6](#) and based on the benchmark system in [subsection 3.2.1](#), is further analysed in [chapter 7](#).

First, the context of this approach is given by the description of a few relevant concepts in [section 3.1](#). The applied network properties such as boundary conditions and subsystem structure can be found in [section 3.2](#). Some key elements concerning the topology generation can be found in [section 3.3](#), like as the design space exploration and the ATG tool. The objective functions used are described in [section 3.4](#) and [section 3.5](#). The last two sections provide an overview of the networks analysed by [de Vos \(2018\)](#) and a chapter summary in [section 3.6](#) and [section 3.7](#).

### 3.1 Reliability and Survivability

Stable, consistent, repeatable measures of effectiveness or metrics are required to compare ship designs ([Chalfant, 2015](#)). However, some relevant and desirable measures, such as costs, survivability, reliability, effectiveness and flexibility, are relatively difficult to compute. These measures are combined and individually studied in several papers, both applied to naval ships and commercial vessels ([Wang et al., 2019](#); [Sui et al., 2019](#)). Two measures, survivability and reliability, are discussed since they are considered more related to this study than the other measures. These concepts are included in [Figure A.2](#).

#### Reliability

Reliability is previously discussed in [subsection 2.4.3](#); however, that section discusses improving reliability but does not discuss the definition of this concept. [de Vos \(2018\)](#) states that system reliability and safety require distribution systems onboard ships to operate reliably and safely in all operational modes and circumstances. [Chalfant \(2015\)](#) provides a more narrow definition of reliability, stating that it is a measure of how consistently equipment works under normal operating conditions. Reliability research is mainly focused on systems that cannot withstand power interruptions, which is not part of this literature study's scope.

#### Survivability

[Habben Jansen et al. \(2018\)](#) defines survivability as "the capability of a ship and its shipboard systems to avoid and withstand a weapons effects environment without sustaining impairment of their ability to accomplish designated missions." This survivability is the combination of three categories: susceptibility, vulnerability and recoverability. This author defines vulnerability as the inability of a ship to withstand damage from one or more hits and recoverability as the ability of a ship and its crew to prevent loss and restore essential functions, given one or more hits. According to [Chalfant \(2015\)](#), survivability is a measure of how well a ship and its systems can perform in adverse circumstances. This author includes detectability in the survivability definition: a measure of the probability that a ship will be discovered. Current methods for studying the survivability of a ship in early-stage ship design have a running time

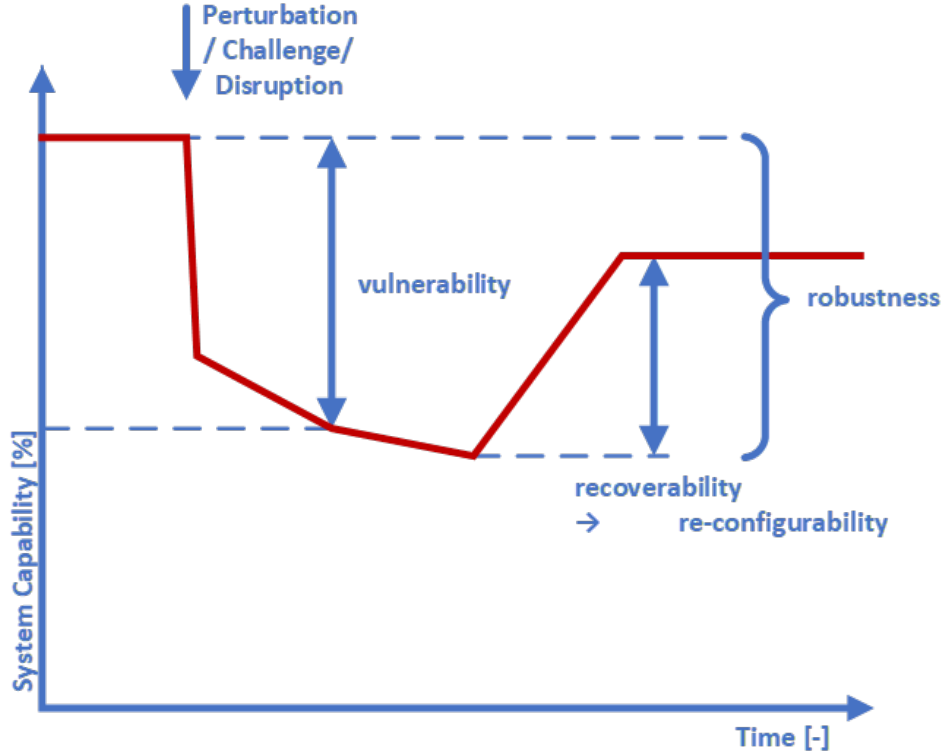


Figure 3.1: General System Response Curve to a Disruption, adapted from de Vos (2018) based on Ashe et al. (2006)

ranging between days and weeks, dependent on the level of detail in which ship functions are analysed (Chalfant, 2015). Moreover, there is no clear consensus on what a navy vessel should be able to withstand. Therefore, survivability cannot yet be considered as an unambiguous objective measure.

Robustness and vulnerability are closely related concepts; Habben Jansen et al. (2020) states that three state of the art robustness measures are identified to decrease systems' vulnerability from an operationally oriented point of perspective. Figure 3.1 contains a system response curve showing the system capability over time including related robustness concepts. Naval ships have been the main focus of robustness research within the maritime industry since survivability is a more tangible concept in hostile situations. Currently, the robustness of systems is improved using design rules, which have been described in subsection 2.4.3. A number of robustness and vulnerability studies have taken place, with the shared goal of creating a quantifiable definition of the robustness of ships (van Oers & Van Ingens, G., Stapersma, D., 2012; Leeuwen, 2017; Habben Jansen et al., 2020; de Vos, 2018). This chapter further elaborates the robustness approach as described by de Vos (2018)<sup>1</sup>.

## 3.2 Network Properties

To determine what type of architecture, or which overlap between architectures, is used within this robustness approach, the name of the method is already a major give-away: automated *topology* generation tool. Therefore, the main focus of this tool is the network topology layer (Van Mieghem, Doerr, et al., 2010) or the logical architecture (Brefort et al., 2018). de Vos (2018) has provided two statements to support this idea. First, it is stated that no different modes of operation of a certain system are studied, supporting the approach to model an accumulator as either a supplier or a user. The idea behind this example is emphasised with a more general mention of time, saying that transient behaviour is outside the scope of early-stage system design and therefore outside the scope of the study. Since the temporal information is required to make an analysis based on the operational architecture, this type of architecture, including its overlap, is not included here.

The second statement is based on the objective function *system claim*, which is further elaborated in

<sup>1</sup>The main source of chapter 3 is de Vos (2018) unless explicitly stated differently

section 3.4. As an alternative to the simplified function, as used throughout the study, a second approach to system claim is defined. This definition includes the estimated length of connections between different system components to determine the installation cost part of the system claim of. The estimation is based on a grove spatial division of the ship. Therefore, this approach is part of the overlap between the logical architecture and the physical architecture, since the topology as well as the physical locations are required information. However, the study continues with the simplified system claim function instead of this spacial system claim function, since this second function requires more information while barely increasing the accuracy of the overall system claim. This means that the ATG Tool by de Vos (2018) is purely based on the logical architecture, disregarding the operational and physical architectures as defined by Brefort et al. (2018).

### 3.2.1 Network Boundary Conditions

In contrary to the *graph theory robustness approach* (Van Mieghem, Doerr, et al., 2010), the *marine robustness approach* is applicable on one specific network type: distribution systems on-board of (naval) ships. The main advantage of having such a concrete application of the theory is that additional assumptions can be made, leading to a less abstract node-edge structure. First, the distribution system properties as described in section 2.2 are assumed. de Vos (2018) has based three *declarations* on these properties, which are described below.

**Declaration 1: A node can be either a supplier or a user in a specific distribution system**

This first declaration follows directly from the system properties described in section 2.2. The flow is the stream or supply of distributed goods or fluids, such as cooling water with a certain pressure and temperature, lubrication oil, electricity with a certain Voltage or data. Distribution systems distributing a certain flow can be connected; in that case, a node can be a user for the first system and a supplier in the second system. Two distribution systems can share a certain node as user, for example, if a system needs both fuel and cooling water. In some cases, the flow direction within a system can be changed. In these systems, a node can switch from being a supplier to a user; however, it cannot fulfil both functions when the system is running.

**Declaration 2: Edges are connections of specific distribution systems, i.e. an edge that belongs to a specific distribution system can "carry" only the specific (predefined) flow type that comes from its suppliers; it cannot distribute any other flow types**

This declaration is based on physical principles: a fluid distribution system requires pipes as edges, while a mechanical or electric distribution system requires completely different edges. Even within certain physical boundaries, different distribution systems can exist. The effort or flow can be different; the temperature of a fluid or a system's voltage are variable. The different variants are all assumed to be separate distribution systems that can be connected using a converter. This converter functions as user for the first system and as supplier for the second system.

**Declaration 3: When a node is not a converter (i.e. supplier in one and/or user in another specific distribution system), it is a hub in a specific distribution system.**

This declaration is, in line with the first declaration, differentiating the nodes within a network. It states that all suppliers, users, converters and accumulators are one node type: the converters. All these converter nodes convert the flow in a certain way. The "leftover" nodes are called hubs, of which the switchboard is the most obvious example. A switchboard does not change the flow between the input and the output; it simply redirects or redistributes this flow. Fluid distribution systems contain distributed hubs as well, such as main pipes. Both main pipes and switchboard are assumed to be single nodes in the category hubs. One advance of explicitly stating the existence of hubs in early-stage ship design is that the chances of these hubs being included in preliminary layouts and drawings increases.

### 3.2.2 Benchmark System & Subsystems

Based on the network description and boundary conditions explained in subsection 3.2.1, the ATG tool is tested with the use of two case studies. More information on these case studies, as well as the verification study, can be found in section 3.6. First, it is important to note that the distribution systems in the first and second case study contain several distribution systems, also known as subsystems. The distinction between these systems is based on the second declaration: edge differentiation. All edges within a single subsystem "carry" the same predefined flow type. Hub nodes are exclusively used by a single subsystem, e.g., a main pipe node only contains water with a predefined pressure and temperature. In Figure 3.2, a

benchmark system of the first case study is introduced. This system contains four connected distribution systems, represented by alternating *hub layers (HL)* and *converter layers (CL)*.

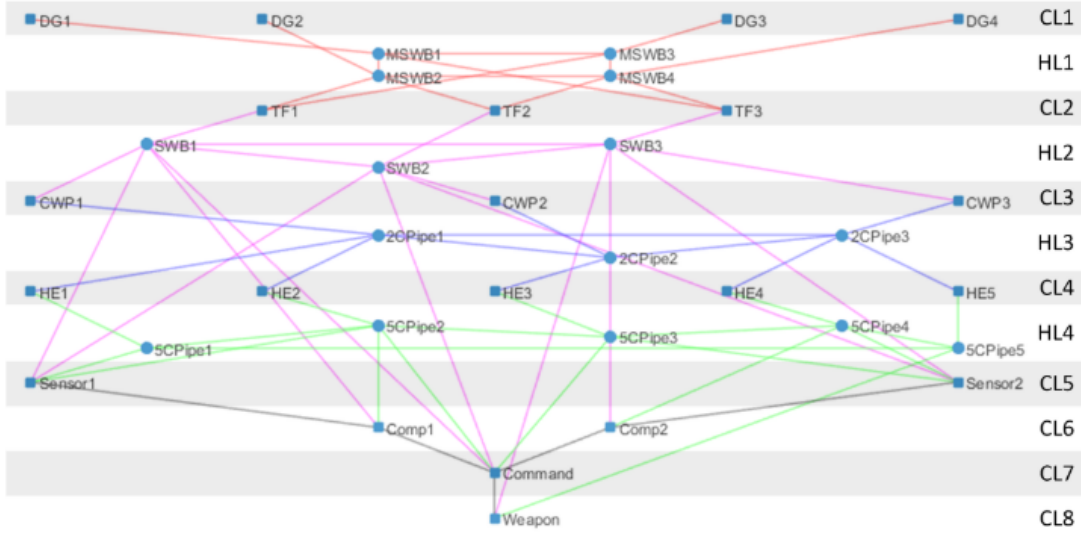


Figure 3.2: Benchmark System of Case Study I (de Vos, 2018)

### 3.3 Topology Generation

Early-stage ship design can be approached using one (or more combined) design methods, such as the classic design spiral (Evans, 1959), concurrent design (Sohlenius, 1992) or set-based design (DOERRY et al., 2014). de Vos (2018) applies *design space exploration (DSE)* as the preferred approach to design onboard distribution systems.

#### 3.3.1 Design Space Exploration: Theoretical Background

Calinescu & Jackson (2011) refers to design space exploration (DSE) as the activity of discovering and evaluating design alternatives during system development. HE discusses three possible uses of this design approach: rapid prototyping, optimisation and system integration. Optimisation methods include multi-objective optimisation, genetic algorithms and particle-swarm optimisation (Chalfant, 2015). Calinescu & Jackson (2011) states that the pitfall of DSE is the number of design alternatives to be explored; in some cases, the design space may be infinite. The following components are crucial in decreasing the design space:

- Representation: This should be formal, more objective and stat-based. Next to that, the representation should be expressive enough to capture more complex constraints.
- Analysis: Machine-assisted techniques discover potential design solutions and check whether they comply with the constraints.
- Exploration Method: Some solutions can be considered equivalent; the framework must provide a method for navigating to interesting solutions.

Chalfant (2015) defines a non-dominated *Pareto front* as edges of feasible regions of specific properties, for which no better design can exist for one property without degrading the other properties. In Figure 3.3, a two-dimensional nondominated front is shown. This graph has a Pareto front in the lower-left corner of the plot since this is the optimum area for the objective functions 1 and 2 (de Vos, 2018). The objective functions, as defined by de Vos (2018), are discussed in section 3.4 and section 3.5.

#### 3.3.2 Design Space Exploration: Application in ATG Tool

Three constraints are added to the declarations in subsection 3.2.1 to reduce the design space. There are two reasons to decrease this design space’s size: to reduce the required computing power and remove nonsensical physical topologies of the distribution system. The constraints are:

1. The connections must be physically possible; no fluid system linked to a high voltage cable. This constraint is based on declaration 2.

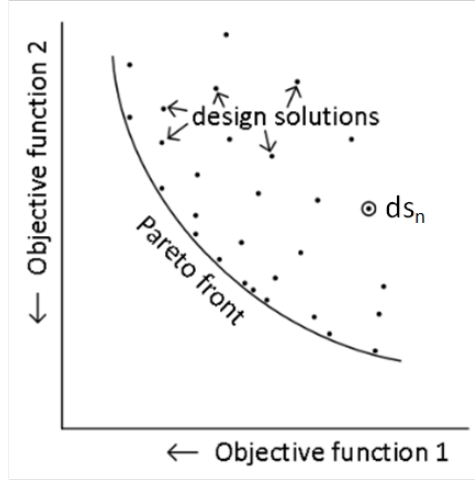


Figure 3.3: Design Space Exploration: Two-Dimensional Pareto Front in Lower Left Corner Based on Two Objective Functions , adapted from de Vos (2018)

2. Converters cannot be linked to other converters, which means that all flow passes at least one hub. Direct connections between converters do exist, such as two pumps in series. Combined components are regarded as a single node within this approach.
3. The system must be a connected graph.

Figure 3.3 shows a sketch of the two-dimensional design space, including the Pareto front, representing this research. In this design space, all solutions  $ds_n$  represent a specific system configuration.

### 3.3.3 Automatic Topology Generation Tool

The automatic topology generation (ATG) is used to fill a design space, in line with the constraints and declarations mentioned before. Each solution is a complete system topology (Figure 3.2), represented by a single point in the design space in Figure 3.4. The ATG tool combines the topological model of the system with a *genetic algorithm*. All topologies have the same number of nodes because the number of nodes is an input value for the ATG tool. With the generation  $n - 1$  of topology solutions, a generation  $n$  is generated, which approaches the Pareto front in the lower left corner slightly.

This method is based on two objective functions; these form the design space in which the Pareto front exists. The first function is the *system claim*, which represents the system costs, weight, volume and operability. The second function is the system robustness, consisting of the system weakness and recoverability.

## 3.4 Objective Function I: System Claim

The first function is the *system claim*, which represents the *system costs, weight, volume and operability*. It is assumed that the system claim can be reduced by minimising the number of nodes and the number and length of edges. The first system claim function can be found in Equation 3.1. To understand this function, the *adjacency matrix* and *distance matrix* are first introduced.

**Adjacency Matrix** Two nodes that are the endpoints of a specific edge are called adjacent. The adjacency matrix  $A(G)$  contains the entry  $a_{i,j}$  that provides the number of edges from node  $i$  to node  $j$  (West, 2001). In case of a simple matrix, it contains the weight of an edge instead of the number of edges. The labelling of the nodes and edges is done arbitrarily and influences the adjacency matrix of the graph. The adjacency matrix is symmetric as long as the graph is not a directed graph and has  $n$ -by- $n$  entries, in which  $n$  represents the number of nodes.

**Distance Matrix** The distance  $d_{ij}$  between nodes  $i$  and  $j$  is the minimum number of edges in series that forms the path between the two nodes. The graph matrix containing all distances  $d_{ij}$  is called the *distance matrix*. The diameter of a graph is the maximum of all distances  $d_{ij}$ ; therefore, this is also called the *longest shortest path*.

The number of edges can be found using nonzero values in the adjacency matrix  $A(x)$  of the generated

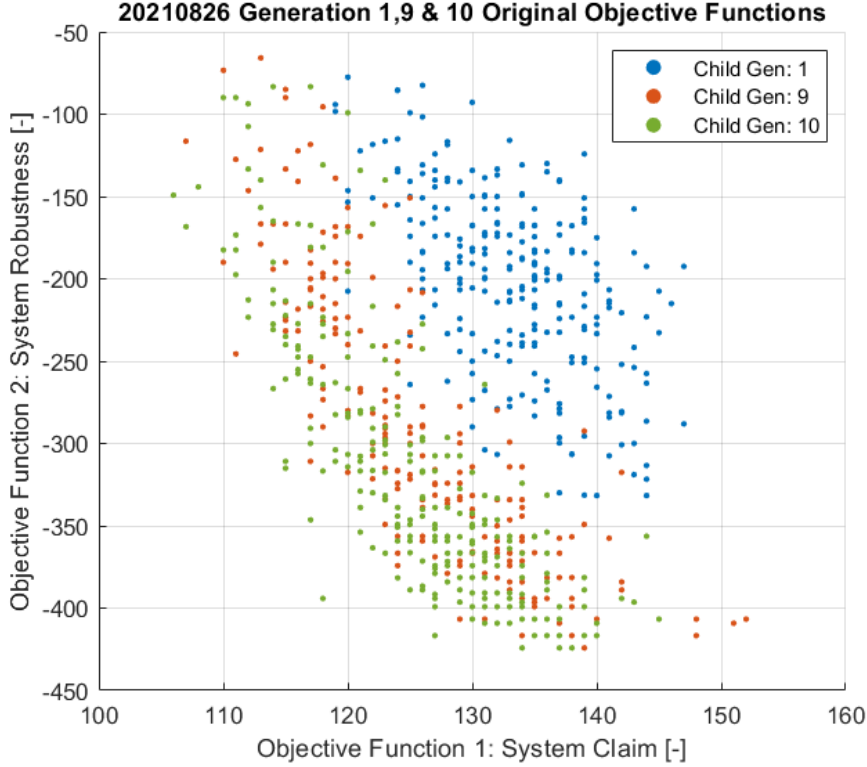


Figure 3.4: Design Space Exploration: Results of Application ATG Tool, adapted from [de Vos \(2018\)](#). Note that a lower F2 value is considered "better"

system topology  $x$ . This number is divided by 2 to compensate for the fact that all edges appear twice in the matrix ( $A_{ij} = A_{ji}$ ). The number of nodes  $nn$  is added to the total number since this an input variable for the ATG tool. [Equation 3.1](#) is only applicable for undirected systems. In case of directed systems, the upper right triangle half of the adjacency matrix can be used when the nodes are ordered starting in the upper left corner of [Figure 3.2](#). The lower boundary of this function  $f_1$  is limited because the system must remain a connected network (constraint 3).

$$f_1 = \min \sum_{i=1}^{nn} \sum_{j=1}^m \frac{A_{i,j}}{2} + nn \quad (3.1)$$

A second option only focuses on the cumulative distance between all nodes, using the minimal length of the distance matrix  $D(x)$  of generated system topology  $x$ . Only values for the distance matrix for which the upper triangle (*triu*) of the adjacency matrix has nonzero values are included in the calculation, shown in [Equation 3.2](#). The ATG-tool continues with the first, simplified, system claim function instead of this spacial system claim function, since this second function requires more information while barely increasing the accuracy of the overall system claim.

$$f_1 = \min \sum_{i=1}^{nn} \sum_{i=1}^m D(\text{triu}(A_{i,j} > 0)) \quad (3.2)$$

### 3.5 Objective Function II: System Robustness

The second function is the *system robustness*, representing the *system weakness and recoverability*. Robustness can be approached from different perspectives. This method approaches system robustness design from three points of view: design for maximum robustness, design for maximum reconfigurability and design for minimum vulnerability.

### 3.5.1 Design for maximum robustness

Design for maximum robustness contains two components: vulnerability and recoverability. A comprehensive study for the definition of robustness can be found in [section 2.4](#). Not all methods used to quantify robustness can simply be applied to ship systems since they do not differentiate between hub type nodes and converter type nodes.

### 3.5.2 Design for maximum reconfigurability

This method's goal, also called the max-flow-between-hubs approach, is increasing the system reconfigurability by increasing the number of disjoint paths between hubs. This method is based on the maximum flow graph measure but only applied to hub-hub connections instead of to all network connections.

**Maximum Flow** According to [Roughgarden \(2016\)](#), maximum flow can only be applied to graphs complying with the following conditions:

- Graph  $G$  is a directed weighted graph with nodes  $V$  and directed edges  $E$
- Graph  $G$  contains a single source node  $s \in V$
- Graph  $G$  contains a single sink node  $t \in V$
- All edges  $e \in E$  have a non-negative and integral capacity

The goal of this measure is to determine the maximum flow that can take place from the source node to the sink node. The maximum capacity of the edges limits this maximum value. In [Figure 3.5](#), the actual flow is shown (in brackets) behind the edge's maximum capacity. The orange, yellow, and light blue arrows indicate the different flow paths, using the edges' full capacity within the graph.

In [de Vos \(2018\)](#), the maximum flow of an undirected graph is determined, which does not comply with the conditions stated by [Roughgarden \(2016\)](#). However, [de Vos \(2018\)](#) used node differentiation to distinguish source nodes, user nodes and hub nodes, which is a distinction made by [Sydney et al. \(2008\)](#) as well (apart from the hub nodes). This distinction remedies non-compliance with the conditions mentioned above.

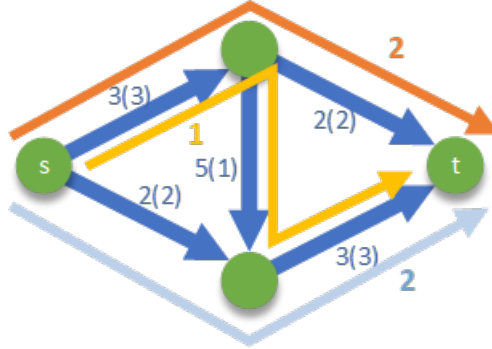


Figure 3.5: Maximum Flow between source node  $s$  and sink node  $t$

[de Vos \(2018\)](#) applies the MATLAB function `mf=maxflow(G,s,t)`, which returns the maximum flow between the nodes  $s$  and  $t$ . This function does not require differentiation between the head node and the tail node, and therefore does not require a directed graph  $G$  as input. However, the source node and sink node must be defined for this function to work. The maximum flow is applied using [Equation 3.3](#).

$$\begin{aligned}
 A_{2_{i,j}} &= \frac{\max \text{ flow } (A_{1(i,j)})}{nh-1} \\
 p(hl) &= \frac{\sum_{i=1}^{nh} \sum_{j=1}^{nh} A_{2_{i,j}}}{nh(nh-1)} \\
 f_2 &= \min \left( - \sum p \cdot 100 \right) - \frac{nh}{nn} \cdot 100
 \end{aligned} \tag{3.3}$$

In this equation,  $A_1$  is a reduced adjacency matrix in which only the hub-hub connections remain nonzero. At the same time, all other entries have are zero.  $nh$  is the number of hubs within a certain layer,  $p(hl)$  gives a value per hub layer  $hl$  of the number of connections between hubs. More connections are considered more important in hub layers with fewer hubs; therefore,  $p(hl)$  decreases with a high number of hubs. In the final equation for  $f_2$ , the total number of hubs is divided by the total number of nodes.

### 3.5.3 Design for minimum vulnerability

This method is based on the percolation theory: how does a system react to a node or edge removal from the system. In this *hurt-state-percolation* method, some nodes are labelled vital, which creates an incentive for a topology generation tool to generate more edges near these nodes. Figure 3.1 shows the system's response curve with the system's capability at the y-axis. The slope and lowest point of the primary damage are dependent on the vulnerability of the system. The recovery is, obviously, dependent on the recoverability of the system.

## 3.6 Case Study and Verification Study

The ATG Tool is applied on three different sets of network systems: case study I, case study II and a verification study. The second case study, a distribution system on-board an ocean-going patrol vessel, is not further analysed within this report and will therefore be disregarded.

### Case Study I: Frigate

The system contains one end user: a weapon on a navy ship. In general, a system contains more users than suppliers, and the number of hubs is in the order of magnitude of the number of suppliers. This means that based on network properties, three node types can be distinguished: suppliers (few nodes, few connections), hubs (few nodes, many connections) and users (many nodes, few connections).

The first case study emphasises the system as an undirected network, which leads to a symmetric adjacency matrix. The choice for an undirected network is made because, in early-stage ship design, having a connection is more important than the flow direction. A second network property is that the number of nodes and the node functions are constant for all generated topologies; the variation is caused by the number and location of the edges.

### Verification Study

The verification of the objective functions  $f_1$  and  $f_2$  is done using the series of system architectures as shown in Figure 5.1a to Figure 5.4c. The distribution systems are converted to the graphs as shown in Figure 5.1b to Figure 5.4d to analyse them using the ATG tool. The network properties of this verification set are discussed in section 5.1.

According to Klein Woud & Stapersma (2016), the systems are ordered from most vulnerable and not-reconfigurable to less vulnerable and more reconfigurable (apart from the first system). The max-flow-between-hubs part of the objective function does not conform to the intuitive robustness sequence. The influence of the number of hubs is greater than is accounted for within the normalisation. To conclude, the author states that the max-flow-between-hubs objective function is of value when considering different distribution systems with a fixed number of hubs.

## 3.7 Conclusion

This chapter can be split in two parts: topology generation and robustness calculation. The topology generation is based on design space exploration with boundaries defined using three declarations; this generation is not part of this study apart from providing the input. The sample set in chapter 7 is a topology set generated by the ATG Tool. Furthermore, the system robustness measure explained in section 3.5 is verified for an extended verification set and for an adapted frigate case study. The verification is done using a robustness approach which complies with general graph theory assumptions; only the case study is in line with these assumptions.

## Chapter 4

# Framework for Computing Topological Network Robustness

The aim of the robustness approach by [Van Mieghem, Doerr, et al. \(2010\)](#)<sup>1</sup> is to define the concept of robustness in such a way that it can be used in all research areas in which network theory is being used. The author's definition of robustness is "a measure of the network's response to perturbations or challenges (such as failures or external attacks) imposed on the network".

Before the calculation of the  $R$ -value is explained in [section 4.2](#), this chapter starts with the applied network properties in [section 4.1](#). A side track of the  $R$ -value calculation is described in [section 4.3](#), including the motivation for not including this part in further research. The graph measures required to calculate the robustness can be found in [section 4.4](#). This section introduces the graph measures, their physical meaning and the theoretical background used for the application in [chapter 6](#) and [chapter 7](#). The final section, [section 4.5](#), provides a summary of the robustness approach by [Van Mieghem, Doerr, et al. \(2010\)](#).

### 4.1 Network Properties

The network architecture at the base of this framework is described in [subsection 2.3.2](#); a distinction between *network service* and *network topology* is made in the description and analysis of a network, as shown in [Figure 2.6](#). In [subsection 2.3.3](#), it is briefly mentioned that the network topology layer of the network model by [Van Mieghem, Doerr, et al. \(2010\)](#) does not contain directed links. According to [Van Mieghem \(2018\)](#), the graph representing the network topology consists of a set  $\mathcal{N}$  of  $N$  nodes and a set  $\mathcal{L}$  of  $L$  links in which each link connects two different nodes. This implies that the graphs considered are *simple graphs*; they cannot contain multiple edges or loops ([Bollobás, 1998](#)). A simple graph can be represented by a *symmetric adjacency matrix*, in which only the link existence is specified. [Van Mieghem \(2018\)](#) considers the direction of a link as additional information to the usage, and therefore not part of the graph but part of the network service layer. The loss of linearity when including directed links in the topology layer is added as an additional advantage of excluding directionality from the scope by this author.

### 4.2 R-Value

The "goodness" or the robustness value ( $R$ -value) is a *performance measure that is relevant for the service* and normalised to the interval  $[0, 1]$ . Since this computing framework is meant to be applied in all network theory applications,  $R = 0$  corresponds to the absence of network "goodness" with  $R = 1$  is perfect network "goodness". It is important to realise that the  $R$ -value does not represent a chance of failing; it is merely an abstract goodness measure. One could compare the use of the robustness value with the second objective function ([de Vos, 2018](#)) as defined in [section 3.5](#). The values of this robustness objective function (graphically represented in [Figure 3.4](#)) can be used to perform a comparison between systems but do not have a meaning in itself.

A perturbation is a series of  $n$  *elementary changes* to which the sequence  $\{R[k]\}_{0 \leq k \leq n}$ . A challenge

---

<sup>1</sup>The main source of [chapter 4](#) is [Van Mieghem, Doerr, et al. \(2010\)](#) unless explicitly stated differently

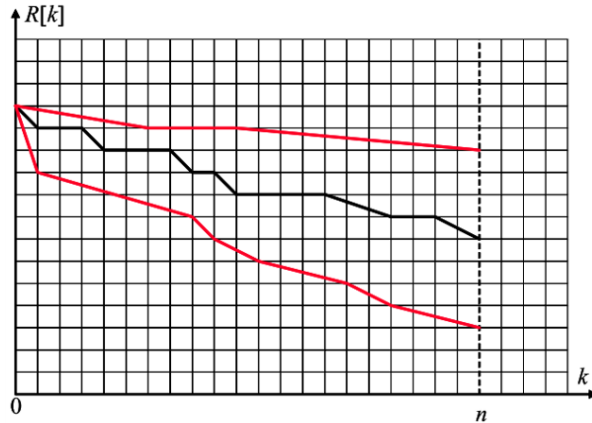


Figure 4.1: A sketch of three realizations of a perturbation of a network consisting of  $n$  elementary changes: the middle curve is a random realization, while the upper and lower curves reflect the maximum and minimum of (possibly several) extreme realizations (Van Mieghem, Doerr, et al., 2010)

can be a complex change in a network. Van Mieghem, Doerr, et al. (2010) assumes that any challenge comprises a series of elementary changes that happen one at a time. Elementary changes consist of six types of modifications:

1. Adding a node to  $G$ ;
2. Removing a node from  $G$ ;
3. Adding a link to  $G$ ;
4. Removing a link from  $G$ ;
5. Rewiring a link in  $G$ ;
6. In weighted graphs, changing the link (and/or node) weight

If no perturbation takes place, the  $R$ -value at time  $t_1$  is  $R(t_1) = R(t_0) = 1$ . The perturbation as described here exists of  $n$  elementary changes, and one elementary change happens at each  $t_k$ . However, sometimes it is not known a priori the exact order of the  $n$  elementary changes. Therefore, these situations ask for a lower and upper bound of the  $R$ -value, respectively defined as  $\min(R_G[k]) = R_{\min}[k]$  and  $\max(R_G[k]) = R_{\max}[k]$ . These values are found by analysing best and worst-case scenarios at  $R[1], R[2] \dots R[n]$ . Not all those maximum and minimum values are expected in one realisation. In that case, the most extreme values of all realisations combined are used. Any random combination of  $n$  elementary changes will show a series  $R_G[k]$  between  $R_{\min}[k]$  and  $R_{\max}[k]$ . If all elementary changes are completely independent,  $R_{\min}[n]$  and  $R_{\max}[n]$  have the same value. In Figure 4.1, the different curves for the minimum, maximum and random  $R$ -values are shown. The area between the two red curves is called the perturbation envelope and can be considered the amount of risk due to a perturbation.

#### 4.2.1 Computation

The proposed computation of the robustness metric:  $R = \sum_{k=1}^m s_k t_k$  consists of two vectors of  $m$  components. The weight vector  $s$  contains  $m$  components which reflect the importance of the corresponding values in the topological vector for the service. Therefore, the  $R$ -value computed using a specific weight and topology vector is applicable to a single service performed by the network. To compute the total  $R$ -value of a network for all services, the  $R$ -values per service  $R_{S_1}, R_{S_2}, \dots, R_{S_K}$  are summed with a weight factor per service:  $R = w_1 R_{S_1} + w_2 R_{S_2} + \dots + w_K R_{S_K}$ .

The topology vector  $t$  contains  $m$  components that characterise the topology or graph, such as average hop-count, minimum degree, or algebraic connectivity. Since a high  $R$ -value corresponds to high robustness, the components  $t_k$  need to reflect this by having a higher value in case of higher robustness.

The constrained model  $R_C = 1_{\{\cap_{k=1}^m t_k \in [t_{\min;k}, t_{\max;k}]\}} \sum_{k=1}^m s_k t_k$  adds confinements or constraints to the topological metrics.  $R_C = R$  if all  $m$  considered topological metrics satisfy the minimum and maximum levels. This  $R_C$  definition avoids that high values of some topological metrics may compensate unacceptably low values of other topological metrics, still leading to an  $R$ -value that passes the overall requirement  $R_{thresh}$ .

## 4.2.2 Normalisation

The  $R$ -value is normalised by taking the  $q$ -norm of the weight vector  $s$  and the topology vector  $t$ . The variable  $q$  is a positive integer, usually  $q = 1, 2$  or  $\infty$ . The  $q$ -norm is defined as  $\|x\|_q^q = \sum_{k=1}^m x_k^q$ , in other terms  $\|x\|_q = \sqrt[q]{x_1^q + x_2^q + \dots + x_m^q}$ . If  $q = 1$ , the  $q$ -norm provides the sum of the absolute values in the vector, while a  $q$ -norm of  $q = 2$  provides the length of the vector. A  $q$ -norm of  $q = \infty$  gives the largest value of the vector. With a  $q$ -norm of  $q = 3, \dots, \infty - 1$ , the largest value of the vector becomes increasingly important with an increasing  $q$ -value. This can prove useful but makes the topology constraint values of the constraint model increasingly influential of the  $R$ -value.

With the  $q$ -norm defined, the  $\tilde{R}$  can be calculated, which is the unnormalised form of the  $R$ -value.

$$|\tilde{R}| \leq \|s\|_q \cdot \|t\|_q \quad (4.1)$$

from which normalisation follows as

$$0 \leq R = \frac{|s^T t|}{\|s\|_q \cdot \|t\|_q} \leq 1 \quad (4.2)$$

For this study, the  $q$ -norm is set to be 2, which is the "standard" normalisation approach and the Euclidian norm. The separate inputs for the topology vector  $|t|$  are the normalised graph measures; the normalisation of these measures is explained in [subsection 5.2.7](#).

## 4.3 Temporal Aspects

The  $R$ -value contains time-dependent and time-independent aspects. Within part II of this report, only the time-independent aspects are used. However, the explanation of this robustness framework is not complete without mentioning the three time-dependent robustness comparison approaches and the recoverability.

### 4.3.1 Elementary Change

As mentioned before, the two main goals of a framework to compute robustness are: improving a network to achieve a desirable level of robustness and comparing different networks on robustness. Three criteria can be used to compare different graphs on robustness. For these criteria, the initially connected graphs  $G_1$  and  $G_2$  are used, with respective initial  $R$ -values of  $R_{G_1}[0]$  and  $R_{G_2}[0]$ .

#### Criterion 1: Envelope Overlap

When the lowest extreme of  $G_1$ ,  $R_{G_1, \min}[k]$ , is always larger than the highest extreme of  $G_2$ ,  $R_{G_2, \max}[k]$ , graph  $G_1$  is said to be more robust than graph  $G_2$  with respect to perturbation  $P$  and metric  $R$ . In this case the envelopes do not overlap, for example in case that the perturbation  $P$  is an elementary change ( $n = 1$ ).

#### Criterion 2: Partial Envelope Overlap

If there exists an overlap between both robustness envelopes, the first criterion cannot be applied. A second criterion is defined for those more common cases, using the sum over all  $R$ -values per graph. Since the comparison is based on all possible realisations of perturbation  $P$ , those realisations' expectation is used. This means that if  $E[r_{G_1}[n]] > E[r_{G_2}[n]]$  with  $r[k] = \sum_{j=0}^k R[j]$ , graph  $G_1$  is said to be more robust than graph  $G_2$  with respect to perturbation  $P$  and the metric  $R$ .

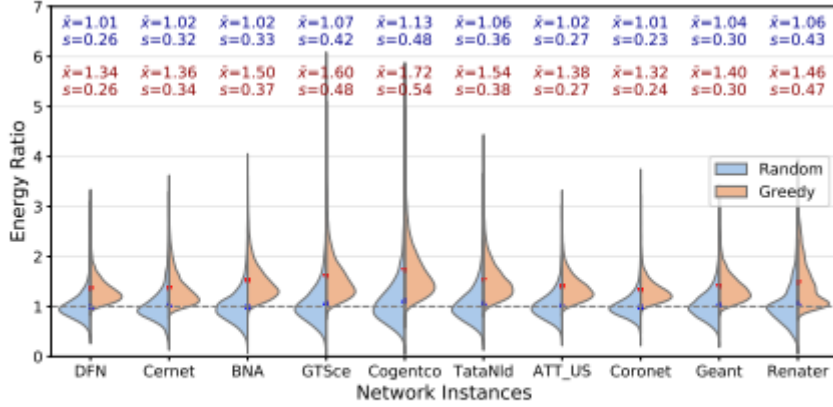
#### Criterion 3: Hitting Time

The hitting time is denoted by  $k_j$ , with  $R_{G_j}[k_j] = \rho$  and  $\rho$  being some threshold value  $R(t) = \rho$ . If  $k_1 > k_2$ , the graph  $G_1$  is said to be more robust than graph  $G_2$  with respect to perturbation  $P$  and metric  $R$ .

### 4.3.2 Recoverability

The robustness approach by [Van Mieghem, Doerr, et al. \(2010\)](#) is used by [He \(2020\)](#) to define *network recoverability*<sup>2</sup>. The definition of network recoverability is 'the ability of a network to return to a desired performance level after suffering malicious attacks or random failures'. Two recovery scenarios are analysed: the recovery of damaged connections on the one hand and any disconnected pair of nodes can be connected on the other hand. For example, the first scenario applies to virtual circuits, while the

<sup>2</sup>The primary source of this section is [\(He, 2020\)](#) unless explicitly stated differently



(c) Scenario B:  $r_G^{-1}$

Figure 4.2: Probability density of energy ratio's of different communication networks (He, 2020)

second approach can be used for physical (communication networks). The attacks, i.e. the elimination of edges, is done until  $R$  reaches the threshold value of  $\rho = 0.8$ . At that moment, the recovery process starts and edges are added to the system.

### Energy Ratio

The energy ratio  $\eta_{E(G,\rho)}$  is an indicator to measure compensation of the recovery process for the attack process. The recoverability indicator used is the robustness energy  $S(G,\rho)$ , which is the sum of the  $R$ -values during the attack or recovery process. The calculation of the energy ratio and the robustness energies can be found in Equation 4.3.

$$\begin{aligned}
 S_a(G,\rho) &= \sum_{k=0}^{K_a} (1 - R[k]) \\
 S_r(G,\rho) &= \sum_{k=0}^{K_a} (R[k] - \rho) \\
 \eta_E(G,\rho) &= \frac{S_r}{S_a}
 \end{aligned} \tag{4.3}$$

In this equation,  $K_a$  is the number of *attack challenges*; the number of edges that are, one-by-one, being removed from the system. If the energy ratio is higher than 1  $\eta_{E(G,\rho)} > 1$ , the recovery measures can compensate for the loss of network performance. This means that a system with a higher energy ratio has a higher network recovery capability. Since the order in which the edges are removed influences the  $R$ -value, an envelope of the attack and recovery processes can be created.

### Recovery Strategies

The main goal of this recovery model is approaching a real system; therefore, the attacks are considered random attacks. This assumption is simplified by considering the attacks as uniform and independent. However, the recovery process can be influenced, three possible recovery strategies:

- *Random recovery*: The order of recovered edges is random. This strategy follows the same analogy as the attack strategy.
- *Metric-based recovery*: The goal of this strategy is to improve a specific graph metric, such as algebraic connectivity or the minimum degree. This strategy can prove useful in restoring vital edges or bottlenecks.
- *Greedy recovery*: In the greedy recovery strategy, the damaged element (node or edge) which improves the network performance most has the highest priority to be recovered; adding an edge that makes the  $R$ -value increase most in each challenge. This recovery strategy is considered practical and intuitive.

This research shows that the  $R$ -value increases most when using a greedy recovery strategy. Figure 4.2 shows the probability density of energy ratio  $\eta_E$  of different communication networks. The violin graphs show a higher mean energy ratio for greedy recovery than for random recovery, which suggests a higher recovery capability of the network.

### 4.3.3 Scope Concerning Time-Related Concepts

As mentioned in the introduction of this section, time related concepts are not part of this thesis research. Only the network at  $t = 0$  is analysed, this is where the limits of the study are placed. A discrete time-domain simulation is an interesting following up step for this research. However, the time-independent robustness measures are first analysed before adding the additional time-variable to the analysis.

## 4.4 Graph Measures

The  $R$ -value, as introduced in [section 4.2](#), is a measure for the network “goodness” or robustness. However, it does not have a physical meaning in itself, e.a. it is a measure used to compare different networks and their robustness. On the other hand, the  $m$  graph measures within the topology vector  $t$  represent a less abstract (sometimes even physical) concept. A selection of graph measures and their physical meaning is described in this section. The physical meaning is focused on the robustness criteria as described in [subsection 2.4.3](#): independent subsystems, redundancy and reconfigurability. This graph measure collection aims to create and analyse a broad general used field of graph measures but is in no sense a complete or ideal collection of measures, the following graph measures are discussed:

- Degree
- Connectivity
- Modularity
- Eccentricity
- Cycle Basis
- Effective Resistance

### 4.4.1 Degree

The first and most fundamental graph measure is the node degree, for which the local measure is reduced to a single global graph measure using the mean value. This measure is introduced in [section 3.4](#), where it functions as the base of the system claim objective function. The network degree distribution or mean degree is related to robustness or reliability because a node with more links can be reconnected in different ways in case of damage or failure. The edge connectivity and the  $degree_{hub-hub}$  are similar measures, however, the single point of focus of both measures is different. While the edge connectivity purely focuses on the weakest link, the mean hub-hub degree takes all hub node degrees into account, using the reduced hub graph explained below and shown in [Figure 4.3b](#). In case of directed networks, two types of degree can be considered: *in degree* and *out degree*. The names of these measures are self-explanatory, respectively the number of edges directed to a node and the number of edge originating at a node. The mean value of the in degree and out degree over the total network and over the reduced hub network is identical because all edges begin and end at a certain node.

**Degree & Degree Matrix** The degree of a node is the number of incident edges of the node ([West, 2001](#)). In case of a loop, the same node is the endpoint of an edge twice, which gives it a degree of 2. The degree matrix  $D(G)$  is a  $n$ -by- $n$  matrix with the degree of the nodes at the diagonal. With a directed graph, the degree matrix can be filled with either the indegree or the outdegree of the nodes, dependent on type of graph analysis. The degree matrix of a directed graph could be considered as an undirected graph degree matrix as well.

### 4.4.2 Connectivity

A distinction can be made between the three types of connectivity. The first connectivity,  $\kappa$ , is a binary value that determines whether a graph is connected  $\kappa = 1$  or unconnected  $\kappa = 0$ . Within a connected graph, as mentioned before, all pairs of nodes are connected by edges through a particular path. The second connectivity is vertex connectivity  $\kappa_v$ ; this is the minimum number of nodes that need to be removed from a connected graph to become unconnected. Edge connectivity  $\kappa_e$  follows the same analogy, i.e. the minimum number of edges that have to be removed. [Ellens & Kooij \(2013\)](#) states that, in general, a higher node or edge connectivity means a more robust graph. The minimum value within the degree matrix,  $\delta_{min}$ , can be used to determine the upper bound of the connectivity measure, as shown in [Equation 4.4](#).

$$\kappa_v \leq \kappa_e \leq \delta_{min} \quad (4.4)$$

Connectivity can also be approached in a probabilistic way, for example, using a *reliability polynomial*.

This polynomial  $Rel(G)$  is equal to the probability that the graph is connected based on which edges are present. Another probabilistic approach to connectivity is using *degree distribution*. Britton et al. (2006) defines  $p_k^{(n)}$  as the probability of a randomly chosen node of a set of  $n$  nodes to have degree  $k$ . With this probability, a probability distribution can be determined:  $F = \{p_k; k \geq 0\}$ . According to Britton et al. (2006), complex networks typically have a more heavy-tailed degree distribution, these types of graphs are often referred to as *scale-free graphs*.

An example is provided to explain what type of connectivity measure is used within this study: Figure 4.3a shows a complete connected ring distribution network that contains eight hubs. This and other networks are further introduced in section 5.1. Since the network is connected, the total connectivity  $\kappa = 1$ . All networks are connected, and, therefore, this connectivity measure is of little value. The same applies to the second and third connectivity measures, respectively  $\kappa_v$  and  $\kappa_e$ . However, this time the value  $\kappa_v = \kappa_e = 1$  because the removal of *one* specific node or edge reduces the graph to an unconnected graph. The graph analysed is, therefore, not the complete graph but the reduced hubgraph. This graph only contains the hub-hub connections and disregards all but the hub nodes and edges, which is displayed in Figure 4.3b. Because most supplier and user nodes are connected to a single hub, the connection of this hub to other hubs plays an essential role in the total reliability of the network. The analysed connectivity measure,  $\kappa_{e, hub-hub}$ , rates the reconfigurability of the network. In case of a single edge failure, a *hub-hub edge connectivity*  $\geq 1$  means that the hub does not fail. Dependent on which edge, only one supplier or user might stop functioning, but the damage remains limited.

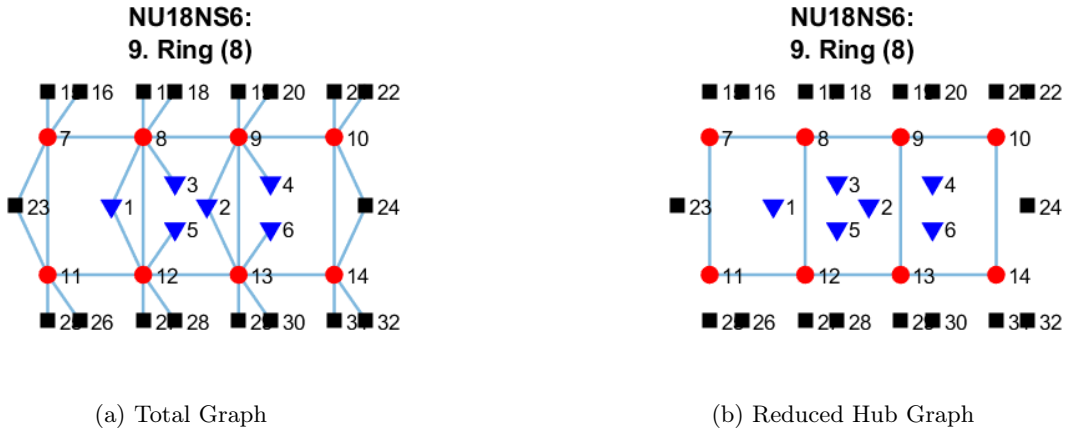


Figure 4.3: Ring Distribution NU18NS6 (8 hubs, 18 users, 6 suppliers)

### 4.4.3 Modularity

Modularity is a global graph measure representing the extent to which a graph can be divided into clearly separated communities (Mijalkov et al., 2017). These separated communities are based on a previously determined community structure. Since this structure is constructed manually, the separated communities can be defined as *independent subsystems*. Currently, one of the main applications of modularity as graph measure is within brain studies, specifically concerning Alzheimer's Disease (Brier et al., 2014). Modularity is large when nodes are maximally connected within a subsystem but minimally connected between communities, this value decreases over age and during the advanced stages of the disease. It can be calculated using Equation 4.5 in which  $E$  is the number of edges in the graph,  $A_{ij}$  the connectivity or adjacency matrix,  $d_i$  the degree of a node and  $\delta_{ij}$  is 1 if the two nodes belong to the same community and 0 otherwise.

$$\frac{1}{E} \sum_{ij} \left[ A_{ij} - \frac{d_i d_j}{E} \right] \delta_{ij} \quad (4.5)$$

### 4.4.4 Eccentricity

According to Ellens & Kooij (2013), the meaning of the diameter and average distance is that a shorter path means a more robust graph. However, backup paths are not considered within this graph measure. In line with this reasoning is the *node eccentricity*, which provides the maximum distance of a given

node to another node within the connected graph. According to [Ellens & Kooij \(2013\)](#), a more compact network has a higher efficiency and is therefore more robust.

#### 4.4.5 Cycle Basis

Cycle Bases are a compact description of the set of all cycles of a graph ([Kavitha et al., 2009](#)). A cycle is a simple graph or subgraph with as many nodes as edges ([West, 2001](#)). The nodes are placed in a way that they form a closed cycle together with the edges. A tree subgraph or graph, on the other hand, is a connected graph that does not contain cycles ([Gross et al., 2014](#)). The presence of rings or cycles within a network is considered "good practice" when it comes to reconfigurability and robustness. In [Figure 4.4](#), some graphs including the present cycles can be found. This figure shows that, in case of undirected graphs, the number of cycles is not only dependent on the hub-hub connections, but on the number of connections to supplier and user nodes as well. Therefore, the number of cycles or cycle bases can be used to analyse the redundancy and the reconfigurability within a network.

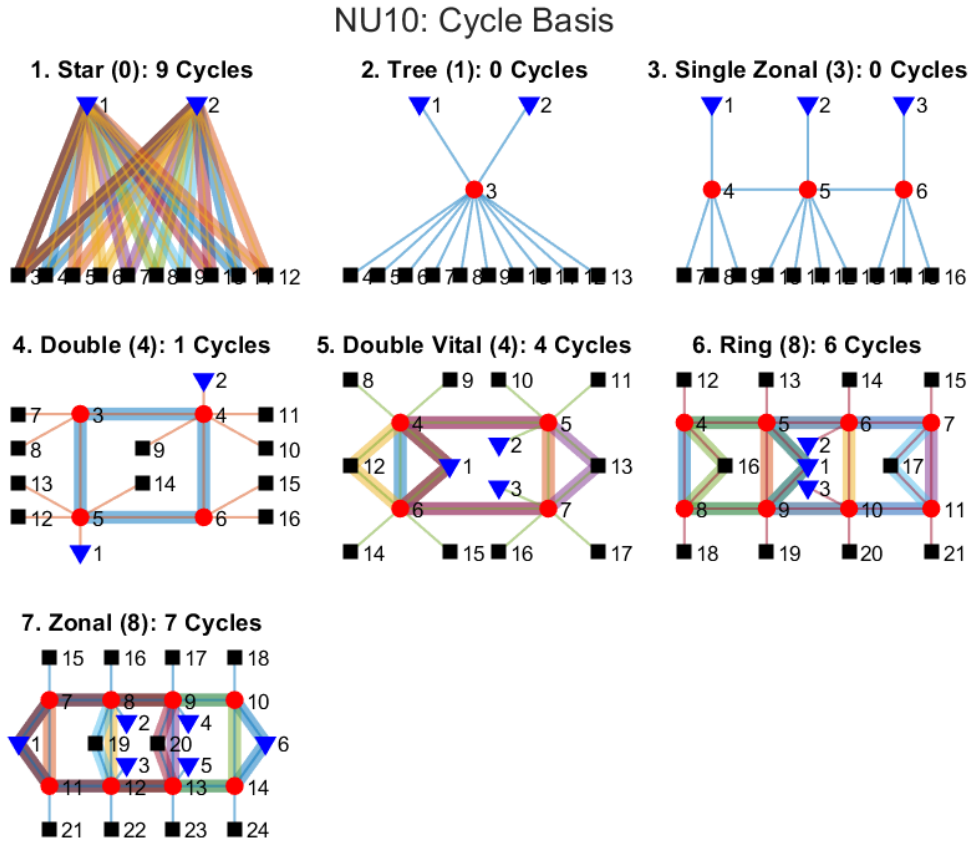


Figure 4.4: Cycle Bases of Verification Set I: NU10

#### 4.4.6 Effective Resistance

The graph measure *effective resistance* has its origin in the electrical circuits, where resistance is measured in Ohm ( $\Omega$ ). The effective graph resistance or total effective resistance or Kirchhoff index is, according to [Ellens & Kooij \(2013\)](#), the sum of the effective resistance over all given pairs of nodes. The resistance decreases when an edge is added to the graph, which means a more robust network. The effective resistance can be calculated using the eigenvalues of the Laplacian matrix. [Van Mieghem, Doerr, et al. \(2010\)](#) defines effective graph resistance  $R_G$  by [Equation 4.6](#), where  $\mu_k$  is the  $k$ th largest eigenvalue of the Laplacian matrix.

$$R_G = N \sum_{\mu_k > 0}^{N_1} \frac{1}{\mu_k} \quad (4.6)$$

## 4.5 Conclusion

First, the graph measures used within the topology vector  $|t|$  of the  $R$ -value calculation are selected based on a literature sample. The graph measures applied within this study are:

- Degree
- Connectivity
- Modularity
- Eccentricity
- Cycle Basis
- Effective Resistance

The scope of the study is further limited by disregarding the temporal aspects part of this robustness approach. These temporal aspects are elementary changes over discrete time and the recoverability. These limitations also form the assumptions required to apply the  $R$ -value on onboard distribution systems. This robustness measure is further analysed in Part II of this report.

## Part II: Network Analysis

# Chapter 5

## Network Set Introduction

The second part of this study, the network analysis, starts with this chapter. While the previous three chapters ([chapter 2](#) to [chapter 4](#)) are based on literature, the following chapters aim to extend the current knowledge by creating new insights. This first chapter of Part II, [chapter 5](#), introduces the different analysed networks: five verification sets and 12 frigate systems based on the benchmark system by [de Vos \(2018\)](#).

Verification Set I can be considered as reference set since it directly originates from [de Vos \(2018\)](#). This first network set is described in [section 5.1](#); here, the different graphs and their network properties are discussed. [section 5.2](#) introduce verification set II to V and the maximum and minimum connected sets, all used in [chapter 6](#). For [chapter 7](#), another set is introduced: the sample set. This set can be found in [section 5.3](#), followed by a general conclusion in [section 5.4](#).

To describe the different sets, certain abbreviations and symbols are used:

- $NN$  number of nodes per graph
- $NS$  number of supplier nodes per graph (**blue triangles**)
- $NH$  number of hub nodes per graph (**red circles**)
- $NU$  number of user nodes per graph (**black squares**)

The sets have been given names based on the most remarkable node properties, for example, Verification Set I or  $NU10$  includes a constant number of *user nodes*; the total number of nodes ( $NN$ ), number of hub nodes ( $NH$ ) and number of supplier nodes ( $NS$ ) is variable.

### 5.1 Verification Set in Literature

In [subsection 2.3.3](#), some examples of physical topologies are mentioned, such as mesh, star, ring and bus topology. These different topologies influence the reliability and efficiency of a given network on the logical architecture level as defined by [Brefort et al. \(2018\)](#). Three topology approaches to improve the reliability are: independent subsystems, redundancy and reconfigurability ([Woud & Stapersma, 2003](#)). The design rules (rules of thumb) as described by [Spruit et al. \(2009\)](#) are based on these approaches. [Woud & Stapersma \(2003\)](#) has defined a set of network topologies with an intuitively increasing level of reliability; e.a., based on the design rules used during actual ship design. This set functions as the basis of the five verification sets, which are further introduced in [section 5.2](#).

[Figure 5.1](#) shows the first topology: a radial distribution or star network. The corresponding graph is bipartite, meaning that it exists of two independent sets of nodes (partite sets) ([West, 2001](#)). The links or edges have one endpoint in each group, they cannot connect two nodes within the same set. This topology can be considered very efficient due to the low hop-count or the number of edges in an arbitrary shortest path in the graph [Van Mieghem, Doerr, et al. \(2010\)](#) GE. On the other hand, when considering the system claim as defined by [de Vos \(2018\)](#) in [section 3.4](#), one could find the number of edges within topology to be disproportionately large, which represents a differently defined low efficiency. Despite being the first in the set, this topology is not considered the least reliable structure; the high system claim makes it a less realistic option for most systems.

[Figure 5.1a](#) and [Figure 5.1b](#) contain two *supplier nodes*, [de Vos \(2018\)](#) standardised the number of *user*

nodes to ten for all graphs within the set  $NU10$  (directed). A second difference between the original and adapted topology is the directionality: [Woud & Stapersma \(2003\)](#) implies directed links within this topology but shows undirected links, while [de Vos \(2018\)](#), on the other hand, explicitly defined the links as directed.

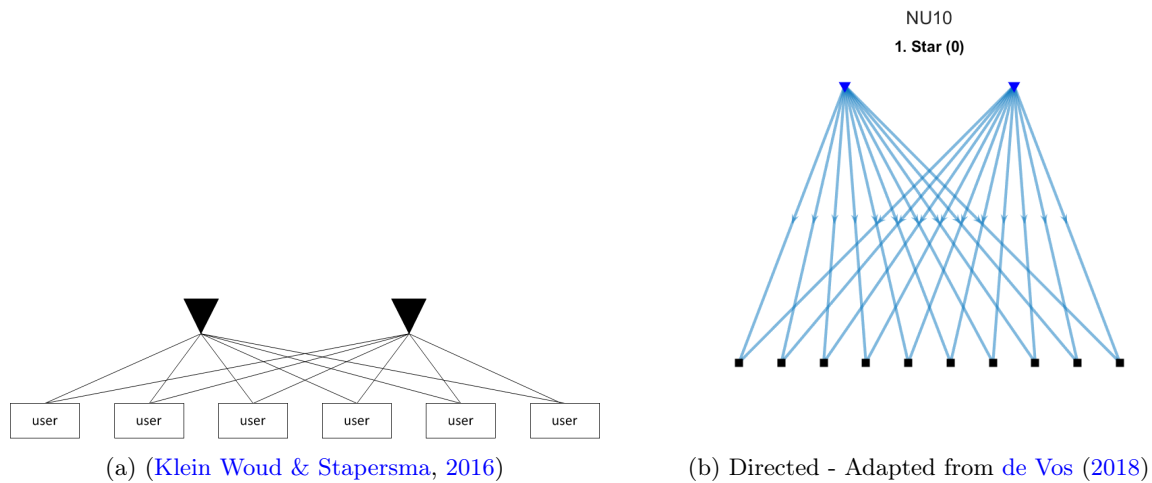
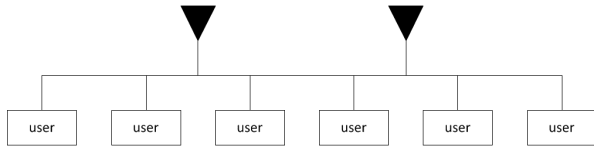
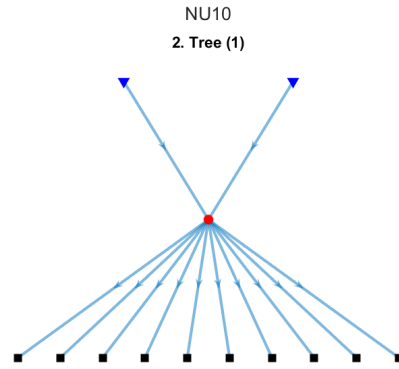


Figure 5.1: Radial Distribution (Star Network)

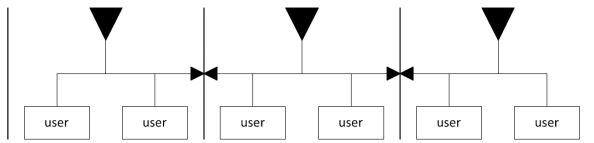
The second and third topology can be found in [Figure 5.2](#), showing a single and a single zonal distribution. [Figure 5.2b](#) first introduces the *hub node*, representing the main pipeline as drawn in [Figure 5.2a](#). This topology has a low system claim because of the centralised distribution, also causing a lower reliability through a single point of failure. The reliability can be improved by added redundancy or *independent subsystems*; separate islands that can function independently and are connected by means of standard open or standard closed valves. This system, including valves or hubs, is shown in respectively [Figure 5.2c](#) and [Figure 5.2d](#). The directed connections between the hubs are made bidirectional using a double connection, which provides additional reconfigurability to the system.



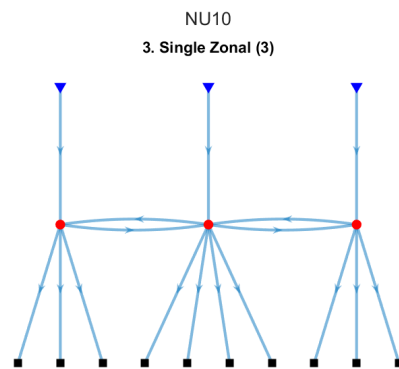
(a) Single Distribution - (Klein Woud & Stapersma, 2016)



(b) Single Distribution (directed) - Adapted from de Vos (2018)



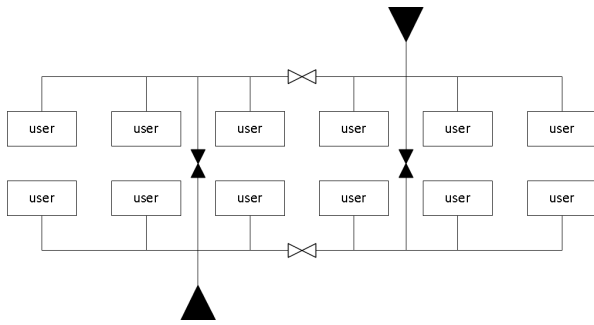
(c) Single, Zonal Distribution - (Klein Woud & Stapersma, 2016)



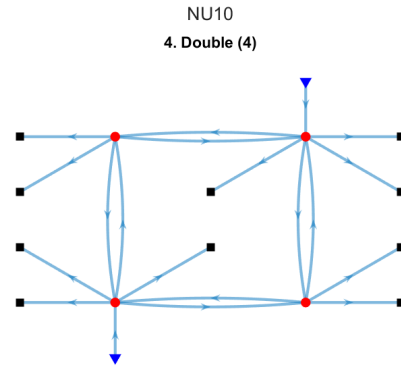
(d) Single, Zonal Distribution (directed) - Adapted from de Vos (2018)

Figure 5.2: Single Distribution (Tree Network) & Single, Zonal Distribution

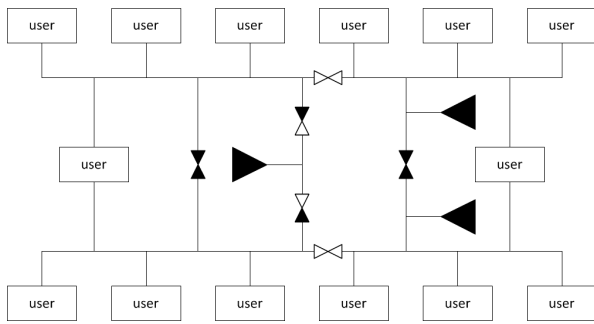
Figure 5.3 shows a distribution system with redundancy in both the set of suppliers and the set of users. Moreover, a failure can be isolated by closing off valves connecting the upper and lower part or the left and right part of the system. All users can be connected to both suppliers, which means that there is not only redundancy but also reconfigurability in case of a supplier failure. The main difference between the double distribution and the double *vital* distribution is that the two *vital users*, node 12 and 13 in Figure 5.3d, can be supplied via two different hubs. The function of the vital users can only be interrupted in case of a failure within the user component itself or if two hubs fail simultaneously.



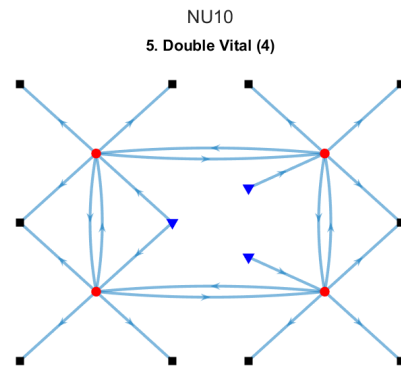
(a) Double Distribution - (Klein Woud & Stapersma, 2016)



(b) Double Distribution (directed) - Adapted from de Vos (2018)



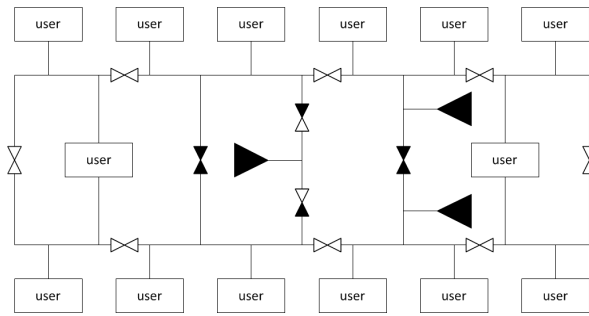
(c) Double Vital Distribution (Klein Woud & Stapersma, 2016)



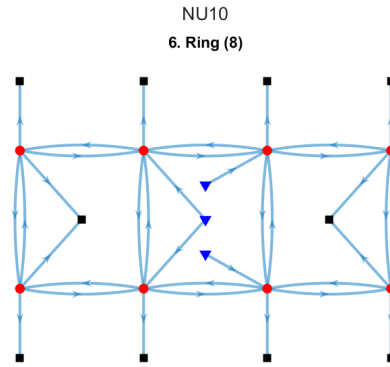
(d) Double Vital Distribution (directed) - Adapted from de Vos (2018)

Figure 5.3: Double distribution with communication between the two supply lines and separation valves - Double distribution: without and with vital and non-vital consumers and separate and combined suppliers

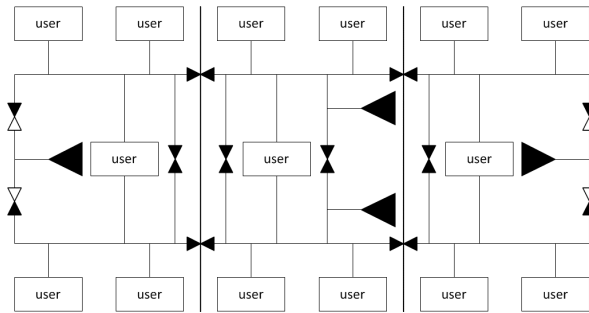
Figure 5.3c can be improved further by adding an additional connection between the lower and upper part of the system, which creates a circle or ring. The reconfigurability of a *ring distribution* is increased in comparison to the double distribution, all users are connected to suppliers via multiple paths. However, independent subsystems are less applicable within this system, since not all parts are connected to a supplier nodes. Therefore, extra supplier nodes are added, to ensure this subsystem functionality again, as shown in Figure 5.4c and Figure 5.4d. Therefore, this system is considered the most reliable system within the set.



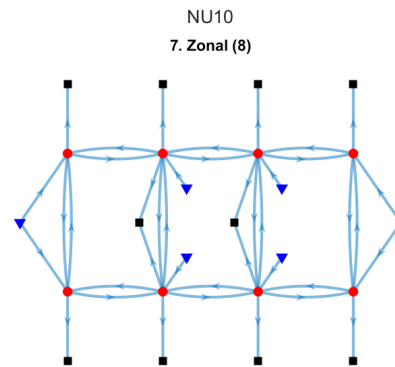
(a) Ring Distribution - (Klein Woud & Stapersma, 2016)



(b) Ring Distribution (directed) - Adapted from de Vos (2018)



(c) Zonal Distribution - (Klein Woud & Stapersma, 2016)



(d) Zonal Distribution (directed) - Adapted from de Vos (2018)

Figure 5.4: Ring and Zonal Distribution

## 5.2 Development Verification Sets

chapter 3 and chapter 4 introduce to robustness approaches, each with corresponding assumptions concerning the definition of a network or distribution system. The first verification set by de Vos (2018) is adjusted in order to analyse the assumptions in both methods. The first step of these adjustments, defining networks with a constant number of user nodes, is described in the verification study by de Vos (2018) (section 6.3).

### 5.2.1 Verification Set I: *NU10*

The set is modified from directed graphs to undirected graphs for the succeeding step, as shown in Figure 5.5. This adjustment also includes reducing the two directed edges between hub nodes to a single bidirectional or undirected edge. The main advance of the first verification set is that it remains close to the original set. However, undirected edges do not distinguish between different node types. Therefore, some graph measures might not provide a realistic value when flow travels past supplier nodes instead of merely starting at such nodes.

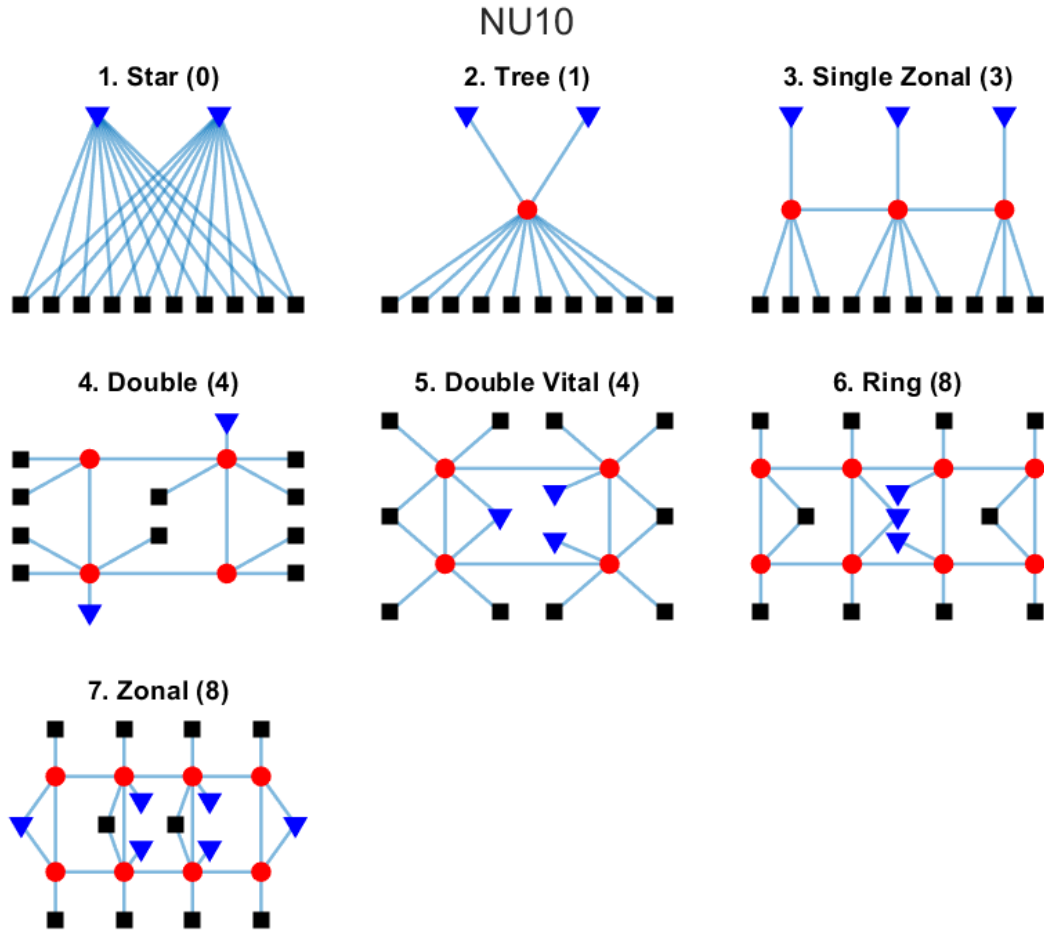


Figure 5.5: Verification Set I: Undirected Graph with 10 users and varying number of suppliers, hubs and total nodes

### 5.2.2 Verification Set II: *NN24*

According to [Van Mieghem, Doerr, et al. \(2010\)](#), one could not compare graphs with a different number of nodes when it comes to absolute graph measures. Such a comparison is being made impossible by the definition of graphs using matrices. A comparison between the eigenvalues of matrices or matrices themselves of varying sizes is like *"comparing something in different spatial dimensions"*. To overcome this limitation in the applicability of graph theory, user nodes have been added to the *NU10* set to the point that all graphs contain the same number of nodes.

In [Figure 5.6](#), an overview of this undirected set can be found. The main advantage, as mentioned before, is that it can be compared according to graph theory. However, the physical meaning and applicability of this comparison is unclear. The number of suppliers, hubs and users is varying, therefore, the network type is still not standardised. Ultimately, the system revolves around the number of users it can serve, so this number should preferably be kept constant.

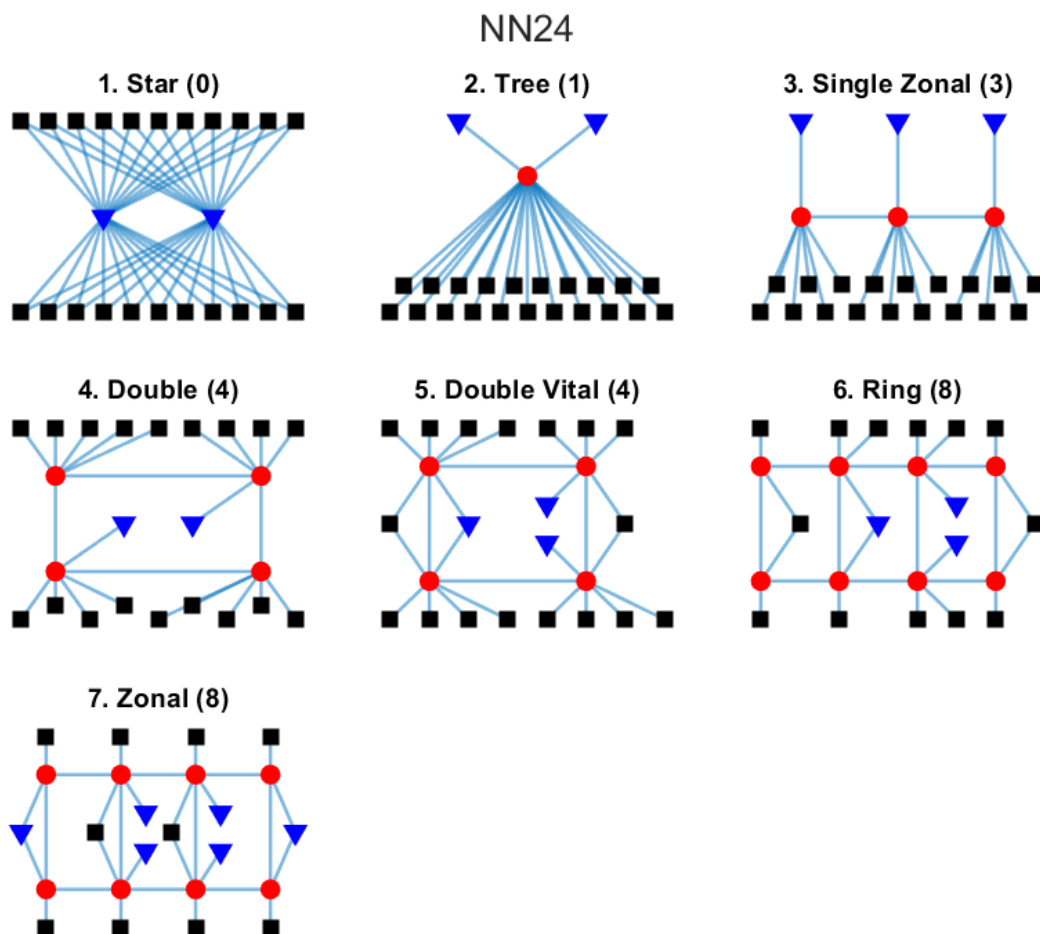


Figure 5.6: Verification Set II: Undirected Graph with 24 total nodes and varying number of suppliers, hubs and users

### 5.2.3 Verification Set III: $NN24NS6$

Like verification set II, this set has a constant total number of nodes, moreover, the number of suppliers is kept constant as well within the set  $NN24NS6$ . However, the main difference between the previous sets and this set is the addition of the graphs 3, 5 and 8. Figure 5.7 shows the set of 10 undirected graphs, the number of hub nodes is in parentheses after the graph number and name.

First, the third graph is added to provide an extra step in number of hubs between the graph 2 and graph 4. These networks are all (combined) tree networks, which are efficient concerning system claim, but vulnerable due to their single points of failure. Intuitively, the graph 4 is the most robust of the three graphs, due to the independent subsystems and increased number of nodes. This theory is tested using the added graph 3.

Second, graph 5 is meant to bridge the different structures of graph 4 and 6. While the number of hubs is constant for graph 4 and 5, it is expected that graph 5 and 6 show more similarities in behaviour due to the comparable topologies. Since graph 4 and 5 have the same node distribution and therefore a nearly equal system claim, the difference in reliability by adding a single link is considered interesting and meaningful. The final graph added, graph 8, is the least significant addition of the three added graphs. This graph is added to reduce the step in number of hub nodes, from 4 to 8 between graph 7 and 9, to an addition of two nodes per step.

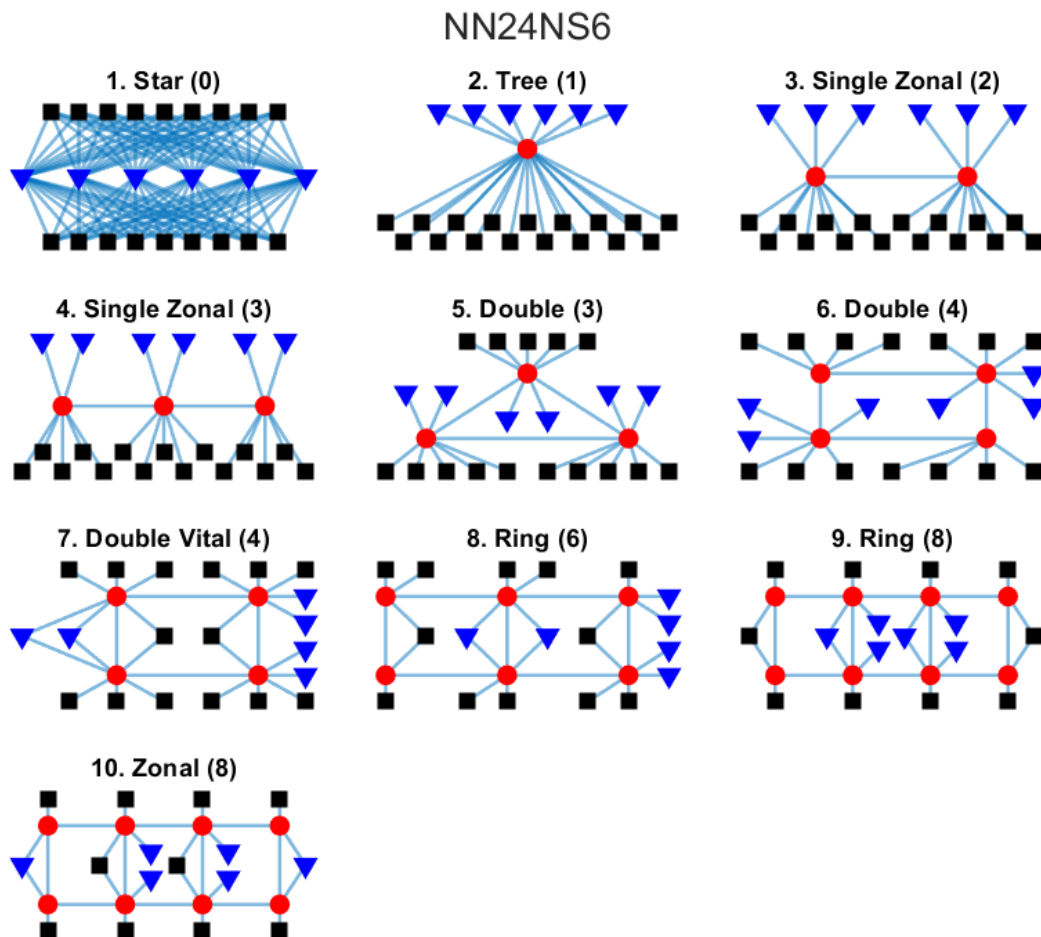


Figure 5.7: Verification Set III: Undirected Graph with 24 nodes and 6 suppliers total and varying number of hubs and users

### 5.2.4 Verification Set IV: *NU18NS6*

Circling back to the first verification set is set *NU18NS6*, since this set has once again a constant number of user nodes. The supplier nodes are kept constant as well, meaning that with a varying number of hub nodes, the total number of nodes is varying. While the mathematical meaning is less reliable, the comparison between different network topologies with a constant number of suppliers and users is a more applicable comparison for distribution systems onboard ships. The ten topologies can be found in Figure 5.8.

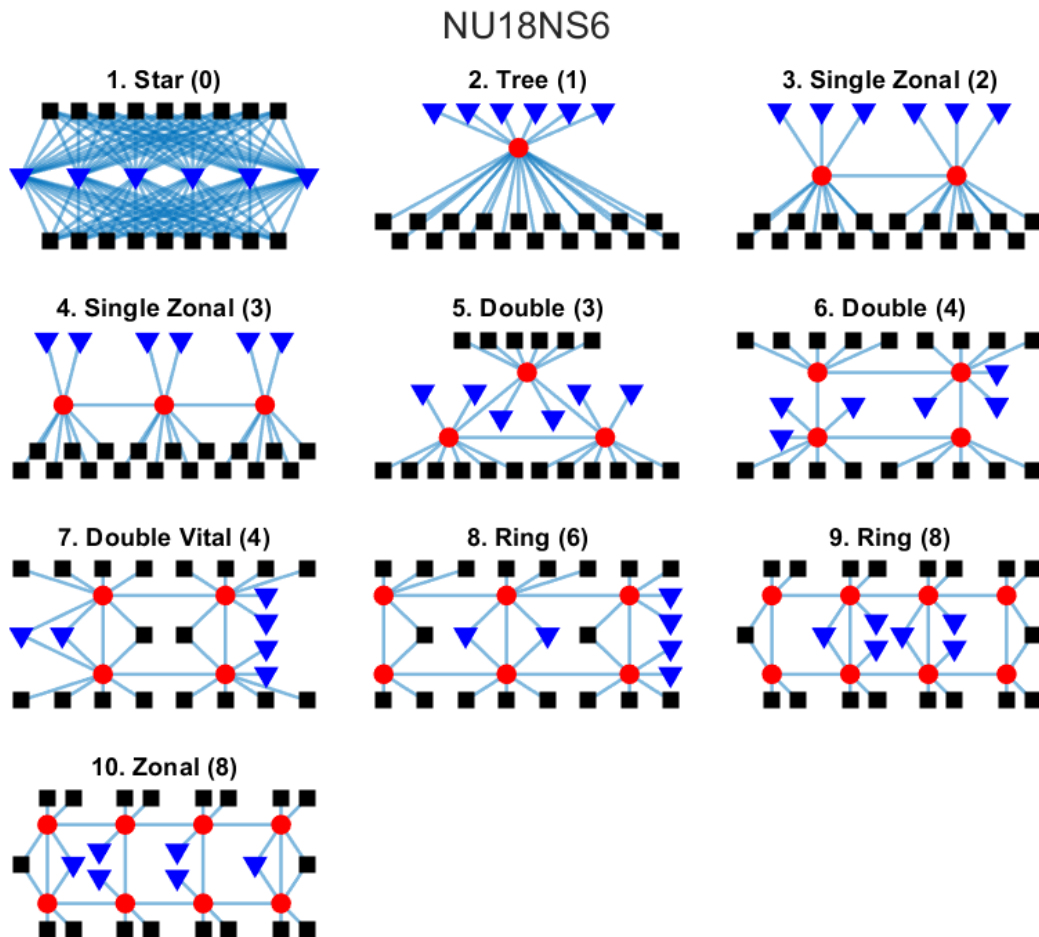


Figure 5.8: Verification Set IV: Undirected Graph with 18 users, 6 suppliers and varying number of hubs and total nodes

### 5.2.5 Verification Set V: *NH8NS8*

Set *NH8NS8* form a deviant set from the previous sets, as seen in [Figure 5.9](#). The sets is based on the zonal distribution network, graph 10, of verification set IV (*NU18NS6*). This set has a constant number of supplier, hub and user nodes, only the number of connections between hub nodes is varying. It is assumed that any link added means added reconfigurability and therefore added reliability. The number of graphs in this set is seven, the addition of three extra graphs would provide no additional information and therefore only costs computational power.

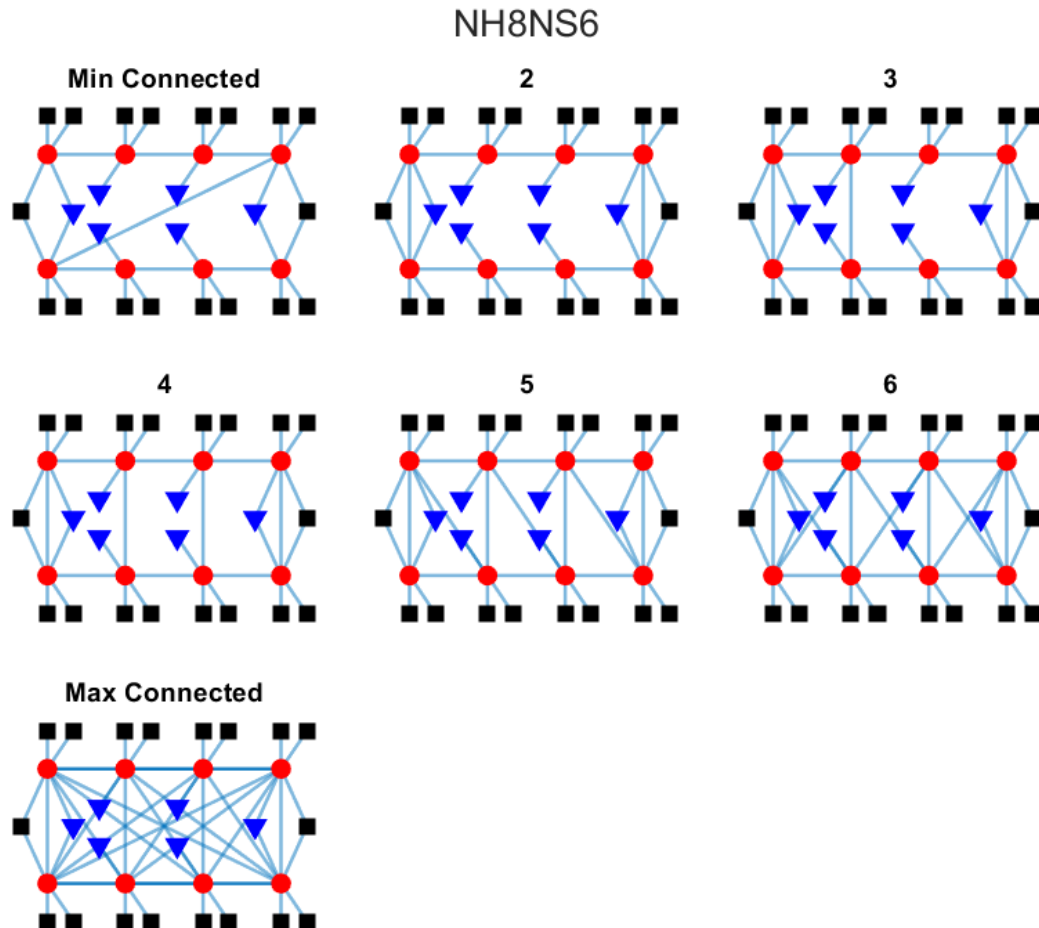


Figure 5.9: Verification Set V: Undirected Graph with 6 suppliers, 8 hubs, 10 users and 32 total nodes with varying number of connections

### 5.2.6 Overview Verification Sets

The verification sets, introduced in [subsection 5.2.1](#) to [subsection 5.2.5](#), are also depicted in [Appendix E](#). This separate insert is provided to aid the reader in understanding the figures in the next chapter, so not all sets are to be memorised by heart. In [Table 5.1](#), an overview of the properties of the network set from literature ([Woud & Stapersma, 2003](#)), the verification set by [de Vos \(2018\)](#) and the four verification sets developed can be found. Despite the notion that all five verification sets are developed as directed and undirected sets, the application in [chapter 6](#) is limited to the undirected sets. This consideration is made because the network analysis is limited to the logical architecture, which only includes the existence of edges and disregards their direction.

Verification Set	Directed	NN (number of nodes)	NS (number of suppliers)	NH (number of hubs)	NU (number of users)
Literature (KLEIN)	No	Varying	Varying	Varying	Varying
1. NU10 (Vos)	Yes/No	Varying	Varying	Varying	10
2. NN24	Yes/No	24	Varying	Varying	Varying
3. NN24NS6	Yes/No	24	6	Varying	Varying
4. NU18NS6	Yes/No	Varying	6	Varying	18
5. NH8NS6	Yes/No	32	6	8	18

Table 5.1: Overview node and edge properties verification sets

### 5.2.7 Minimum and Maximum Values

The sets from the previous section are analysed using a number of graph measures. To normalise these graph measures, minimum and maximum values must be determined, following the calculation as shown in Equation 5.1. By means of normalising the graph measure values, the normalised value is  $0 \leq GM \leq 1$  in which GM is a random graph measure. Therefore, in terms of robustness, the maximum value is considered the highest feasible value a measure can have. The minimum value represents the lowest value for which the graph remains a connected graph. For this determination, two adaptations of the five verification sets are developed: the minimum and maximum connected sets.

$$GM_{norm} = \frac{GM - GM_{min}}{GM_{max} - GM_{min}} \quad (5.1)$$

#### Maximum Connected Set

A network that is *maximal connected* is a complete graph. This means that the undirected adjacency matrix  $A$  is completely filled, apart from the diagonal. Such a network, as shown in Figure 5.10, is not considered physically realistic because of the number of connections.

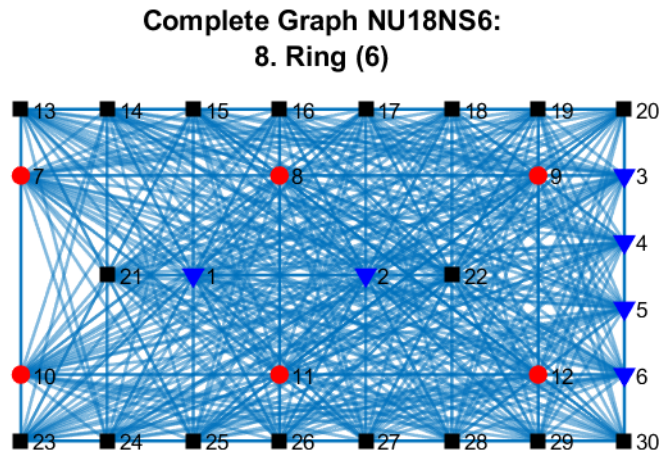


Figure 5.10: Verification Set V. NU18NS6: Complete Graph

For the network used in this example, the number of edges is  $(30^2 - 30)/2 = 435$  edges. Moreover, distribution networks as defined by de Vos (2018) only contain supplier-hub, hub-hub and hub-user connections (except in case of absence of hub nodes). Therefore, the maximum connected set is defined as equal to the normal set, but with a complete connected hub graph, meaning that all possible hub-hub connections are available. The supplier-hub and hub-user connections remain the same, as shown in Figure 5.11.

### NU18NS6 7. Double Vital (4): Min/Max Connected

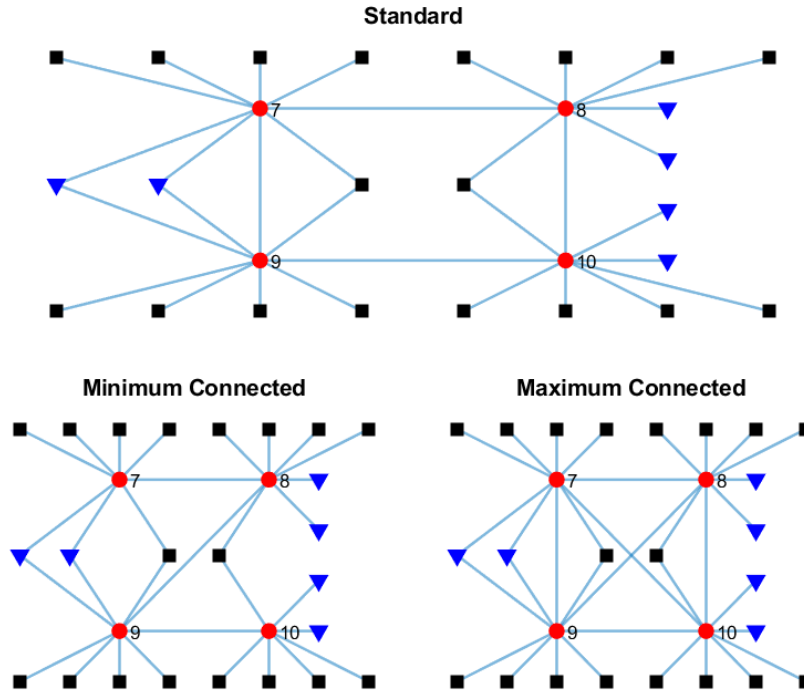


Figure 5.11: Verification Set V. NU18NS6: Maximum Connected Hub Graph

#### Minimum Connected Set

In the third graph of Figure 5.11, the *minimum connected set* can be found. In this set, all hubs are connected in through a single path while the supplier-hub and hub-user connections remained the same. This single path means that no ring distribution is possible, however, the set is more arbitrary than the maximum connected set. For example, a network with 4 hub nodes can have a single path through the nodes in the order 7 – 8 – 9 – 10 or 7 – 8 – 10 – 9. The first order is applied within these minimum connected sets due to programming reasons, but might not always provide "the worst" outcome.

#### Absolute versus Relative Robustness

The determination of the minimum and maximum values relates to the decision what scale to use for the normalisation of the graph measures, and therefore, the robustness. Four commonly known measurement scales are: *nominal*, *ordinal*, *interval* and *ratio scale*. Ascending in the list, more and more information about the data must be available. The nominal scale is literally comparing apples to oranges, while the ordinal scale contains a clear order amongst the possible values (i.e. a service satisfaction query). The difference between the last two scales is that, for the ratio scale, an absolute zero value is known. To normalise the graph measures, the maximum connected and minimum connected hubmatrix are used. Therefore, the normalised graph measures rate along a ratio scale with an arbitrary zero value.

The calculation of the  $R$ -value includes additional normalisation to formulate a single robustness measure. In the process of doing so, the maximum and minimum value stay intact, respectively 0 and 1. However, this robustness measure cannot be used on the interval scale because the difference between the values is not known. One can simply state that  $R_{G_1} > R_{G_2}$ , thus, the  $R$ -value can only be measured along an ordinal scale. Despite this limitation, this robustness measure is a composition of a number of crucial robustness aspects and should therefore not be disfavoured over a ratio scaled measure such as failure likeliness.

### 5.3 Selection Sample Set

For the case study, as performed in chapter 7, a new set of networks is required. This set is the same set as used in the first case study by de Vos (2018) and represents a network onboard a frigate. The model used to represent this network can be found in Figure 3.2. Since a single network cannot be compared,

multiple topologies have been generated using the ATG Tool described in [section 3.3](#). Using this tool, a set of topologies has been generating consisting of ten generations (*child001* to *child010*) each containing 256 topologies. [Figure 3.4](#) shows the 1<sup>st</sup>, the 9<sup>th</sup> and the 10<sup>th</sup> generation; generation 2 to 8 have been left out to keep the figure clear. Of this set of 2560 topologies, 12 topologies have been selected as sample set. The topologies are shown as single points with the two objective functions on the x-axis and y-axis, respectively the system claim and the system robustness. The topologies have a "higher score" on the objective functions if they have a lower value, therefore, the lower left corner contains the best topologies. The selection of the 12 analysed topologies is based on their value for both the system claim and system robustness objective function.

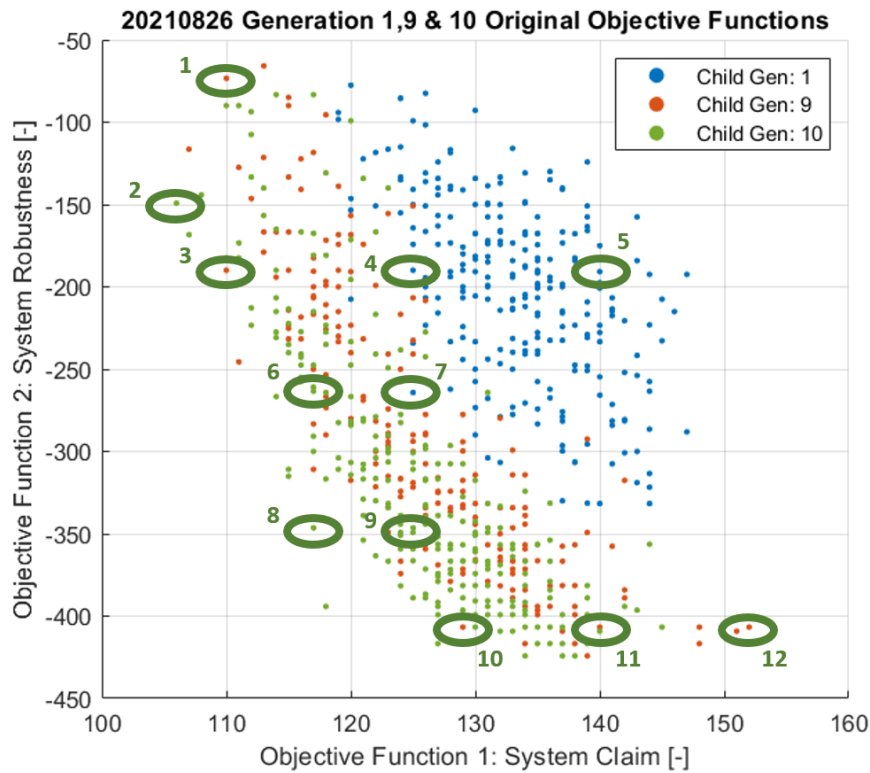


Figure 5.12: Selected Topologies: Results of Application ATG Tool, adapted from [de Vos \(2018\)](#)

The selected set has an increasing value for the system robustness measure, mirroring the values for the verification sets. [Figure 5.13](#) shows the values for the system claim and system robustness, calculated according to [Equation 3.1](#) and [Equation 3.3](#). The vertical and horizontal lines in [Figure 5.12](#) show that the selected topologies contain sets with similar objective function values; a conscious choice made to even the playing field for the graph measures.

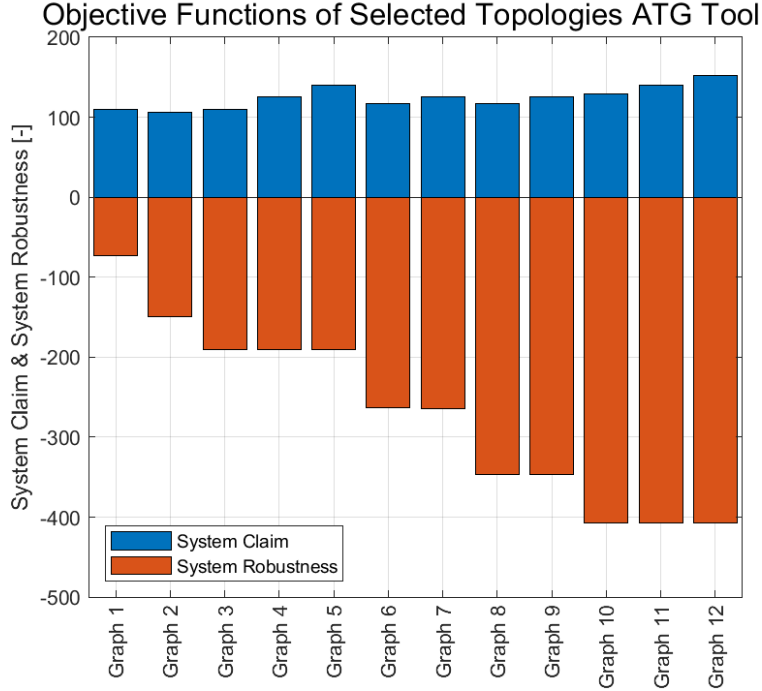


Figure 5.13: F1 System Claim and F2 System Robustness of Selected Topologies

### 5.3.1 Total System to Separate Subsystems

Figure 5.14 shows one of the selected topologies: Graph 2. This graph contains five subsystems, coloured red, pink, blue, green and grey respectively. To analyse the total system using graph measures, the five subsystems have been separated. An overview of these subsystems can be found in Figure 5.15, for which the legend below can be used.

Sample Set	Colour	Flow Type
Subsystem 1	Red	6600 Volt
Subsystem 2	Pink	440 Volt
Subsystem 3	Blue	Water 2°C
Subsystem 4	Green	Water 5°C
Subsystem 5	Grey	Data

Table 5.2: Overview system properties sample sets for case study

One should note that subgraph 5 does not contain any hub nodes. Therefore, this set is treated like the first graph of verification set I to IV; the graph measures dependent on the presence of a *hubmatrix* are zero. Moreover, all networks within a subgraph set contain a *constant number of supplier nodes, hub nodes and user nodes*. It is expected that the sets behave in a similar fashion as *NH8NS6*, which has been designed according to the same network properties.

Sample Set	Directed	NN (number of nodes)	NS (number of suppliers)	NH (number of hubs)	NU (number of users)
Complete System	No	36	-	15	-
Subsystem 1	No	11	4	4	3
Subsystem 2	No	15	3	3	9
Subsystem 3	No	11	3	3	5
Subsystem 4	No	16	5	5	6
Subsystem 5	No	6	2	0	4

Table 5.3: Overview node and edge properties sample sets for case study

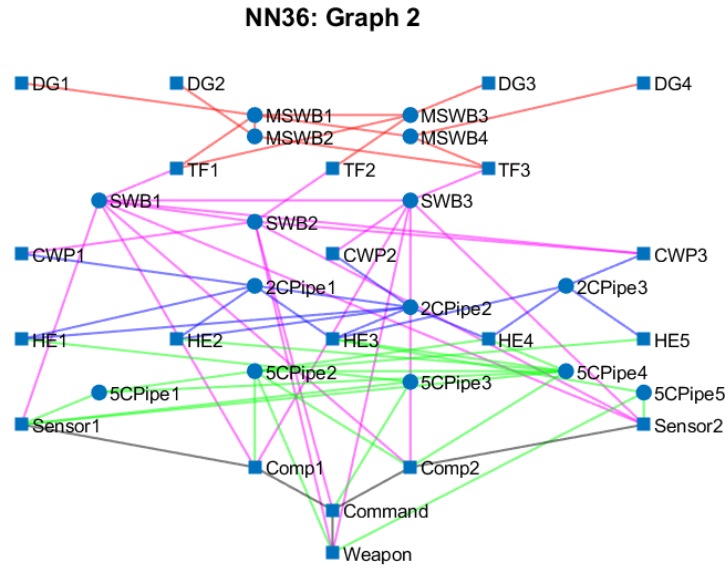


Figure 5.14: Total Graph Case Study: NN36 Graph 2 with Colour-Coded Subsystems

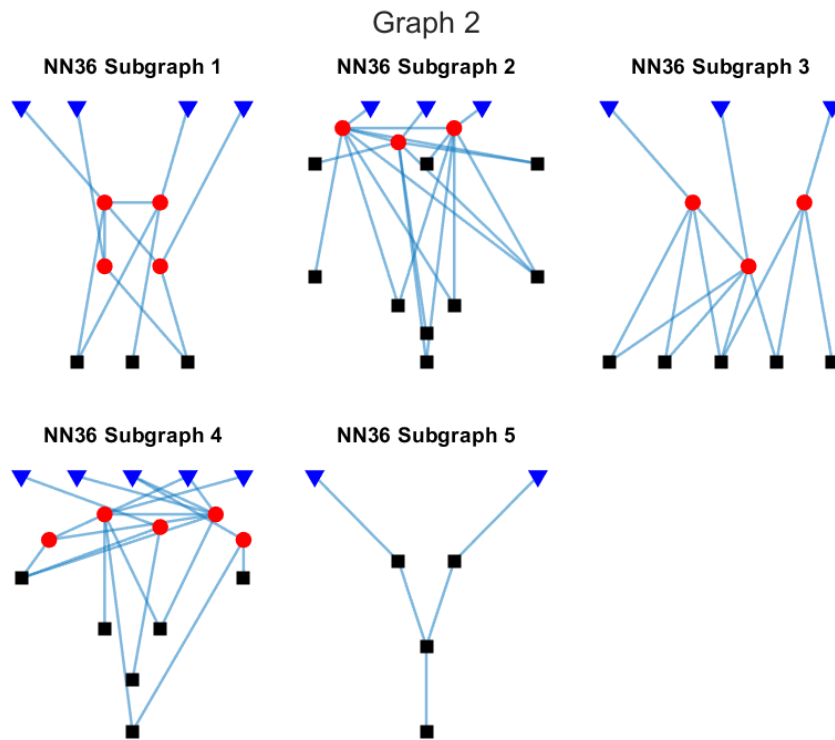


Figure 5.15: Five Subsystems Graph Case Study: NN36 Graph 2

## 5.4 Network Set Conclusion

In this chapter, [chapter 5](#), two network sets are introduced: a verification set and a sample set. First, the verification sets can be split in two groups: the sets with a constant number of users ( $NU10$ ,  $NU18NS6$  and  $NH8NS8$ ) and the sets with a constant number of total nodes ( $NN24$ ,  $NN24NS6$  and  $NH8NS8$ ). The first group has a better usability in actual ship design: the support system is often designed with the number of (main) users known. However, in graph theory it is considered good practice to compare graphs with the same number of nodes. The only set that fulfills both conditions is  $NH8NS8$ ; this set also mirrors the network properties of the first four subgraphs of the sample set.

The minimum and maximum values required for the normalisation of the graph measures are defined using the minimum and maximum connected hubgraph. The normalised graph measures have relative instead of absolute values since the supplier-hub and hub-user connections are not maximised or minimised. This approach is reconsidered in [section 7.2](#) following the verification set analysis in [chapter 6](#).

## Chapter 6

# Verification Set Network Analysis

In [chapter 5](#), five verification sets and the case study sample set are introduced. The network robustness of these verification sets is calculated and analysed in this chapter. First, the total  $R$ -value calculation is presented in [section 6.1](#), in which an example is used. The next two sections, [section 6.2](#) and [section 6.3](#), focus on two steps within the calculation process, respectively the calculation of the graph measures and the normalisation of the  $R$ -value. In [section 6.4](#), the system claim and system robustness ((de Vos, 2018)) of the verification sets are calculated. To conclude this chapter, the system robustness is compared to the  $R$ -value in [section 6.5](#).

### 6.1 R-calculation

The robustness or  $R$ -value of the verification sets is calculated according to the flowchart shown in [Figure 6.1](#). The four steps are:

1. Define the input graph, the weight vector and the normalisation value
2. Calculate the graph measure value for each graph
3. Normalise the graph measure value
4. Calculate the  $R$ -value using the normalised graph measure, the weight vector and the  $q$ -norm

Within this section, the four steps are followed for a single verification set and graph measure; respectively *NN24NS6* and *hub-hub degree*.

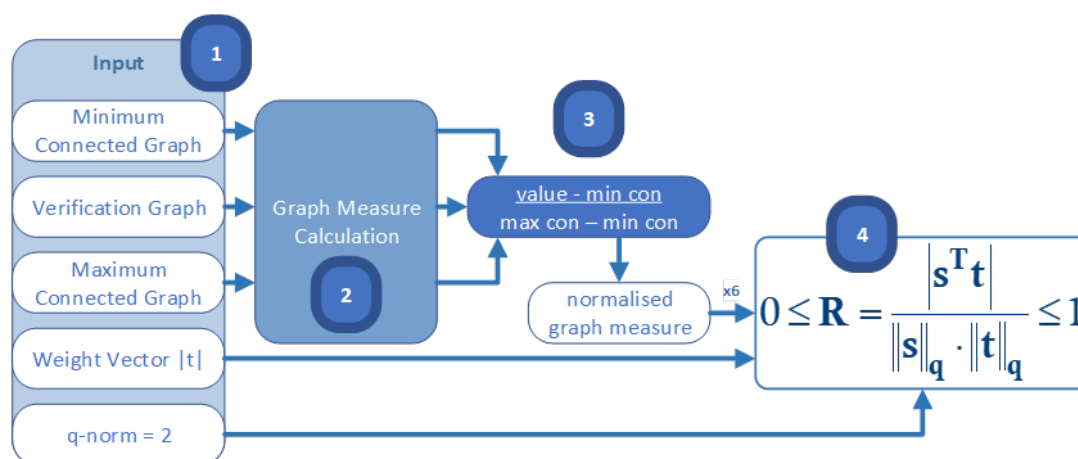


Figure 6.1: Flowchart R-value Calculation

### 6.1.1 Step 1: Input

In subsection 5.2.7, the minimum and maximum connected graph are defined. These graphs connect the absolute value of a certain graph measure to a relative value between 0 and 1. Figure 6.2 shows the seventh graph (a double vital network) of the third verification set (NN24NS6). The three graphs contain an equal number and placement of supplier-hub connections and hub-user connections. The minimum connected graph contains a single path passing the four hub nodes: 7 – 8 – 9 – 10. All hub nodes are connected to all other hub nodes within the maximum connected graph; the hub-matrix is fully connected.

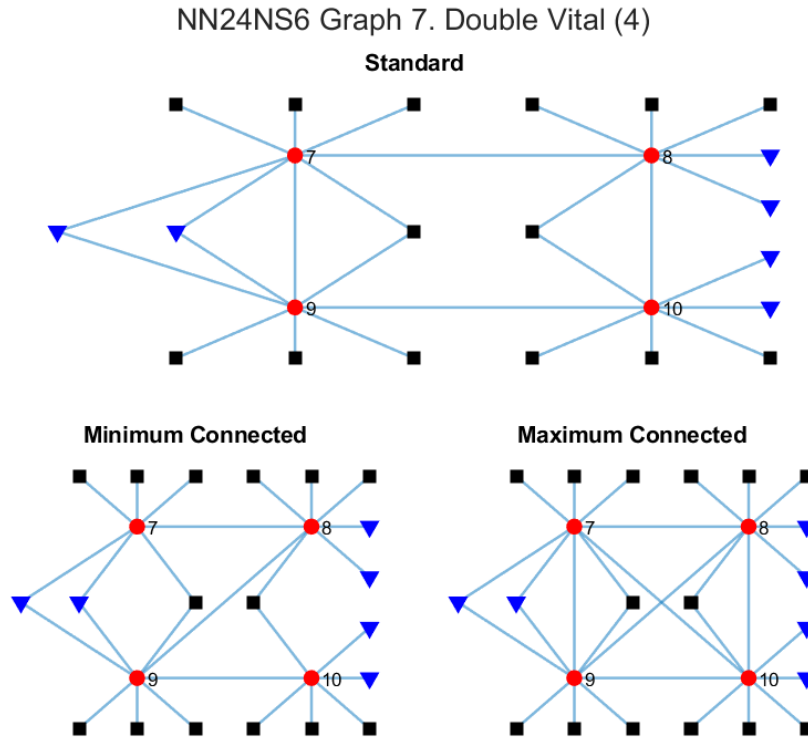


Figure 6.2: Standard, Minimum and Maximum Connected Double Vital Network with 24 nodes and 6 suppliers (NN24NS6)

The input for the  $R$ -calculation contains two other elements: the weight vector  $|s|$  and the  $q$ -norm. All elements within the weight vector  $|s|$  are 1, so  $s = [1, 1, 1, 1, 1, 1]^T$ . This means that, for a given  $R$ -calculation, the six graph measures are valued equally. More research into valuing graph measures differently is recommended, however, not part of this study. The norm is decided to be  $q = 2$ , generally known as the Euclidian norm. With  $q = 2$ , the vector norm can be calculated using Equation 6.1.

$$\|s\|_2 = \sqrt{s_1^2 + s_2^2 + \dots + s_n^2} \quad (6.1)$$

### 6.1.2 Step 2: Graph Measure Calculation

The second step is calculation the values of the graph measure; the minimum and maximum connected graphs are shown in [Figure 6.4a](#). Within this example, the *mean hub-hub degree* is calculated for the third verification set: *NN24NS6*. The values of this graph measure can be found in [Figure 6.3](#). Due to the absence of hub nodes in general and the absence of hub-hub connections, the star network and tree network have a NaN value and zero value, respectively. The other graphs show a step-wise increasing trend; with only a change in supplier-hub or hub-user connections, the hub-matrix itself does not change.

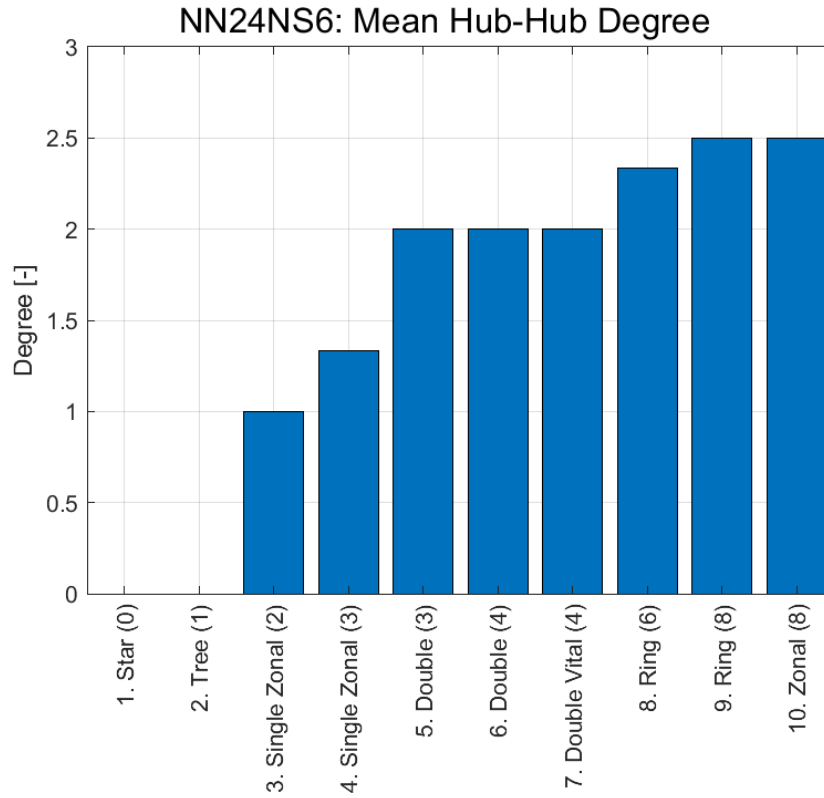


Figure 6.3: Mean Hub-Hub Degree (NN24NS6)

### 6.1.3 Step 3: Graph Measure Normalisation

The degree of the minimum and maximum connected graph is determined in step 2 and can be found in [Figure 6.4a](#). The values of these graphs are shown using a line plot to improve the clarity of the figure; the independent values are not continuous. For this graph measure, the maximum connected graph is considered to have a higher robustness than the minimum connected graph. Therefore, the maximum connected graph is marked green while the minimum connected graph is marked orange. The light blue area between the minimum and maximum connected graph provides the envelope of possible graph measure values.

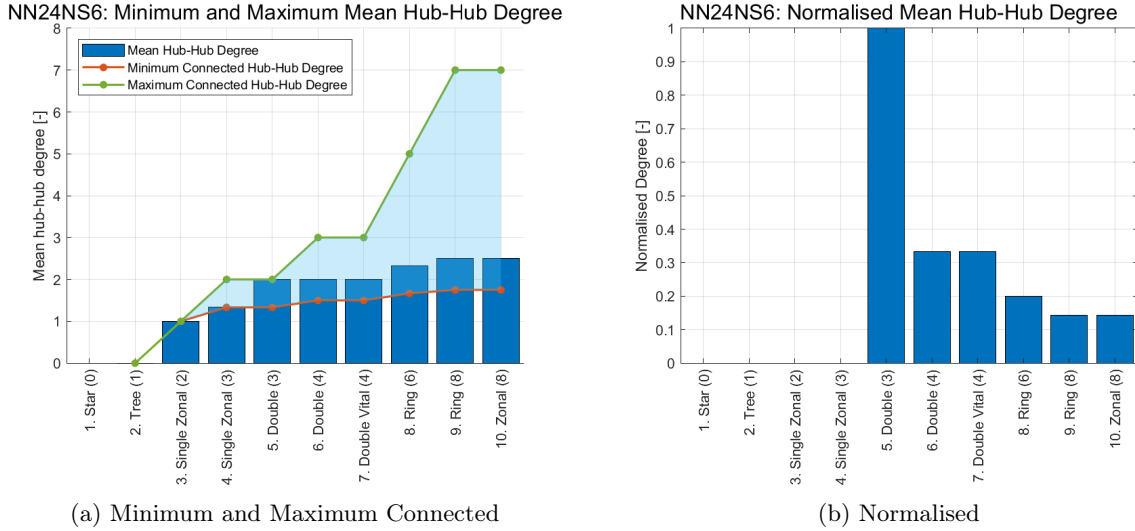


Figure 6.4: Mean Hub-Hub Degree (NN24NS6)

The normalised values are calculated using [Equation 6.2](#) and are shown in [Figure 6.4](#). In contrary to the standard measure, the normalised measure shows a decreasing trend. This is caused by the difference in slope between the maximum connected values and the minimum connected and standard values. The last two show a comparable trend, while the maximum connected set increases significantly starting with an increase in number of hubs.

$$degree_{norm} = \frac{degree - degree_{min}}{degree_{max} - degree_{min}} \quad (6.2)$$

As can be seen in [Equation 6.2](#), when the maximum and minimum graph measures are equal, the normalised degree is undefined. In this thesis, this has been set to a normalised value of 0, to always have an underestimation of the total robustness. If this is taken into account, the normalised value of graphs one to four can be seen to be zero, where this conversion from undefined to *NaN* has been made for graphs one to three. Furthermore, graph four shows a zero value since the actual measure is equal to the minimum value.

### 6.1.4 Step 4: R-value Calculation

The final and fourth step is defining a single robustness value based on the six normalised values calculated in the previous step. Equation 6.3 provides the input vectors and variables used in Equation 6.3. The topology vector  $t$  contains the six normalised measures, with the normalised mean hub-hub degree as  $t_1$ . In the subscript  $j,i$ ,  $j$  refers to the verification set or graph set while  $i$  refers to a specific graph within set  $j$ .

$$t_{j,i} = \begin{bmatrix} \bar{D}_{hubs,j,i} \\ \kappa_{e,j,i} \\ q_{j,i} \\ \bar{E}_{j,i} \\ C_{j,i} \\ R_{eff,j,i} \end{bmatrix}, s_{j,i} = \begin{bmatrix} 1 \\ 1 \\ 1 \\ 1 \\ 1 \\ 1 \end{bmatrix}, q_{norm} = 2 \quad (6.3)$$

$$0 \leq R_{j,i} = \frac{|s^T t|}{\|s\|_q \cdot \|t\|_q} \leq 1 \quad (4.2)$$

Figure 6.5 shows the calculated robustness measure. For clarification, the share of the normalised mean hub-hub degree has also been made visible. The share of the degree measure is not equal to the values shown in Figure 6.4 due to an extra "normalisation layer" in Equation 4.2. This layer values a graph with small deviations between different measures over graphs with higher deviations; a high robustness measure means a relatively high value for all separate graph measures. The influence of the six graph measures on the total robustness value is analysed in section 6.2.

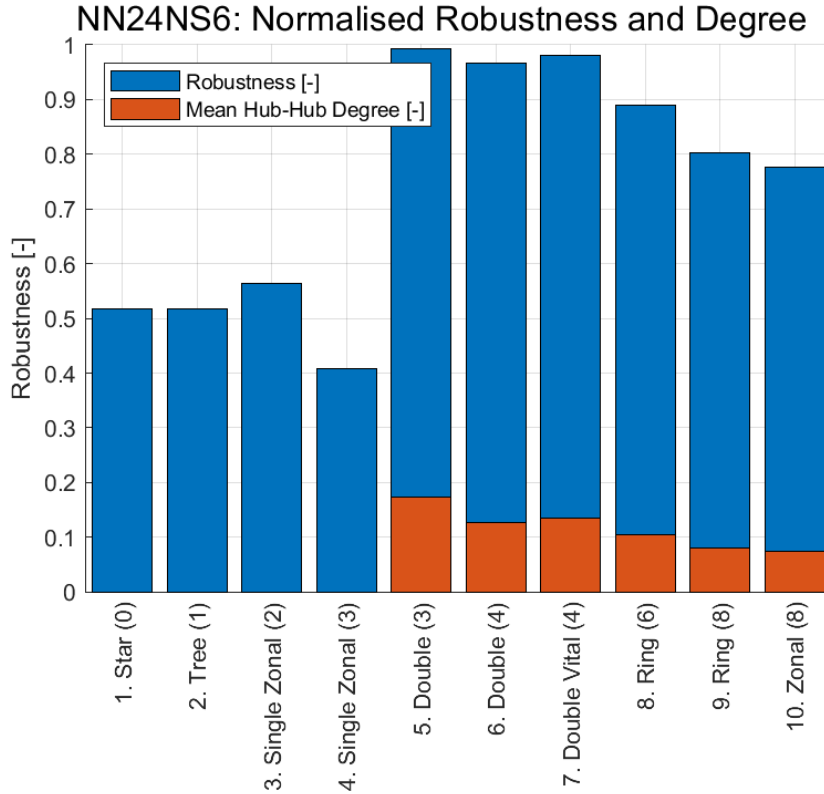


Figure 6.5: Normalised Robustness and Mean Hub-Hub Degree (NN24NS6)

## 6.2 Graph Measure Analysis

The meaning of the six measures is analysed using the five verification sets as introduced in section 5.2. All plots containing the minimum, maximum, standard and normalised graph measure values can be found in Appendix B. The main difference between the first four and the last set is the plot trend of

the minimum and maximum connected graphs; these plots have a significant influence on the graph measure normalisation. For the last set, these plots show a constant line (Figure 6.6) while the other verification sets have a changing slope as minimum or maximum connected value (Figure 6.4a). This difference is apparent for all graph measures apart from modularity, which is explained in later in subsection 6.2.4.

### 6.2.1 Clean Increasing Trend for NH8NS6

The first graph measure is the *mean hub-hub degree* which has been used in the example  $R$ -calculation the previous section. The two plots in Figure 6.4 for  $NN24NS6$  have been combined into one plot in Figure 6.6 for  $NH8NS6$ . The left axis shows the standard, the minimum connected and the maximum connected values while the right axis shows the normalised values. Since this verification set contains both the minimum connected graph (graph 1) as well as the maximum connected graph (graph 7), the normalised and the standard measure show an increasing trend from the minimum value to the maximum value. A similar trend for verification set V ( $NH8NS6$ ) can be found for *cycle basis* and *hub-hub edge connectivity*. Therefore, these measures are, like mean hub-hub degree, mainly dependent on the number of edges within the *hub-matrix*.

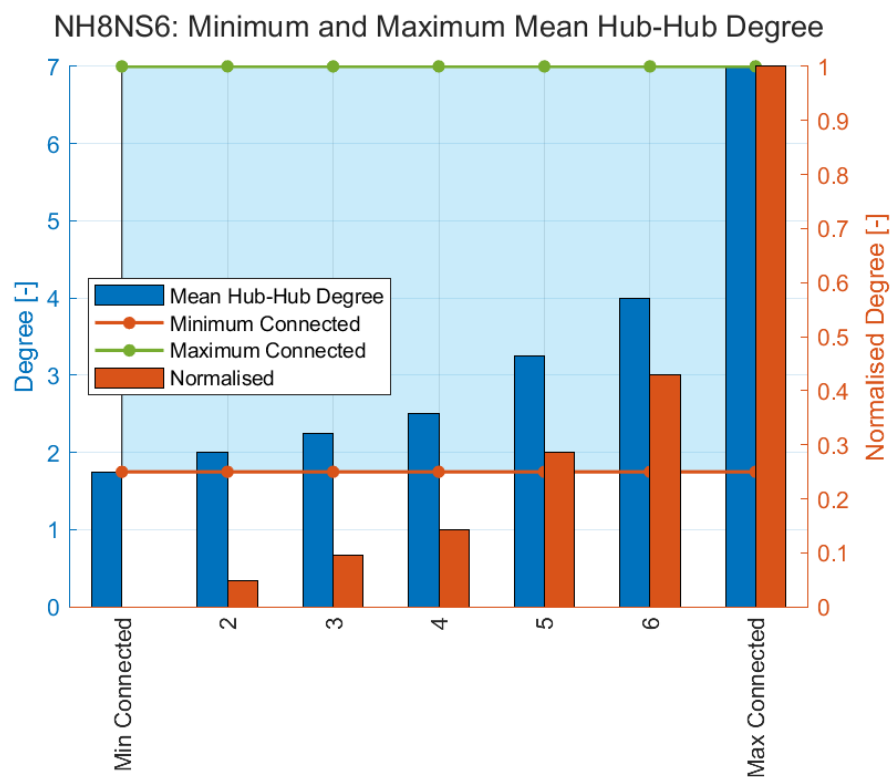


Figure 6.6: Mean Hub-Hub Degree with the normalised values on the right axis (NH8NS6)

### 6.2.2 Clean Decreasing Trend for NH8NS6

Figure 6.7 shows, in contrary to Figure 6.6, a decreasing trend for the un-normalised graph measure. This development can be seen in the *mean node eccentricity* but also in the measure for *effective resistance*. The explanation for this trend is that, for a higher degree hub-matrix, more paths between sets of nodes exist. When the network is considered as an electrical network, an increase in parallel paths causes a lower resistance. Moreover, the chance that a shortest path between a set of nodes decreases with more edges increases, leading to a lower eccentricity. Both developments can be considered positive for the network robustness: a lower resistance means more options to connect a set of nodes and a lower eccentricity means a decrease in dependence from different nodes and edges. Therefore, the normalised values have been corrected to provide a higher value for a lower eccentricity or resistance.

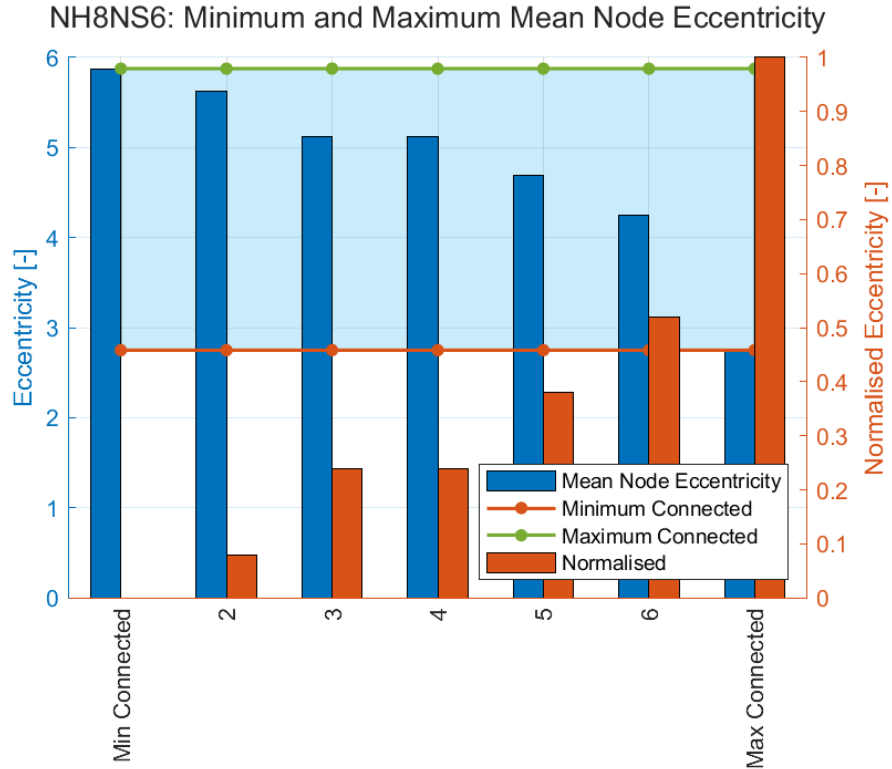


Figure 6.7: Mean Node Eccentricity With Normalised Values on Right Axis (NH8NS6)

### 6.2.3 Variable Results

Most figures have more in common with the plot shown in Figure 6.8 than with the previous two figures. The *mean node eccentricity* shows features similar to the *mean hub-hub degree* in Figure 6.4a. The following trends can be found for verification sets I to IV, more or less dominant for all six graph measures.

- Without the normalisation step, the graph measure shows a step-wise increasing trend.
- The values of the measures remain closer to the minimum connected value; the maximum connected value deviates more with an increasing hub-matrix
- Due to the second point, the values of the normalised measure decrease once they contain a value larger than zero. Only amongst graphs with an equal sized hub-matrix (graph 6 and 7 or graph 9 and 10), an increasing value can be found.
- The zero values are either adapted *NaN* values or "real" zero values.

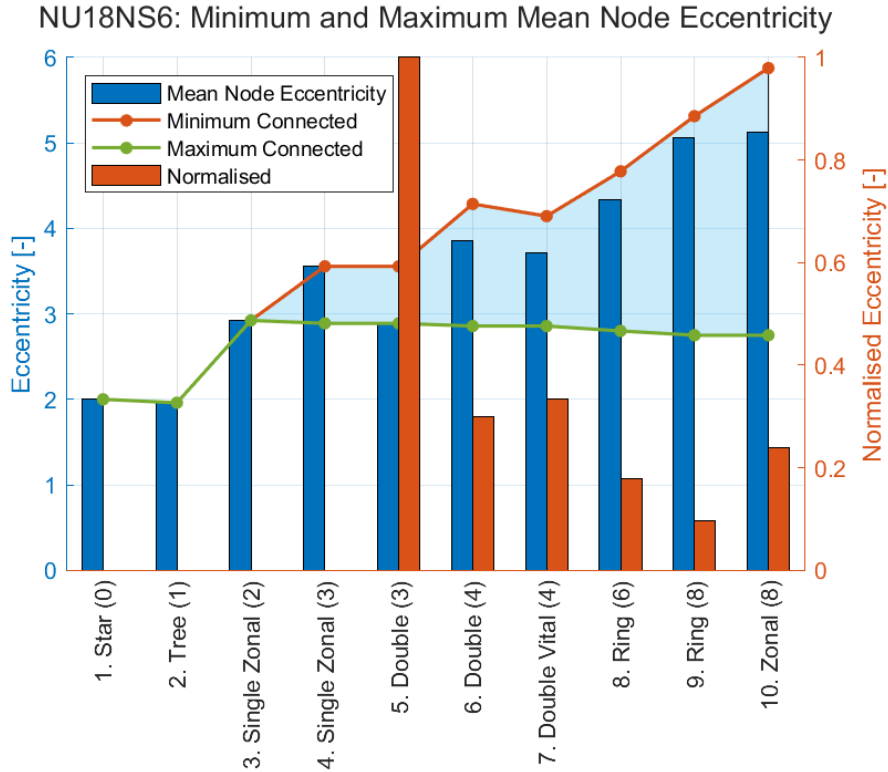


Figure 6.8: Mean Node Eccentricity With Normalised Values on Right Axis (NU18NS6)

Apart from these general trends, some notes specified to this measure can be made. In contrary to the graph measure *mean node eccentricity* before normalisation in Figure 6.7, Figure 6.8 shows an increasing eccentricity value. This increase directly derives from the increase in graph size; with a constant number of users, the number of nodes increases over the 10 graphs. However, the same trend can be found in the eccentricity plot for *NN24NS6*, which has per definition, a constant number of nodes. The mean node eccentricity therefore has a positive relation to the size of the hub-matrix.

### 6.2.4 Independent Modularity Normalisation

For the final graph measure, *modularity*, the normalised values for all verification sets are shown in Figure 6.9. In contrary to the other graph measures, the minimum and maximum modularity is not shown in Figure 6.9 because these values are constant for all networks and respectively  $-0.5$  and  $1$ . The value of this measure is  $> 0$  if the graph is more modular than can be expected based on the number of nodes. The modules or subsystems have been defined manually to ensure that each subsystem contains at least one supplier, one hub node and one user node, creating an *independent subsystem*.

The three graph, containing only a single node, cannot become modular and contains only a single subsystem. Therefore, this graph has a value of  $0$ . The star graphs contain more than one hub node, however, this graph has exactly the same modularity as could be expected based on random networks. For the fifth verification set, the modularity decreases with an increase in hub-hub connections. As described in subsection 4.4.3, modularity decreases when more edges between different subsystems exist, which is what causes this negative trend.

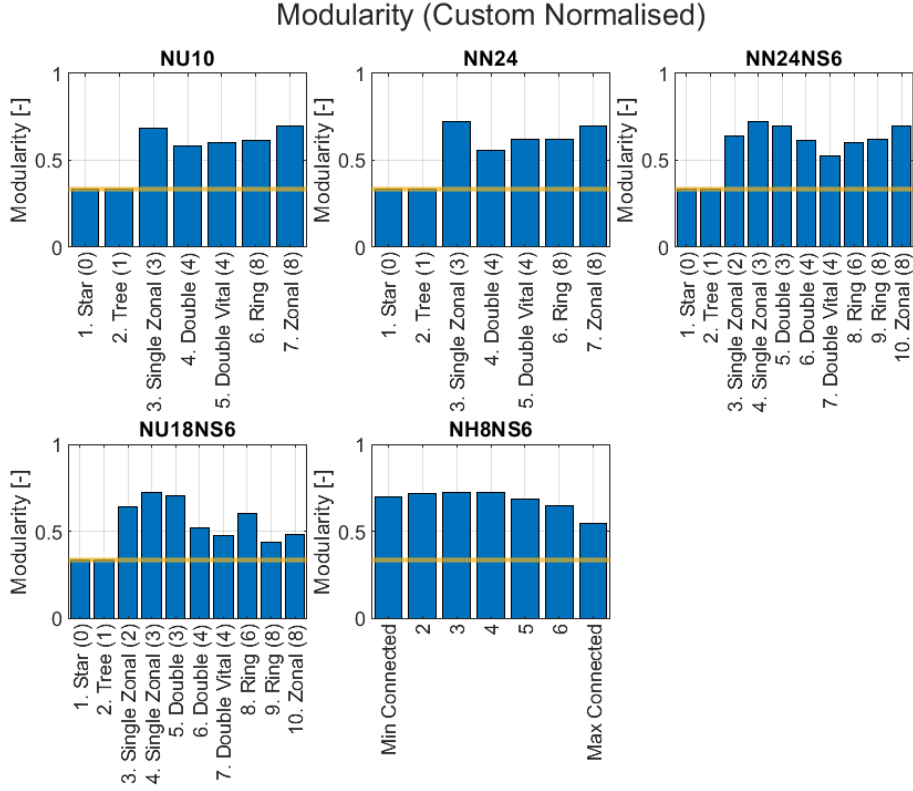


Figure 6.9: Normalised Modularity

### 6.2.5 Graph Measure Noteworthy Plots

Apart from the general trends described before, a more specific comments can be made concerning the separate graph measures and normalisation.

#### High Values for Star Network Cycle Basis Measure

All user nodes can be considered *vital users* within the star networks of different verification sets. Vital users are favoured by the cycle basis graph measure, leading to higher values for such graphs (up to 85 cycles for *NN24NS6*). [Figure 6.10](#) shows such a star network containing 9 cycles. However, these values do not play a role within the normalised graph measure; this is *NaN* since the minimum and maximum connected graphs are equal due to the absence of a hubmatrix.

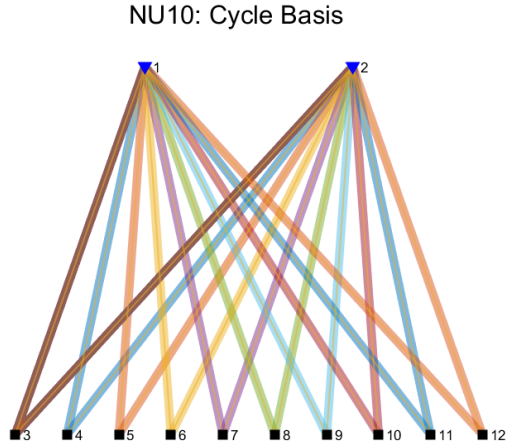


Figure 6.10: Cycle Basis (NU10 Graph 1), for context see [Figure 4.4](#)

### Constant Values for Connectivity Measure

The *hub-hub edge connectivity* graph measure ([Figure 6.11](#)) is inherently dependent on the hubmatrix. Apart from the last two graphs of verification set V, the highest minimum node degree (or edge connectivity) within the hubmatrix is 2, with a minimum connected value of either 0 (in the absence of 2 or more hub nodes) or 1. Therefore, the normalisation is mainly based on the maximum connected value. This value can be manually calculated by  $\kappa_{edge,max} = NH - 1$  and is entirely based on the number of hub nodes. Based on [Figure 6.11](#), one can conclude that the normalised value decreases with an increasing robustness value.

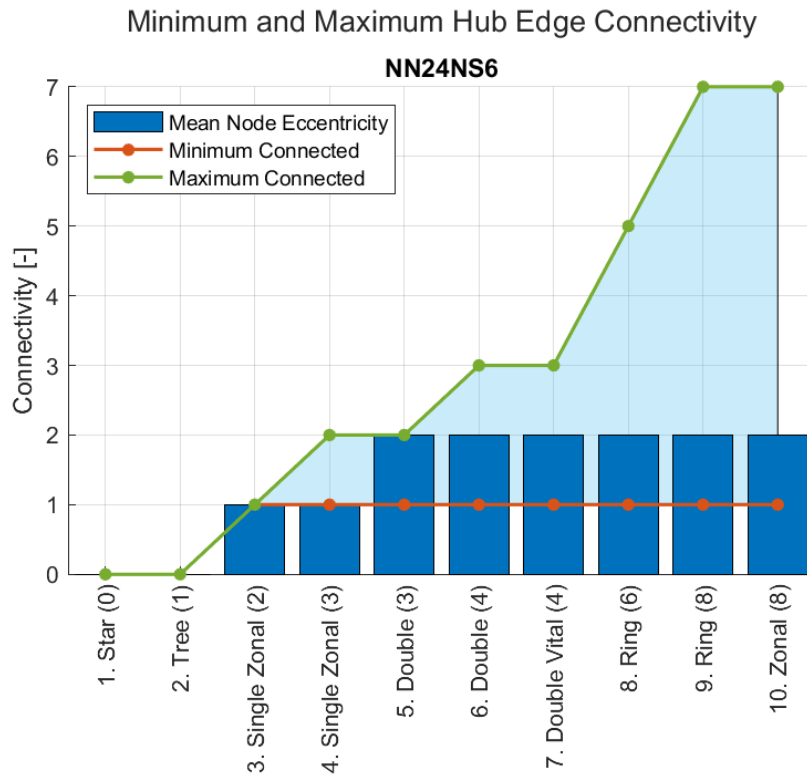


Figure 6.11: Minimum and Maximum Connected Mean Hub-Hub Edge Connectivity (NN24NS6)

### 6.3 Alternative Normalisation

For a network comparison, it is convenient to end up with a single robustness value per graph. The first option to arrive at this point is provided in [section 6.1](#) using the four steps. However, this method is not the sole method to reach a robustness value than can be used to compare different networks.

#### 6.3.1 Un-normalised Graph Measures

A second option to get this single graph is by simply adding up the different graph measures, as shown in [Figure 6.12](#). This figure contains the sum of all graph measures, independent on whether a graph measure represent a more robust graph with a lower or higher value. Despite the clear trend for all verification sets, a star network is robust and the robustness show an upward trend for the other graphs, this figure gives a distorted picture. The distortion is caused by two factors: first, some graph measures represent a more robust graph with a lower value. For example, the node eccentricity and the effective resistance decrease with increasing robustness. Second, the upper and lower limits of the measured values differ significantly. If a measure has values between 0 and 30, it has more influence on the total  $R$ -value than a measure with values between  $-0.5$  and 1. Therefore, a third option is defined: a standard normalised robustness value.

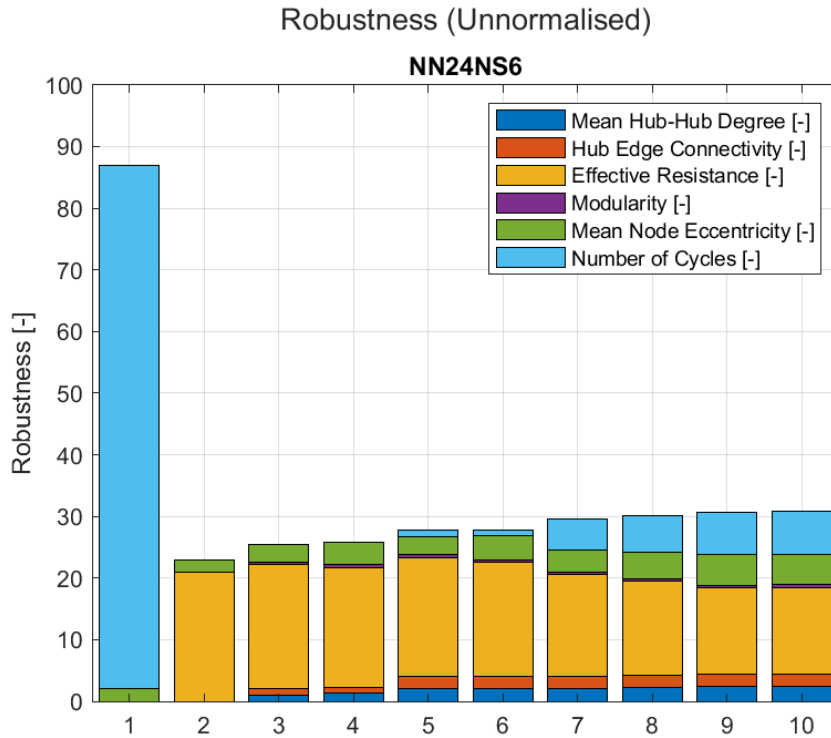


Figure 6.12: Robustness based on Unnormalised Graph Measures (NN24NS6)

#### 6.3.2 Graph Measures Normalised per Set

An example of the third robustness option is shown in [Figure 6.13](#). This robustness has been calculated by dividing each graph measure by the norm of the graph measure within the verification set. For example, the mean node eccentricity for the third graph of verification set I ( $NU10$ ) is calculated using [Equation 6.4](#). In doing so, the problem concerning the difference in upper and lower limits has been solved. However, the measures with a lower value for a more robust graph are still represented incorrectly. Moreover, the robustness calculated here is dependent on the used verification set. By adding, removing or changing a graph within a set, the all robustness values is changed because the norm of the graph measures is dependent of the entire set.

$$Ec_{norm}(NU10, 3) = \frac{1}{6} \frac{Ec(NU10, 3)}{norm(Ec(NU10, all))} \quad (6.4)$$

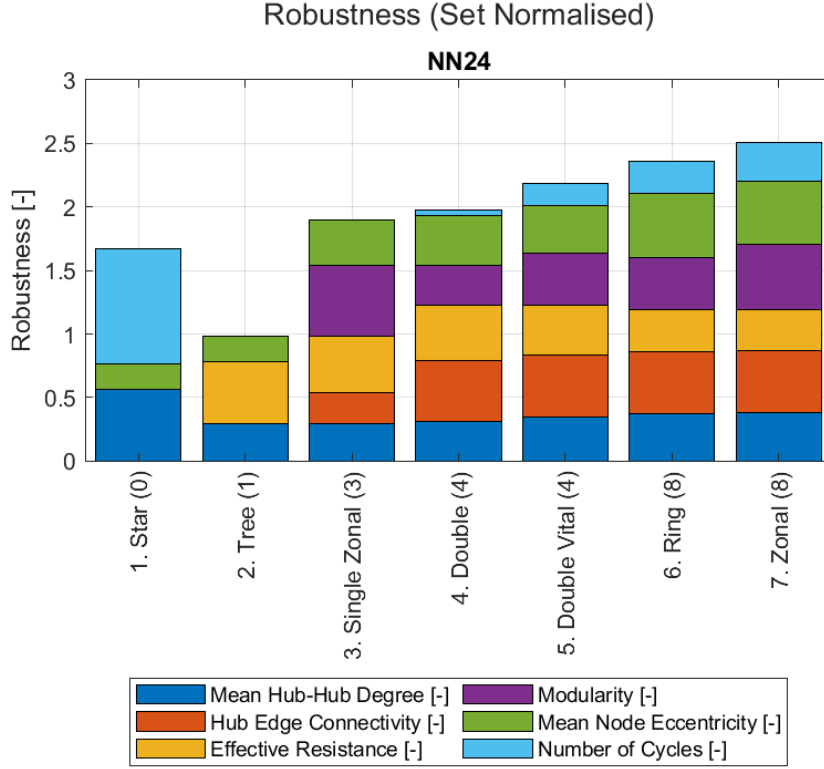


Figure 6.13: Robustness based on Graph Measures Normalised per Set (NN24)

### 6.3.3 Graph Measures Normalised per Graph Measure

The last robustness option is closest to the  $R$ -value calculation since both approaches share two main characteristics. First, the robustness value of a specific graph is not dependent on other graphs within the set. Second, all graph measures share the same interval  $0 \leq GM \leq 1$  with 1 being the most robust. The main disadvantage of this method is that two high graph measures can compensate for extremely low values of other measures. The  $R$ -value calculation prevents the occurrence of such a situation by adding an extra normalisation layer. This layer favours a graph with comparable values for all graph measures over a graph with a topology vector like  $[1, 1, 1, 0, 0, 0]^T$ . Figure 6.14 shows the robustness values for the fourth normalisation option; the calculation of this robustness can be found in Equation 6.5.

$$R_{norm}(NU10, 3) = \frac{1}{6}(D_{norm}(NU10,3) + \dots + C_{norm}(NU10,3)) \quad (6.5)$$

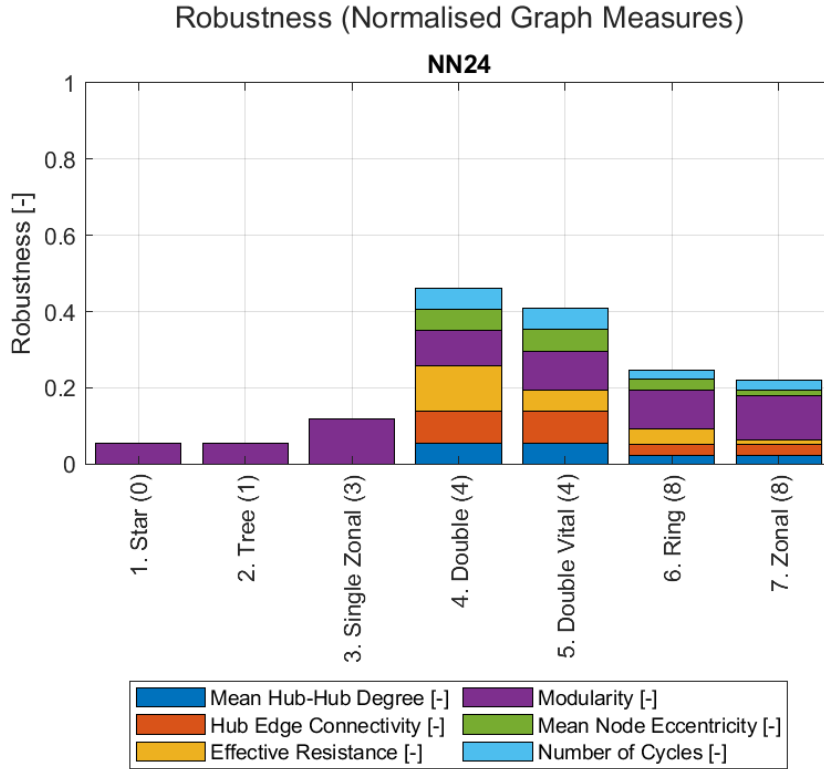
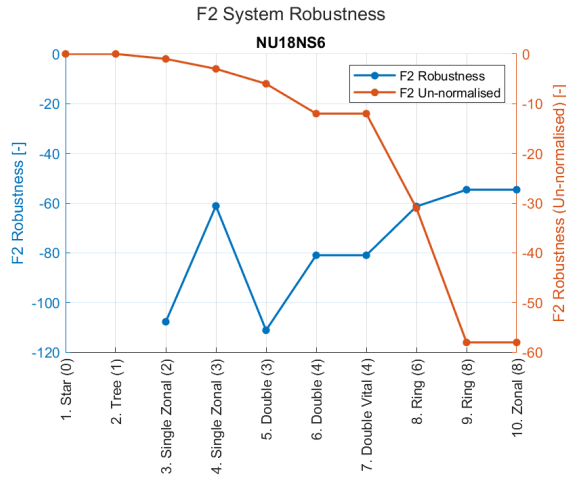


Figure 6.14: Robustness based on Normalised Graph Measures (NN24)

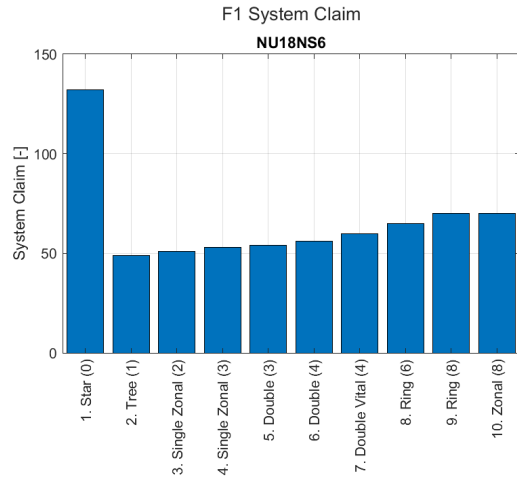
## 6.4 Objective Function Analysis

In [section 6.5](#), the  $R$ -values are compared to the system robustness  $F2$ . Values for the first and second objective function ([\(de Vos, 2018\)](#)) for two selected verification sets can be found in [Figure 6.15](#) and [Figure 6.16](#). [Figure 6.15a](#) shows the normalised and standard second objective function ([\(de Vos, 2018\)](#)): the system robustness. Note that the robustness in this plot is considered "better" for a lower value of  $F2$ , this is not in line with the  $R$ -value. Moreover, a line plot is used for a clear comparison, the separate values still remain independent of other values within the plot.

The normalisation of this measure is based on the number of hubs within the network instead of a maximum and minimum connected reference network. Despite this difference in normalisation, the standard normalised version shows a comparable trend to i.e. the normalised mean node eccentricity in [Figure 6.8](#). This conclusion resonates with the conclusion by [de Vos \(2018\)](#); the normalisation does not show the expected decreasing trend with a variable number of hubs. In [Figure 6.16a](#), this conclusion is confirmed since a continuously decreasing trend can be found for a constant number of hub nodes. Within the case study, the compared networks contain a constant number of hub nodes, therefore, the standard system robustness measure is used.



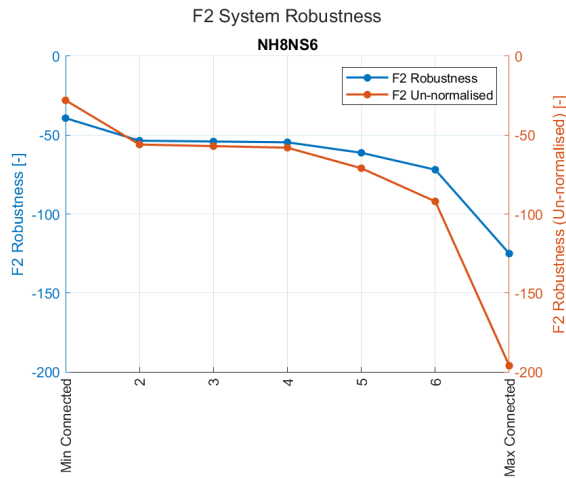
(a) F2 System Robustness: Standard and Un-Normalised



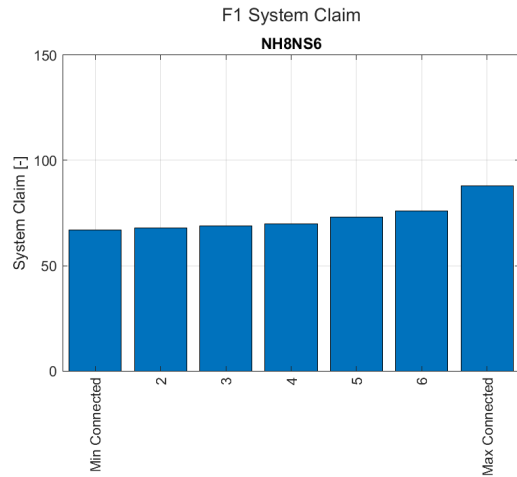
(b) F1 System Claim

Figure 6.15: Objective Functions F1 System Claim and F2 System Robustness (NU18NS6)

The first objective function, system claim, is shown in Figure 6.15b and Figure 6.16b. Both plots increase step-wise, with exception of the first network of *NU18NS6*. This high outlier is a star network with 6 supplier nodes and 18 user nodes in which the all supplier nodes are connected to all user nodes. This sixfold redundancy requires  $6 \cdot 18 = 108$  connections, which creates the peak in system claim. In Figure 6.16b, the number of nodes is constant, meaning that the system claim is only dependent on the number of connections.



(a) F2 System Robustness: Standard and Un-Normalised



(b) F1 System Claim

Figure 6.16: Objective Functions F1 System Claim and F2 System Robustness (NH8NS6)

## 6.5 Robustness Measure Comparison

Figure 6.17 and Figure 6.18 show the final comparison of the verification study: the plots for the  $R$ -value and the F2 system robustness. The system robustness is adapted to show positive values for a higher robustness to facilitate the comparison.

For Figure 6.17, the most significant slope is between network 4 and 5. Both networks have three hub nodes but the networks have a minimum and maximum connected hubmatrix, respectively. The decreasing trend starting at the fifth network is caused by the normalisation based on the minimum and maximum connected hubmatrix: this value shifts with an increase in number of hub nodes. The normalisation also causes a constant  $R$ -value for the first four networks; only modularity has a non-zero value for these graphs since this measure is independently normalised. The normalisation used for the system robustness causes the absence of values for the first two graphs; both networks lead to a division by 0. In conclusion, the two trends show comparable results. However, both plots are not in line with the expected increasing trend based on the design rules.

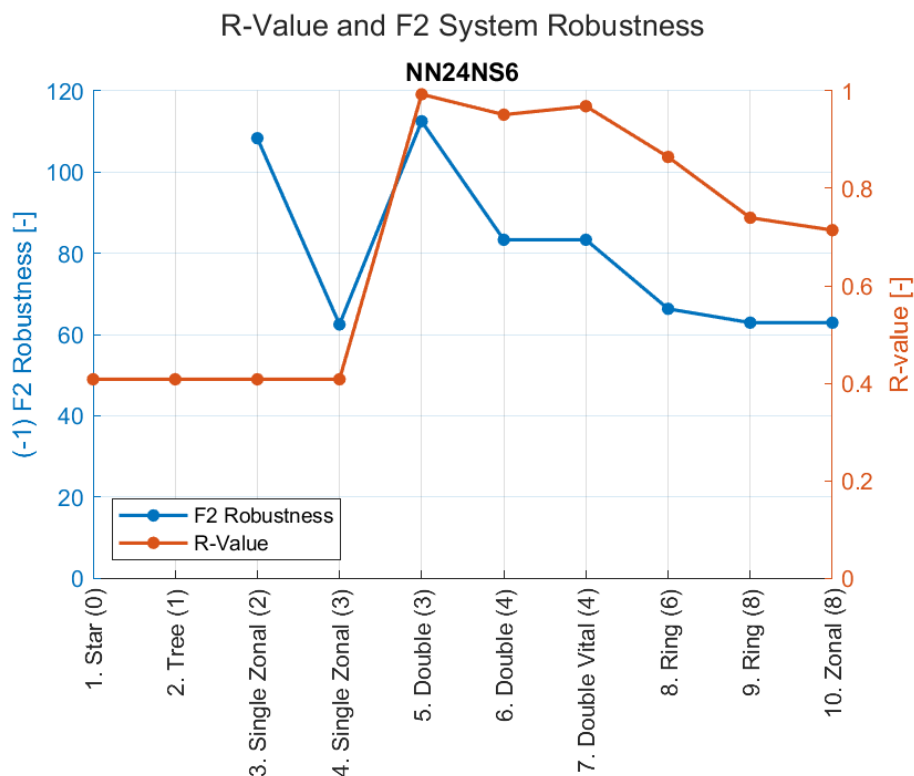


Figure 6.17: R-Value and F2 System Robustness (NN24NS6)

Figure 6.18 shows an increasing trend for both measures, however, the curve of both plots differs. First, the system robustness shows a trend that directly relates to the number of edges present in the hubmatrix. The highest increments are between the last two networks and between the first two networks, respectively. This is in line with the number of edges added to the network, as shown in Figure 6.16b. The system robustness is represented by the sum of the maximum flow between two hub nodes; the direct relation with the number of edges is therefore makes sense.

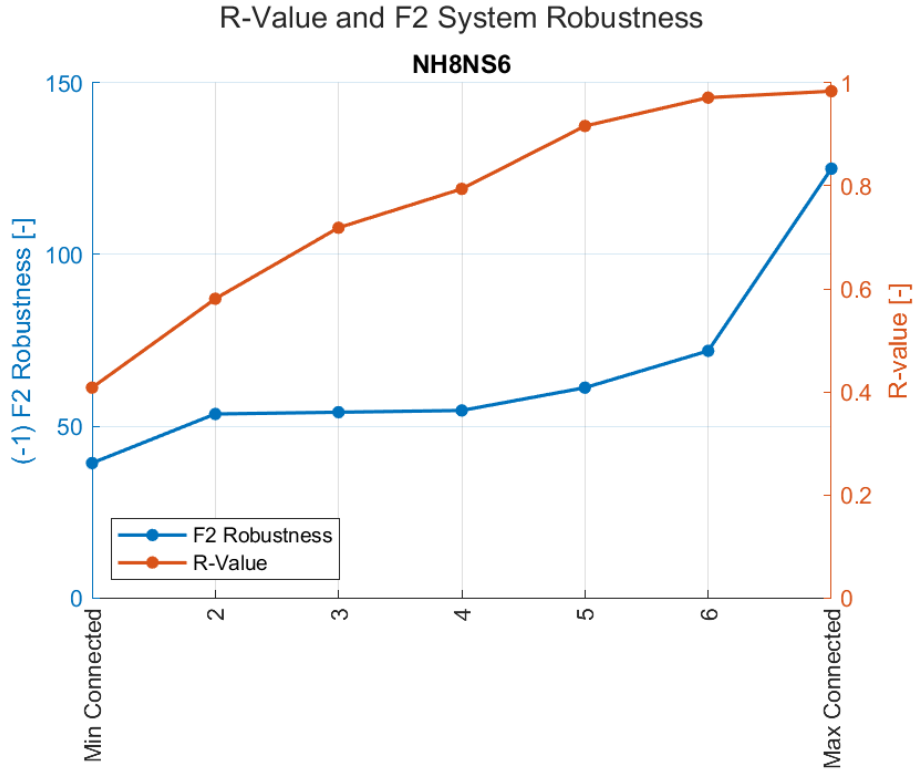
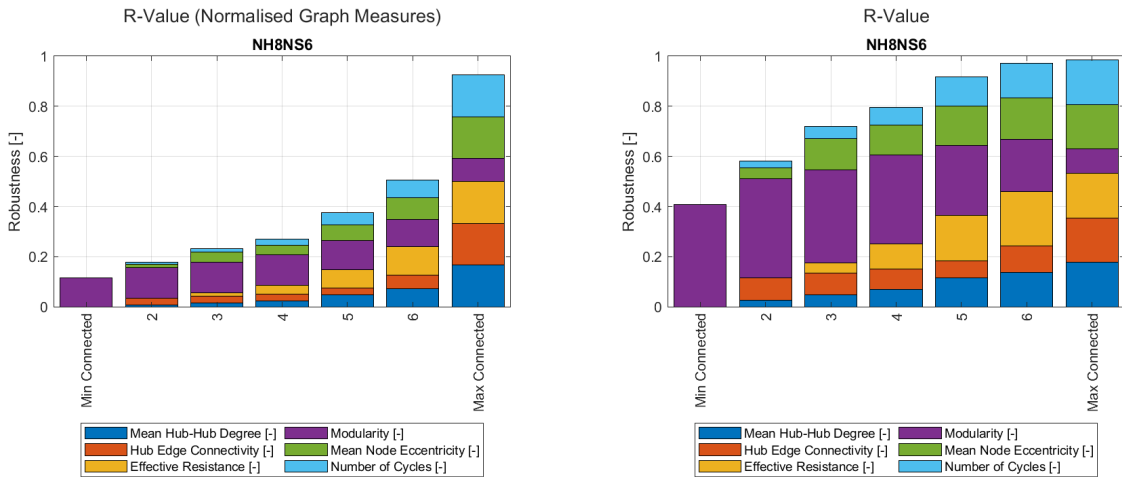


Figure 6.18: R-Value and F2 System Robustness (NH8NS6)

The  $R$ -value demonstrates a flattening of the curve, which results from the decrease in modularity over the sets. As mentioned in subsection 6.3.3, the  $R$ -value favours comparable values over a wide range in measured values. Figure 6.19a shows a decreasing modularity value; more connections between modules causes less independent islands and therefore a lower modularity. The deviation between the graph measures increases since the other five graph measures increase in value, which results in an  $R$ -value as shown in Figure 6.19b and Figure 6.16a.



(a) Robustness Normalised Graph Measures

(b) R-Value

Figure 6.19: Two Robustness Approaches: Normalised Graph Measures and R-Value (NH8NS6)

### 6.5.1 Verification Study Conclusion

Based on the results found in this chapter, it can be concluded that the  $R$ -value verifies the F2 System Robustness based on the max-flow-between-hubs. Moreover, the  $R$ -value includes more aspects of robustness than covered by the max-flow-between-hubs. For example, the graph measure modularity also includes the *independent subsystems* as robustness property. However, this conclusion is limited in its application:

- The normalised graph measures forming the  $R$ -value do not follow the intuitive increase in robustness over the verification sets except when the number and function of the nodes within the network remain constant.
- To ensure the intuitive increasing trend, the minimum and maximum values must be constant for a networks within a set.
- The weight vector is not part of the  $R$ -value for this verification study, however, the influence of this vector's absence is not part of this study.
- While *unnormalised* and *set-normalised* robustness have been studied, they do not seem to be good alternatives for the actual  $R$ -measure.
- The robustness measure as introduced in [Figure 6.14](#) and further found in [Figure 6.19](#) shows a more comparable trend to the F2 system robustness than the actual  $R$ -measure. However, the effect of outlying graph measures is not included within this measure. The robustness study application determines which measure is more appropriate.
- Some graph measures provide a measure of the same network property, i.e. hub-edge connectivity and mean hub-hub degree have overlap in calculated values. This effect is disregarded within this study.

Two statements can be made based on the results and the conclusions found in this chapter. First, the verification study as performed by [de Vos \(2018\)](#) in chapter 6.3 cannot be regarded as a verification for the objective functions. Not only does that study contain directed graphs ([ZIE CHAPTER 5](#)), the number and function of the nodes differs as well. However, the first case study performed by [de Vos \(2018\)](#) falls within the limitations of the  $R$ -value and the F2 System Robustness. This case study is further studied in the next chapter, [Case Study Network Analysis](#).

# Chapter 7

## Case Study Network Analysis

This chapter contains a second network analysis, based on the frigate case study by de Vos (2018). The case study in this thesis research aims to confirm the conclusions drawn following the verification study. More importantly, the case study bridges the theoretically approached verification study and the actual ship design. The study approach is described in section 7.1 and consists of five steps. The first step, defining the input, has already been performed in subsection 5.3.1 but is briefly recapitulated in section 7.1. The second step is part of the input as well; the definition of the minimum and maximum values is described in section 7.2. The calculated  $R$ -values for the separate subsystems can be found in section 7.3, this is the third step. The combination of the robustness measures for the five subsystems is the fourth step, in section 7.4. The fifth and final step is, in line with the verification study, the comparison between the  $R$ -values and the F2 system robustness values.

### 7.1 Case Study Approach

Figure 7.1 shows the different parts of this case study; these parts form the structure for this chapter. However, structure of the diagram itself remained unmentioned within the introduction. The upper white box (*Case Study frigate: 12 Systems*) represents the 12 topologies selected in Figure 5.12. These 12 topologies are compared using three robustness measures: the original F2 Robustness, the F2 robustness of the 5 combined subsystems (left dark-blue box) and the  $R$ -value of the 5 combined subsystems (right dark-blue box). This comparison takes place in **step 4** (original F2 versus combined F2) and **step 5** (original F2 versus  $R$ -value). The topologies are generated and selected using their values for the objective functions, mainly focusing on the second objective function (F2 System Robustness). These values are represented by the dark blue box on top of the flowchart.

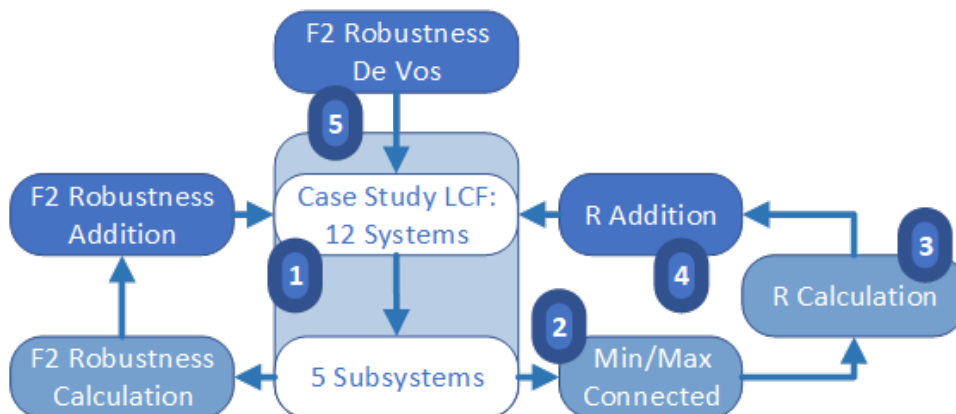


Figure 7.1: Flowchart Case Study Approach

The lower white box (*5 Subsystems*) represents the five subsystems which can be found in Figure 5.15. **Step 1** is the adaption from the total frigate system (Figure 5.14) to the five subsystems based on difference in flow for each connection. The five steps of the case study are:

1. Convert the sample set graphs into separate subsystems
2. Define the minimum and maximum connected graphs
3. Calculate the R-value for the separate subsystems
4. Combine the separate R-values to a single robustness value for the total system
5. Compare total R value to the system robustness

## 7.2 Minimum and Maximum Connected Graph

For the second step, the maximum and minimum values are defined. The maximum and minimum values can be defined in two ways based on the conclusions from the verification set: a constant topology generation or a constant maximum/minimum topology.

### 7.2.1 Constant Topology Generation

The first option is based on the programming approach of the minimum and maximum connected set. In line with the verification study, the minimum connected set contains a hubmatrix in which all hub nodes are minimal connected (5–6–7–8). The maximum connected set includes a fully connected hubmatrix; the supplier-hub and hub-user connections remain constant for the minimum and maximum connected graphs as shown in Figure 7.2. The main advance of this approach is that the maximum and minimum graph are generated automatically. The order in which the hub nodes are connected remains arbitrary for the minimum connected set; apart from this choice, the software determines the graphs.

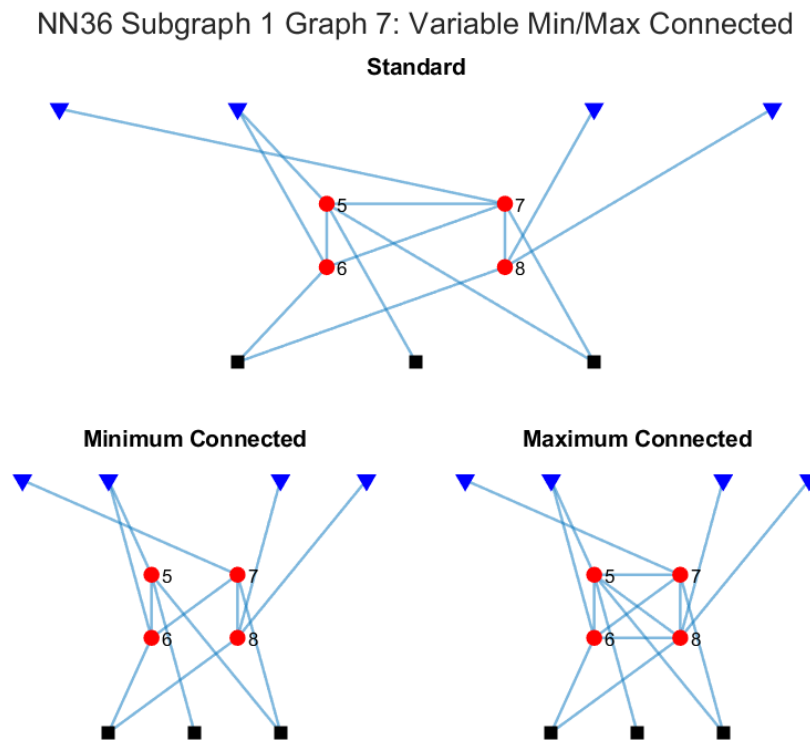
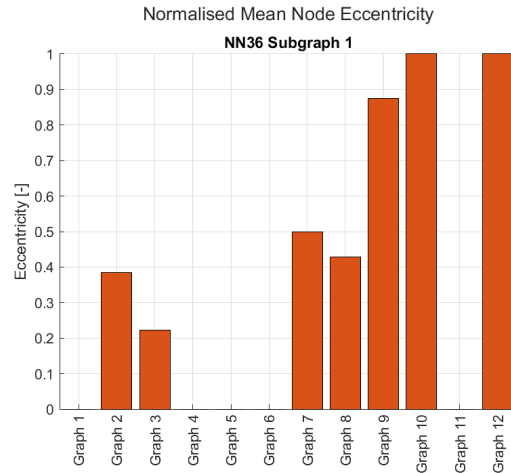
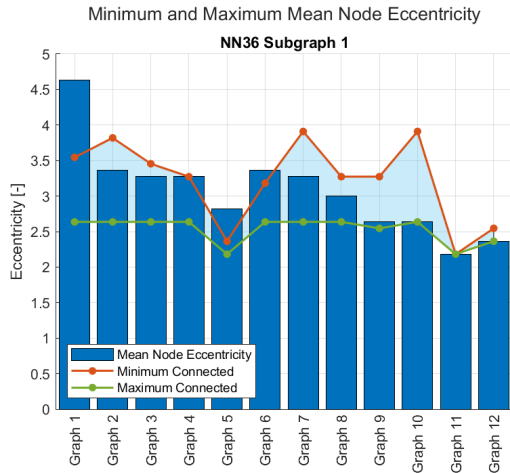


Figure 7.2: Normalised and Unnormalised Objective Function 2: System Robustness (NH8NS6)

The plots for the graph measure *mean node eccentricity* in Figure 7.3 show the disadvantage of this definition for the maximum and minimum connected graphs: the graph measure values are not constant for all graphs. In contrary to the fifth verification set (*NH8NS6*), the way the supplier nodes and user nodes are connected to the hubmatrix differs per graph causing a varying plot instead of a constant line. Moreover, if a supplier or user node is double connected to the hubmatrix, already some redundancy is present within the minimum connected set. Despite the relative nature of the maximum and minimum set, this undermines the normalisation, e.a., the zero value does not represent the worst robustness.



(a) Mean Node Eccentricity with Variable Minimum/- Maximum Connected Graph

(b) Normalised Mean Node Eccentricity with Variable Minimum/Maximum Connected Graph

Figure 7.3: (Normalised) Mean Node Eccentricity with Variable Minimum/Maximum Connected Graph (NN36 Subsystem 1)

### 7.2.2 Constant Maximum/Minimum Topology

The second option for the maximum and minimum connected topology is not generated automatically: the graphs are defined manually. The goal of this method is to recreate the constant plot for the maximum and minimum values, mirroring the constant minimum and maximum plots for *NH8NS6*. The minimum graph consists, again, of two parts: a minimum connected hubmatrix with a single connection (5–6–7–8) and supplier-hub and hub-user connections. The first part is the same as for the first option, the second part only consists of a single connection for each supplier node and user node. The maximum graph is approached similarly: a fully connected hubmatrix as part one with two connections to each supplier node and user node. The minimum and maximum connected graphs are shown in [Figure 7.4](#).

NN36 Subgraph 1 Graph 7: Constant Min/Max Connected

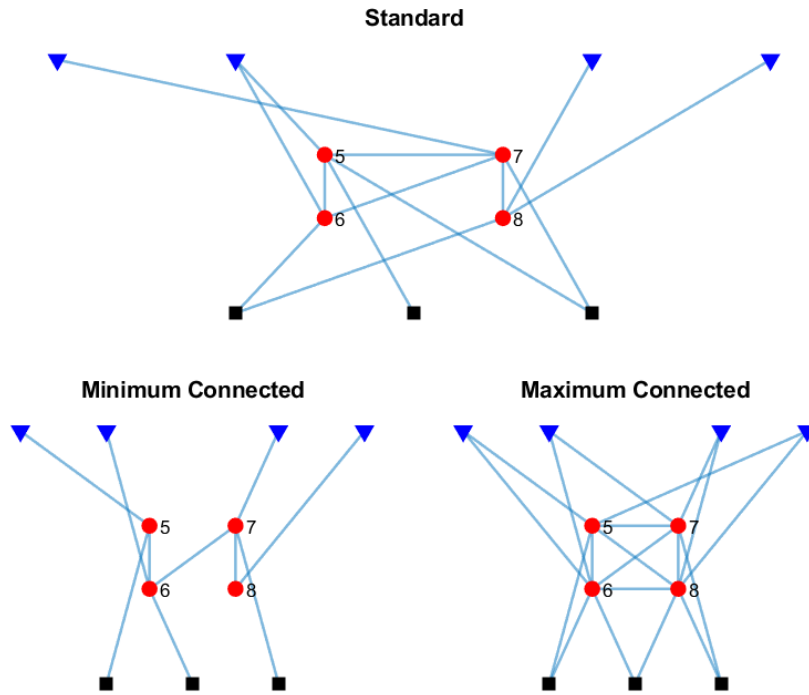
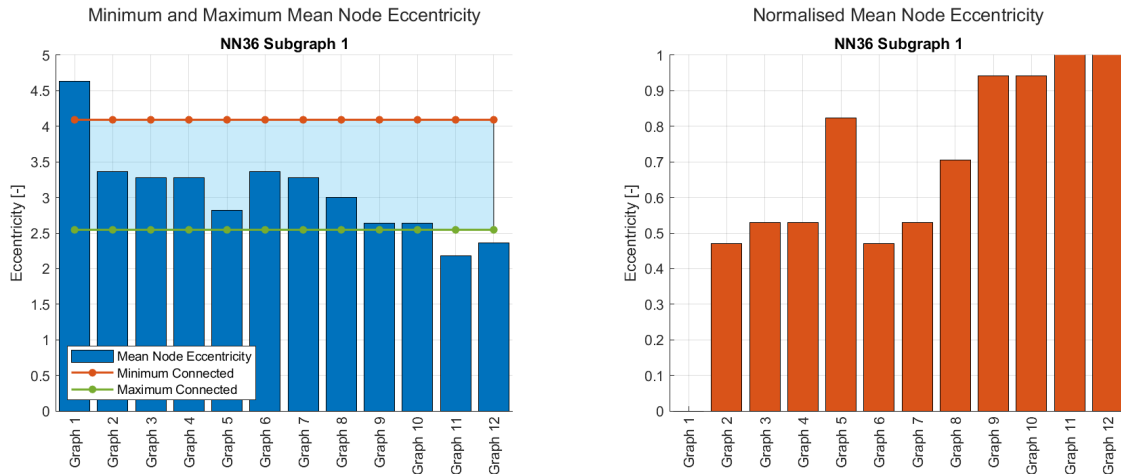


Figure 7.4: Normalised and Unnormalised Objective Function 2: System Robustness (NH8NS6)

The advantage of this option is the constant maximum and minimum plot, in line with *NH8NS6* (Figure 7.5). As mentioned before, the disadvantage is the manual definition of the graphs. Not only does this require a higher time investment, the connections are added arbitrary. Automatically generating these graphs is most definitely possible with better programming, however, improving this is not considered part of this study.



(a) Mean Node Eccentricity with Constant Minimum/Maximum Connected Graph

(b) Normalised Mean Node Eccentricity with Constant Minimum/Maximum Connected Graph

Figure 7.5: Normalised Mean Node Eccentricity with Constant Minimum/Maximum Connected Graph (NN36 Subsystem 1)

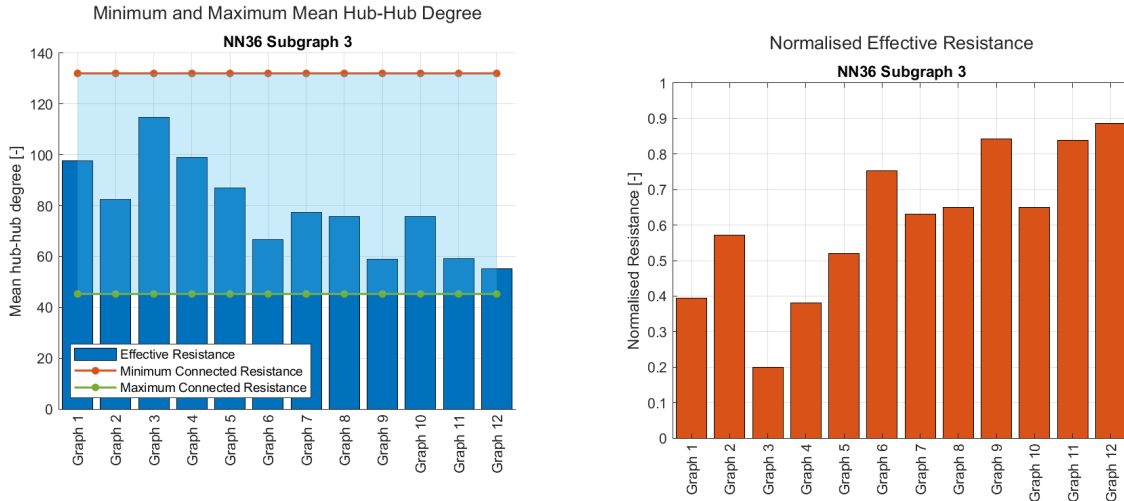
### Maximum/Minimum Value Approach

The second option is selected for this case study because of the more useful results, despite the deviation in programming approach compared to the verification study. An additional pro for the section option is that the last subsystem contains non-zero normalised values with this option, despite the absence of hub nodes. Both options still contain values higher or lower than the maximum/minimum value; some users/suppliers are triple connected or the hubgraph is not connected. These graphs are considered outliers and adjusted to a normalised 0 or 1 value, respectively.

### 7.3 Subsystem R-Calculation

The R-calculation for each subsystem is approached the same way as for the verification sets; this is the **step 3** in the case study. However, one graph measure is not actively included in this case study: *modularity*. To calculate the modularity, a manual grouping of the modules is required. Since the supplier-hub and hub-user connections differ for each graph, such a generally applicable grouping cannot be made for the subsystems. Therefore, all nodes are considered to be part of the same module, meaning that the normalised modularity value is  $\frac{0 - (-0.5)}{1 - (-0.5)} = 0.33$  for all graphs.

The resulting values of the graph measures are comparable to [Figure 7.6](#), which shows the effective resistance measure for the third subgraph. Some increase in values can be found, but since this plot only represents one fifth of the total system, the ascending trend is not without deviations.



(a) TITLE: Constant Minimum/Maximum Connected Graph

(b) Normalised

Figure 7.6: Effective Resistance with Minimum/Maximum Connected Graph (Subsystem 3)

In [Figure 7.7](#), the combined robustness value for the fifth subsystem can be found. The measures *mean hub-hub degree* and *hub-edge connectivity* are obviously zero for this subsystem due to the absence of a hubgraph. Furthermore, only three possible topologies can be found for the fifth subsystem, grouping 2,6&11, 5&12 and the other graphs. The second group only increases the total values slightly in comparison to the third group, mainly based on a higher *number of cycles*.

The robustness for the first five graphs of the second subsystem ([Figure 7.8](#)) does not contain values for the hubgraph-related measures. [Figure 5.15](#) shows that this hubmatrix only contains three nodes, meaning that the graph is either minimum connected (or less) or maximum connected. The rise between the first five and next seven graphs is damped by the second normalization of the *R*-value, which weights comparable graph measure values more heavily than values in a wide range. Since the modularity is constant for all values, this graph measure functions as a damper for the *R*-value.

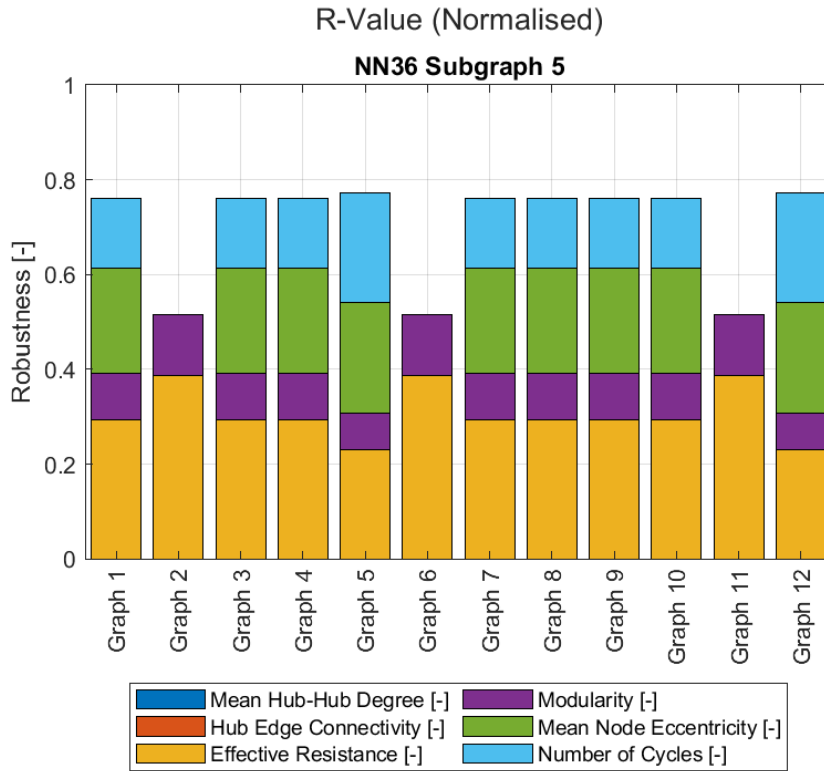


Figure 7.7: R-Value (Subsystem 5)

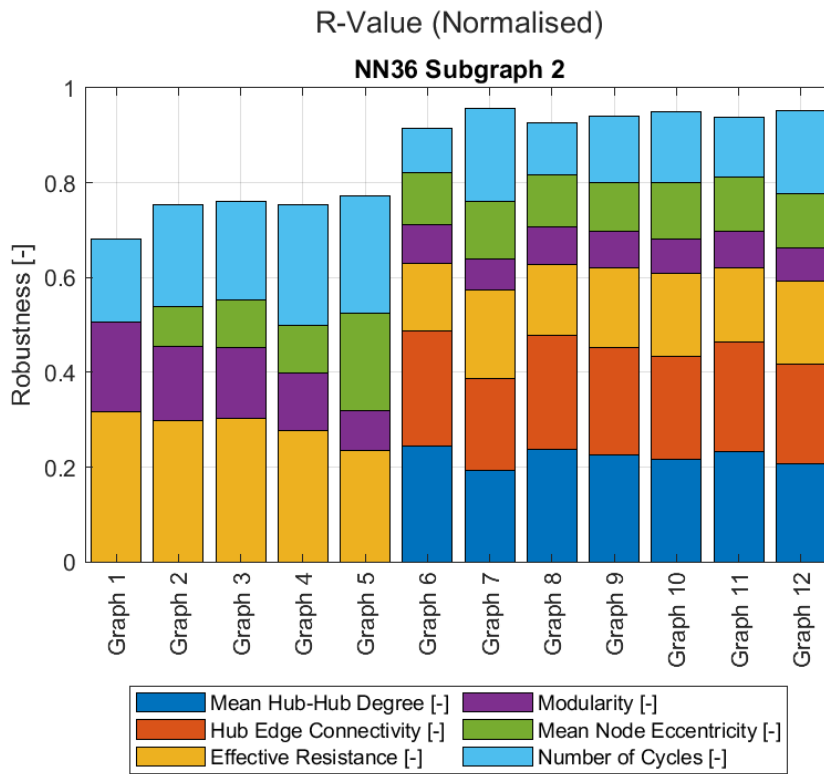


Figure 7.8: R-Value (Subsystem 2)

## 7.4 Combining the R-Values

**Step 4** of the case study is the combining of the robustness values for the five subsystems to a single value. First, the F2 system robustness for the total system is compared to the values of the five added subsystems in [Figure 7.9](#). The two plots show exactly the same downward trend, with a constant vertical shift. This shift originates in the normalisation using the number of nodes: since this is done separately for the combined value, about half of the nodes are counted twice. However, this figure suggests that adding separate values is a valid alternative to calculating the complete system for F2 system robustness.

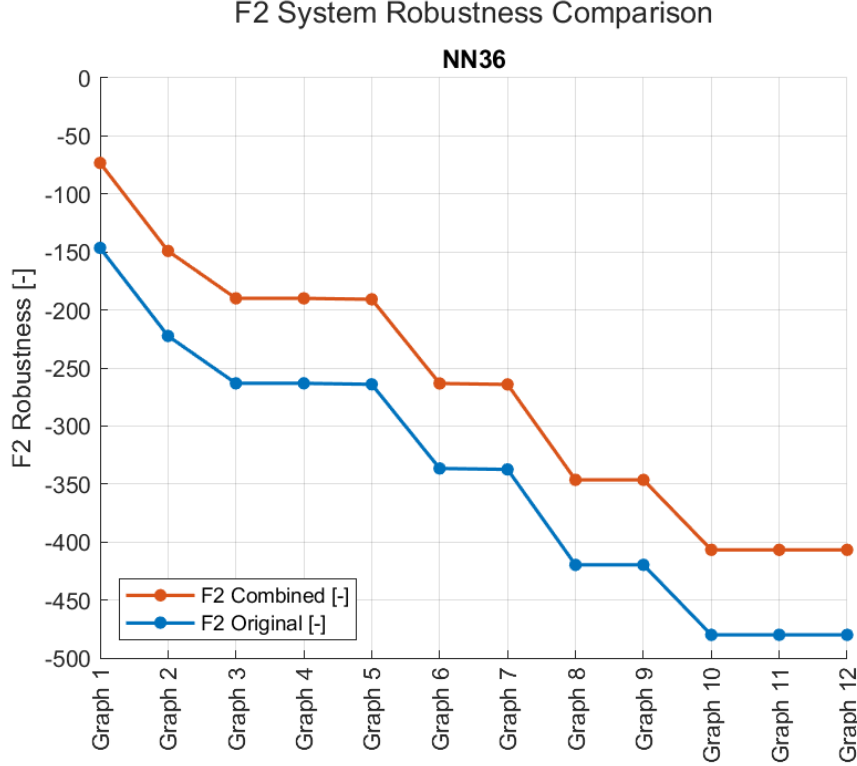


Figure 7.9: Combined and Original R-Value

In [Figure 7.10](#) shows the added  $R$ -values of the five subsystems, the second and fifth shown in [Figure 7.8](#) and [Figure 7.7](#). All five subsystems are valued equally using [Equation 7.1](#); the  $R$ -value ranges between 0 and 1 by simply dividing the total value by 5. The combined  $R$ -value shows an increasing trend apart from two outliers: graph 2 and graph 11. Together with graph 6, these graphs show the lowest  $R$ -value for the fifth subsystem ([Figure 7.7](#)). This subsystem is not included in the F2 System Robustness calculation because of the absence of a hubmatrix; therefore, it provides additional information in rating the graphs.

$$R_{combined} = \frac{1}{5}(R_{sub1} + R_{sub2} + R_{sub3} + R_{sub4} + R_{sub5}) \quad (7.1)$$

[Figure 7.11](#) shows the total  $R$ -value without the final normalisation; the graph measures are normalised but simply added to form the  $R$ -value per subsystem ([subsection 6.3.3](#)). In contrary to [Figure 7.10](#), this figure shows that the normalised graph measure values increase significantly over the range of the graphs. In this plot, lower values are more strongly compensated by higher values due to the higher range in calculated values for each subsystem. This can be considered a negative effect due to the weakest link principle.

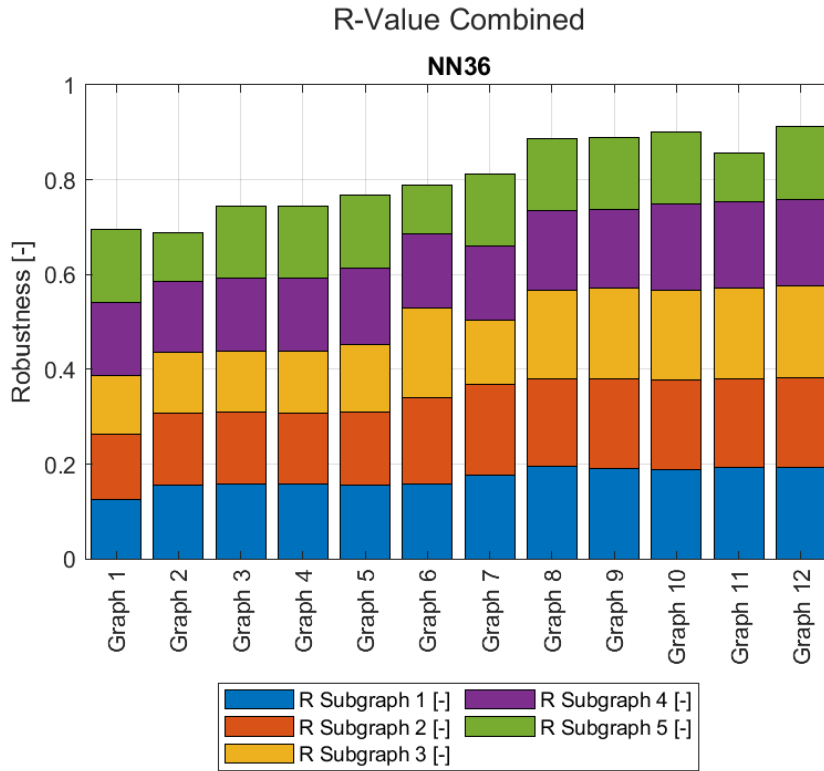


Figure 7.10: R-Value (NN36)

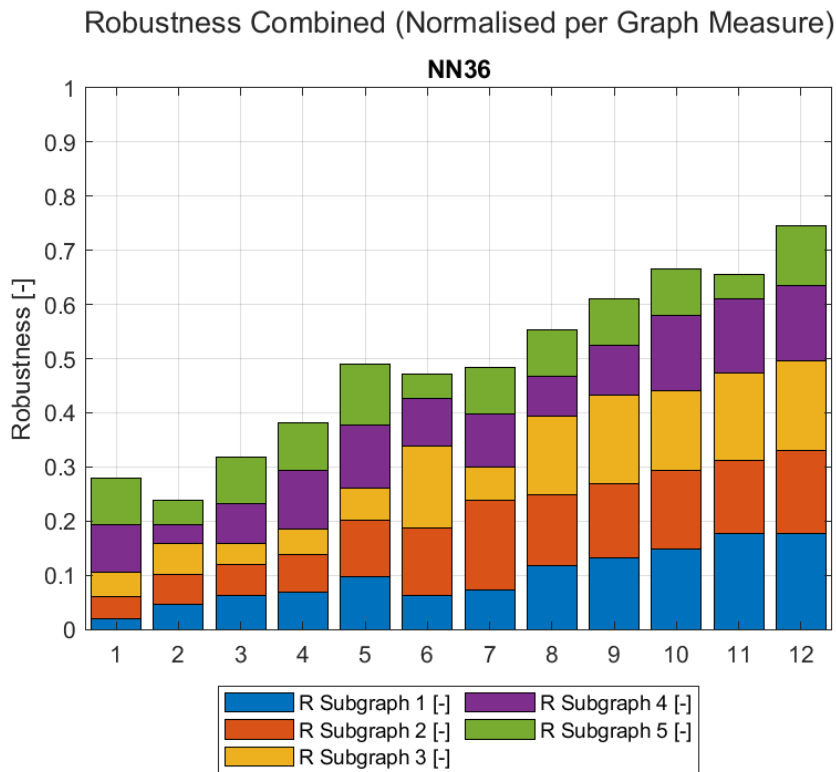


Figure 7.11: Robustness Normalised Graph Measures (NN36)

### 7.4.1 Subsystem Coupling

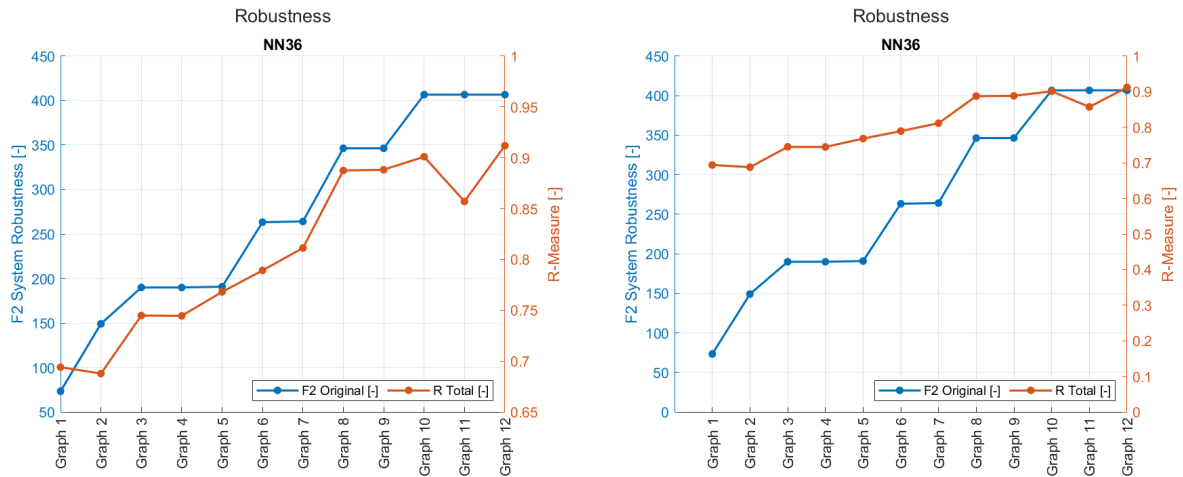
Figure 7.9 shows that, for F2 system robustness, superposition holds; the difference is a constant value but the incline remains the same. However, this statement is not proven for the  $R$ -value. Some considerations can be made to nuance the simply added  $R$ -values for the five subsystems.

- In line with the combined normalisation of the  $R$ -value (the deviation of the graph measures is included in the value), such a normalisation step could be made when adding the subsystems. This leads to a higher overall value for systems with a comparable robustness for the subsystems; one positive outlier does not simply increase the total value.
- Some subsystems have a higher number of nodes than other systems, a correction factor could be included to favour more robust smaller systems over more robust larger systems to increase the robustness value of the weakest link.
- A correlation factor could be included to represent the relation between the subsystems. If a subsystem is connected to multiple other systems, its robustness could be considered more influential than the robustness of less connected systems.

## 7.5 Robustness Comparison

The final part of this case study, **step 5**, is the comparison of the original total F2 system robustness and the total combined  $R$ -value for the sample set. Figure 7.12a and Figure 7.12b show the same plot but with different y-axes. Both figures show positive F2 values to enable a good comparison between the robustness measures. The most noticeable trend in Figure 7.12a is that the measures show a comparable trend up to graph 9. The last three graphs show the flattened curve of the  $R$ -value due to the "modularity normalisation". Moreover, F2 does not include values for subsystem 5 because of the absent hubgraph. The fifth subsystem causes the dip in the  $R$ -value for graph 2 and 11, magnified by this axis selection.

Figure 7.12b intuitively suggests that all  $R$ -values are relatively high with no values below 0.7. The increased values are mainly caused by the second normalisation within the  $R$ -calculation, as shown in Figure 7.10 (with second normalisation layer) and Figure 7.11 (without second normalisation layer). The  $R$ -value plots in Figure 7.12 do not show the step-wise increase that can be found in the F2 plots. This is most likely caused by the effect of supplier-hub and hub-user connections on the robustness of the subsystems and the fifth subsystem; both elements are not included in the F2 system robustness.



(a) Constant Minimum/Maximum Connected Graph

(b) Normalised

Figure 7.12: R-Value and F2 System Robustness (NN36)

### 7.5.1 Application

Figure 7.13 provides an example of the application of the robustness measures in the marine industry. The indicated system claim in Figure 7.13a shows that, in general, a more robust system means a higher system claim. The second figure, Figure 7.13b shows the unit *robustness per system claim*, as calculated using Equation 7.2. This dimensionless plot suggests that graph 8 provides the highest robustness for

the number of nodes and edges present within the system. Graph 9, 10 and 12 have a higher robustness, however, the practical optimum can be found for systems with less edges than those three graphs. On the other hand, graph 5 shows an inefficient use of edges, since the robustness is not compensated by the high system claim.

$$\frac{R}{F1} = \frac{R}{R_{norm}} \cdot \frac{F1_{norm}}{F1} \quad (7.2)$$

$$\frac{F2}{F1} = \frac{F2}{F2_{norm}} \cdot \frac{F1_{norm}}{F1}$$

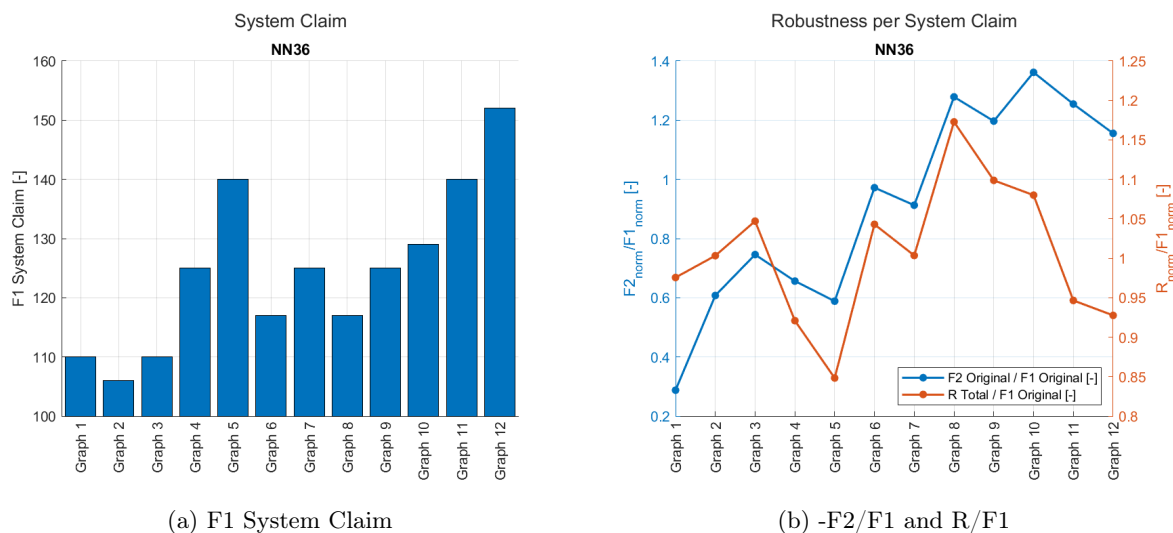


Figure 7.13: System Claim and Robustness per System Claim (NN36)

## 7.5.2 Case Study Conclusion

The main aim of this chapter is twofold: to confirm the conclusions drawn following the verification study and to bridge the theoretically approached verification study and the actual ship design. First, the conclusions of the verification study, including the limitations mentioned, can be confirmed. Again, some limitations are added to the scope concerning the applicability of these conclusions. To begin with, the approach to define the minimum and maximum connected graph is adjusted in comparison to the verification study. This means that the  $R$ -values for the verification study have a different meaning than the  $R$ -values within the case study. However, based on the fifth verification set ( $NH8NS6$ ), this seems like an adjustment in line with the intended purpose of the maximum and minimum values.

Next, modularity is omitted from the calculations because of the limited possibilities using manually defined graph modules. This adjustment is preventable in future studies by automatising the grouping the graph modules, but this step is not yet made.

One of the main differences between the total combined  $R$ -value and the original  $F2$  system robustness measure is the inclusion of subsystem 5 within the  $R$ -calculation. For now, only the robustness of existing topologies is calculated, but this alternative robustness calculation might influence the topology generation and create systems with more robust subsystems and total systems.

Following this statement concerning the topology generation brings us to the bridge to actual early-stage ship design. The two  $R$ -approaches in Figure 7.10 and Figure 7.11 show different trends, but figures both suggest that a system can be split in subsystems in order to calculate the robustness of the total system. A possible next step could be analysing an entire frigate system robustness instead of only the subsystems required to operate a single weapon.

# Chapter 8

## Conclusion, Discussion and Reflection

This chapter is the final chapter of this master thesis and concludes the study performed. In [section 8.1](#), the research goal is addressed. Moreover, the different parts of the knowledge gap are addressed in [subsection 8.1.1](#) and [subsection 8.1.2](#). The discussion forms the second part of this chapter and can be found in [section 8.2](#). This section provides the main limitations of this study and suggests interesting topics for further research. To conclude, [section 8.3](#) reflects on the deliverables defined in [subsection 1.2.6](#).

### 8.1 Conclusions

This study aimed to *improve the approach for on-board distribution system robustness estimation in early-stage ship design*, through comparing and verifying the robustness approach by [de Vos \(2018\)](#) using the robustness approach by [Van Mieghem, Doerr, et al. \(2010\)](#). Based on the conclusions found in literature and this research, on-board distribution system robustness estimation in early-stage ship design is deemed improved in comparison to the robustness approach by [de Vos \(2018\)](#) for the following reasons:

- The concept of robustness is approached from more than just the perspective of reconfigurability. Other aspects, such as independent subsystems and redundancy, are included in the new robustness measure as well. Therefore, the measured network property is more in line with the design rules concerning robustness.
- The supplier-hub and hub-user connections are included in this measure, instead of an exclusive focus on the hub-hub connections. The presence of vital users influences the robustness of the system, however, the choice of graph measures still highly values the properties of the hub-hub graph.
- The fifth subsystem of the case study is included in the robustness calculations. While [de Vos \(2018\)](#) excludes data distribution systems from his scope, the robustness approach by [Van Mieghem, Doerr, et al. \(2010\)](#) is aimed to be applicable to all kinds of networks, with examples such as the internet and power grids. The broad scope of this last approach gives reason to include the data distribution system in the robustness calculation.

#### 8.1.1 Marine Assumptions

The knowledge gap as defined in [subsection 1.2.3](#) exists of two parts. First, if the robustness approach by [Van Mieghem, Doerr, et al. \(2010\)](#) is currently not applicable to on-board distribution systems, what assumptions must be made to transform the this approach to a robustness approach that can be applied to distribution systems on-board ships? The first conclusion to address this knowledge gap is clear: the robustness approach by [Van Mieghem, Doerr, et al. \(2010\)](#) can be used to perform a robustness estimation of on-board distribution systems in early-stage ship design. [Equation 4.2](#) shows a generally applicable robustness measure, which can be used to estimate the robustness of any given network within the boundaries of graph theory. Concerning the second part of this question, for the specific application within maritime context, some considerations have been made.

$$0 \leq R_{j,i} = \frac{|s^T t|}{\|s\|_q \cdot \|t\|_q} \leq 1 \quad (4.2)$$

### Edge Differentiation

The case study system in [chapter 7](#) consists of five subsystems, each distributing a different flow which can only be transported through connections that physically match the flow type. This differentiation is not part of the  $R$ -value as defined by [Van Mieghem, Doerr, et al. \(2010\)](#), but can be included by analysing the separate subsystems independently. Superposition is assumed in determining the total robustness value; no interaction between subsystems is yet included in the robustness measure.

### Topology Vector $|t|$ Definition

[Van Mieghem, Doerr, et al. \(2010\)](#) does not define which graph measures should be part of the  $|t|$ -vector within the robustness calculation. The chosen graph measures are assumed to represent the three robustness properties as defined by [Klein Woud & Stapersma \(2016\)](#) for distribution systems on-board ships: independent subsystems, redundancy and reconfigurability.

### Weight Vector $|s|$ Definition

As stated, the graph measures are selected based on their indication of certain robustness properties. Dependent on the type of distribution system or the operational profile of said system, the relevant robustness properties change. This change can be expressed using the weight vector  $|s|$ , which values the used graph measures. Within this study, the weight vector is not studied; for  $i = 1, \dots, N$ ,  $s_i = 1$ .

### Minimum/Maximum Connected Graph

For the normalisation of the graph measures, the minimum and maximum connected graphs are defined. A subsystem is minimum connected if all nodes are connected with  $N - 1$  edges; the subgraph containing the hub nodes is assumed to be connected too. The second assumption limits the possible minimum topologies but the number of required edges stays constant. The maximum connected graph is a system with a fully connected hub-graph and two edges connecting each supplier node and user node. All connections are at least duplicated, which can be considered as maximally robust for maritime systems. In other words, all suppliers and users within the maximal connected system are considered vital and should be approached as such.

### Time-Independent Analysis

Within early-stage ship design, the distribution systems are described using a list of main components and a single-line diagram. Therefore, the temporal elements of the  $R$ -value analysis are assumed to be out of the scope of this study. The distribution systems are analysed in steady state, providing a single service.

## 8.1.2 Robustness Approach Verification

The second part of the knowledge gap is: to what extent can the robustness approach by [de Vos \(2018\)](#) be verified using a general robustness approach such as the approach by [Van Mieghem, Doerr, et al. \(2010\)](#)? The answer to this question is split in two for the two performed studies by [de Vos \(2018\)](#): a verification study and a case study.

### Verification Study Verification

The verification study as performed by [de Vos \(2018\)](#) cannot be verified using the robustness approach by [Van Mieghem, Doerr, et al. \(2010\)](#) for the following reasons:

- Comparing systems with a different number of nodes is considered a faux-pas within graph theory, which provides the mathematical basis for the  $R$ -value calculation. Not only the total number of nodes varies, also the number of hub-nodes is not constant for the verification set. This leads to robustness values that are not in line with the expected (normalised) values.
- Directed edges are part of the network service ([Van Mieghem, Doerr, et al., 2010](#)) or operational architecture ([Brefort et al., 2018](#)), and not a part of the network service ([Van Mieghem, Doerr, et al., 2010](#)) or logical architecture ([Brefort et al., 2018](#)). Therefore, this network property should not be included when analysing the topology.

### Case Study Verification

In contrary to the verification study, the case study by [de Vos \(2018\)](#) is verified using the robustness approach by [Van Mieghem, Doerr, et al. \(2010\)](#). Within the case study, a system with a constant number

of nodes is compared. These nodes are connected through undirected edges; therefore, only the logical architecture is analysed. Despite the difference in represented robustness properties, the overall trend in robustness value is considered comparable.

## 8.2 Discussion and Recommendations

To complete a comparison study within the given time-frame, assumptions have been made. First, the two robustness approaches have been selected based on their availability and applicability on on-board distribution systems within the *logical architecture* [Brefort et al. \(2018\)](#) context. However, more methods are available and should be studied in order to obtain a full grasp of the state-of-the-art robustness research.

Second, the assumptions done in [subsection 8.1.1](#) have proven useful in limiting the scope and applying the approach by [Van Mieghem, Doerr, et al. \(2010\)](#) to on-board distribution systems, however, most aspects require additional research:

- The interaction between subsystems is not included in the  $R$ -value, while this might prove an interesting point of research. The interaction can appear as a weakest link situation, or a subsystem might take over the functionality of another system in case of a failure or attack.
- Basing the measured robustness properties on marine design rules builds a bridge between maritime research and general robustness research and is therefore desirable. However, the selection of robustness properties and corresponding graph measures is a fundamental aspect that is not thoroughly covered within this study. Especially the graph measure selection and matching weight vector could be covered in more detail. In future research, it is recommended to further study the mutual influence of the graph measures, what robustness property is measured using a certain graph measure and the influence of the weight vector.
- The normalisation of the graph measures has played a more significant role in the robustness calculation than expected. Moreover, the approach for minimum and maximum connected graph differs for the calculated  $R$ -value in [chapter 6](#) and [chapter 7](#), while F2 System Robustness is normalised differently altogether. This normalisation might be the key to comparing distribution systems, possibly with a variable number of nodes. Therefore, these first three points are considered equally important in estimating robustness in early-stage ship design.

### 8.2.1 R-Value Calculation

Due to the normalisation approach of the total  $R$ -value,  $R = 1$  if all entries in  $|t|$  are equal. This means that, if all graph measures are  $t_i = 0.5$ , the  $R$ -value can still have a maximum value. The opposite effect is present as well: if a single graph measure has a deviating value from the other measures, the  $R$ -value decreases. This effect is demonstrated in [Figure 6.19](#); modularity decreases with more connections between independent subsystems. The effect is desirable that a negative measure is valued more heavily than a positive measure; engineering practice favours an underestimation over an overestimation. However, a high  $R$ -value for comparable, low, graph measures should be avoided at all times. The possible influence of a weight vector in changing or avoiding this effect has not been part of this study.

### 8.2.2 Limitation

The  $R$ -value, as applied within this study, provides an insight in the robustness of on-board distribution systems during early-stage ship design. Suppose the three points of discussion are resolved, one major limitation remains: the number of nodes should remain constant for all compared systems. Moreover, the function of these nodes should be constant as well: a fixed number of suppliers, hubs and users. With the restrictions in allowed connections ([de Vos, 2018](#)), only a very strongly limited variation scope remains. This scope allows for a proper graph comparison, but the applicability of the  $R$ -value is limited within maritime industry.

### 8.2.3 Implementation

This study can be applied within the maritime industry in two ways: first, this study provides insight in the measuring approach of different robustness aspects. While a concept such as mean degree or modularity might initially not mean too much to maritime engineers, understanding these graph measures assists in itself in making a trade-off between different system qualities in early-stage ship design. However, not understanding the robustness calculation or the graph measures properly might result in faulty trade-offs leading to unreliable distribution systems.

Second, the long-term application requires comparison between systems with different components and

different number of components. In an ideal situation, maritime engineers can use a topology generation tool that generates a topology with the following input: number and type of user components and type and level of required robustness, system claim, operability and sustainability. The output would be a list of five (or so) topologies containing different robustness values and different supplier and hub components. Such a tool can assist in the transition to renewable fuels or more sustainable system components, since the total design space can be explored for each system.

### 8.3 Reflection

In [subsection 1.2.6](#), a list of deliverables is introduced. The research is considered to be finished when the following *deliverables* have been completed. At the moment, not all deliverables have been completed as initially intended due to a limitation of the scope. The review of the deliverables forms the academic reflection of this study.

- *An overview of assumptions required to apply the robustness approach by Van Mieghem, Doerr, et al. (2010) on simplified networks of distribution systems on-board ships.*

The assumptions have been made throughout this study, both in the literature part as well as in the network comparison part. The overview can be found earlier in this chapter in [subsection 8.1.1](#).

- *A comparison of the resulting robustness measure of both approaches of the graphs in section 6.3 in de Vos (2018), including the assumptions made for both approaches.*

In [chapter 6](#), a comparison of the graphs in section 6.3 and the comparison for four other verification sets can be found.

- *A modified MATLAB script in which the robustness approach by Van Mieghem, Doerr, et al. (2010) is implemented in the robustness approach by de Vos (2018).*

A schematic representation of the calculation of the  $R$ -value using a *MATLAB* script can be found in [Appendix D](#). This  $R$ -value is not implemented in the ATG-Tool; generating new topologies is not part of the scope. However, the ATG-Tool is used to create a sample set for the case study performed in [chapter 7](#).

- *A comparison between the results returned by the modified and original robustness MATLAB script, including the assumptions made for both approaches.*

The comparison and analysis of the robustness values according to the two approaches can be found in [section 7.5](#). The steering effect of the adjusted  $R$ -value has not been studied since it is not part of the scope.

- *A conclusion, stating whether or not the robustness approach by Van Mieghem, Doerr, et al. (2010) improves the robustness approach by de Vos (2018): to what extent and in what way. Does the first approach verify the second robustness approach?*

This final conclusion can be found in the first section of this chapter, [section 8.1](#).

# References

- Alshattnawi, S. K. (2017). Smart water distribution management system architecture based on internet of things and cloud computing. In *2017 international conference on new trends in computing sciences (ictcs)* (pp. 289–294). IEEE. doi: 10.1109/ICTCS.2017.31
- BBC. (2019). Norway cruise ship evacuated after engine problems. *BBC*. Retrieved 2021, from <https://www.bbc.com/news/world-europe-47680055>
- Bollobás, B. (1998). *Modern graph theory* (Vol. 184). New York: Springer International Publishing and Springer.
- Bondavilli, A., Bouchenak, S., & Kopetz, H. (2016). *Cyber-physical systems of systems: Foundations - a conceptual model and some derivations : the amadeos legacy* (Vol. 10099. State-of-the-art survey). Cham: Springer.
- Brefort, D., Shields, C., Habben Jansen, A., Duchateau, E., Pawling, R., Droste, K., . . . Kana, A. A. (2018). An architectural framework for distributed naval ship systems. *Ocean Engineering*, *147*, 375–385. doi: 10.1016/j.oceaneng.2017.10.028
- Brier, M. R., Thomas, J. B., Fagan, A. M., Hassenstab, J., Holtzman, D. M., Benzinger, T. L., . . . Ances, B. M. (2014). Functional connectivity and graph theory in preclinical alzheimer’s disease. *Neurobiology of aging*, *35*(4), 757–768. doi: 10.1016/j.neurobiolaging.2013.10.081
- Britton, T., Deijfen, M., & Martin-Löf, A. (2006). Generating simple random graphs with prescribed degree distribution. *Journal of Statistical Physics*, *124*(6), 1377–1397. doi: 10.1007/s10955-006-9168-x
- Calinescu, R. C., & Jackson, E. (Eds.). (2011). *Foundations of computer software: Modeling, development, and verification of adaptive systems* (Vol. 6662). Heidelberg: Springer.
- Cats, O., Koppenol, G.-J., & Warnier, M. (2017). Robustness assessment of link capacity reduction for complex networks: Application for public transport systems. *Reliability Engineering & System Safety*, *167*, 544–553. doi: 10.1016/j.res.2017.07.009
- Cerulli, R., Raiconi, A., & Voss, S. (Eds.). (2018). *Computational logistics* (1st ed. 2018 ed., Vol. 11184). Cham: Springer International Publishing and Imprint: Springer.
- Çetinay, H., Koç, Y., Kuipers, F. A., & van Mieghem, P. (2019). Topology-driven performance analysis of power grids. In P. Palensky, M. Cvetković, & T. Keviczky (Eds.), *Intelligent integrated energy systems* (pp. 37–54). Cham: Springer International Publishing. doi: 10.1007/978-3-030-00057-8\_{\text{underscore}}2
- Çetinay, H., Kuipers, F. A., & van Mieghem, P. (2018). A topological investigation of power flow. *IEEE Systems Journal*, *12*(3), 2524–2532. doi: 10.1109/JSYST.2016.2573851
- Chalfant, J. (2015). Early-stage design for electric ship. *Proceedings of the IEEE*, *103*(12), 2252–2266. doi: 10.1109/JPROC.2015.2459672
- Cuadra, L., Salcedo-Sanz, S., Del Ser, J., Jiménez-Fernández, S., & Geem, Z. (2015). A critical review of robustness in power grids using complex networks concepts. *Energies*, *8*(9), 9211–9265. doi: 10.3390/en8099211
- de Vos, P. (2018). *On early-stage design of vital distribution systems on board ships* (Doctoral dissertation, Delft University of Technology). doi: 10.4233/UUID:EB604971-30B7-4668-ACE0-4C4B60CD61BD

- de Vos, P., & Stapersma, D. (2018). Automatic topology generation for early design of on-board energy distribution systems. *Ocean Engineering*, *170*, 55–73. doi: 10.1016/j.oceaneng.2018.09.023
- DOERRY, N., Earnesty, M., Weaver, C., Banko, J., Myers, J., Browne, D., ... Balestrini, S. (2014). *Using set-based design in concept exploration*. Arlington, VA, USA.
- Ellens, W., & Kooij, R. E. (2013). Graph measures and network robustness. Retrieved from <http://arxiv.org/pdf/1311.5064v1>
- Evans, J. H. (1959). Basic design concepts. *Journal of the American Society for Naval Engineers*, *71*(4), 671–678. doi: 10.1111/j.1559-3584.1959.tb01836.x
- Gaspar, H. M., Rhodes, D. H., Ross, A. M., & Erikstad, S. O. (2012). Addressing complexity aspects in conceptual ship design: A systems engineering approach. *Journal of Ship Production and Design*, *28*(4), 145–159. doi: 10.5957/JSPD.28.4.120015
- GeeksforGeeks (Ed.). (2021). *Transmission modes in computer networks: Simplex, half-duplex and full-duplex*. Noida. Retrieved from <https://www.geeksforgeeks.org/transmission-modes-computer-networks/>
- Gross, J. L., Yellen, J., & Zhang, P. (Eds.). (2014). *Handbook of graph theory*. Boca Raton: CRC Press.
- Habben Jansen, A. C. (2020). *A markov-based vulnerability assessment of distributed ship systems in the early design stage* (Doctoral dissertation, Delft University of Technology). doi: 10.4233/UUID:F636539F-64A5-4985-B77F-4A0B8C3990F4
- Habben Jansen, A. C., de Vos, P., Duchateau, E. A. E., & Stapersma, D. (2020). A framework for vulnerability reduction in early stage design of naval ship systems. *Naval Engineers Journal*(No. 132-2).
- Habben Jansen, A. C., Duchateau, E. A. E., & Kana, A. A. (2018). Towards a novel design perspective for system vulnerability using a markov chain. In *Proceedings of the international naval engineering conference and exhibition (inec)*. IMarEST. doi: 10.24868/issn.2515-818X.2018.028
- Haimes, Y. Y. (2009). On the definition of resilience in systems. *Risk analysis : an official publication of the Society for Risk Analysis*, *29*(4), 498–501. doi: 10.1111/j.1539-6924.2009.01216.x
- Han, C. H. (2010). Strategies to reduce air pollution in shipping industry. *The Asian Journal of Shipping and Logistics*, *26*(1), 7–29. doi: 10.1016/S2092-5212(10)80009-4
- Handel, T. G., & Sandford, M. T. (1996). Hiding data in the osi network model. In R. Anderson (Ed.), *Information hiding* (pp. 23–38). Berlin, Heidelberg: Springer Berlin Heidelberg.
- Haugen, S., Barros, A., van Gulijk, C., Kongsvik, T., & Vinnem, J. E. (2018). Safety and reliability – safe societies in a changing world.
- He, Z. (2020). *Performance of complex networks* (PhD, Delft University of Technology). doi: 10.4233/UUID:A9AE2B62-0CF8-4CF3-86AF-ABD33BC99080
- Hornby, A. S., & Turnbull, J. (2010). *Oxford advanced learner's dictionary of current english* (8th ed. / managing editor, Joanna Turnbull ed.). Oxford: Oxford University Press.
- ISO/IEC 7498-1 : 1994. (n.d.). Itu-t rec. x.200 (07/94) information technology - open systems interconnection - basic reference model: The basic model.
- Kavitha, T., Liebchen, C., Mehlhorn, K., Michail, D., Rizzi, R., Ueckerdt, T., & Zweig, K. A. (2009). Cycle bases in graphs characterization, algorithms, complexity, and applications. *Computer Science Review*, *3*(4), 199–243. doi: 10.1016/j.cosrev.2009.08.001
- Klein Woud, H., & Stapersma, D. (2016). *Design of auxiliary systems, shafting and flexible mounting: Selected chapters*. Delft.
- Koç, Y., Raman, A., Warnier, M., & Kumar, T. (2016). Structural vulnerability analysis of electric power distribution grids. *International Journal of Critical Infrastructures*, *12*(4), 311. doi: 10.1504/IJCIS.2016.081299
- Lamb, & Thomas (Eds.). (2003). *Ship design and construction: Volume 1* ([New ed.] ed., Vol. I). Jersey City, N.J.: Society of Naval Architects and Marine Engineers.

- Leeuwen, S. P. (2017). *Estimating the vulnerability of ship distributed system topologies* (MSc). Delft University of Technology, Delft.
- Lowe, D. (2020). *Networking for dummies: 12th edition* (12th ed. ed.). Indianapolis: John Wiley and Sons. Retrieved from <https://www.dummies.com/programming/networking/layers-in-the-osi-model-of-a-computer-network/>
- Mijalkov, M., Kakaei, E., Pereira, J. B., Westman, E., & Volpe, G. (2017). Graph: A graph theory software for the analysis of brain connectivity. *PloS one*, *12*(8), e0178798. doi: 10.1371/journal.pone.0178798
- Nguyen, H. P., Hoang, A. T., & Nizetic, S. (2020). The electric propulsion system as a green solution for management strategy of co2 emission in ocean shipping: A comprehensive review. *Int Trans Electr Energ Syst.*(2020;e12580). doi: 10.1002/2050-7038.12580
- Rhodes, D. H., & Ross, A. M. (2010). Five aspects of engineering complex systems emerging constructs and methods. *2010 IEEE International Systems Conference*, 190–195. doi: 10.1109/SYSTEMS.2010.5482431
- Roughgarden, T. (2016). *Course goals and introduction to maximum flow: Lecture #1*. Department of Computer Science, Stanford University.
- Saxena, P. (n.d.). Osi reference model – a seven layered architecture of osi model.
- Scheffers, E. (2021). *Literature review* (Master Thesis Literature Review). Delft University of Technology, Delft.
- Sequeira, A. (2018). *Comptia network+ n10-007 cert guide*. Indianapolis Indiana: Pearson IT Certification.
- Sohlenius, G. (1992). Concurrent engineering. *CIRP Annals*, *41*(2), 645–655. doi: 10.1016/S0007-8506(07)63251-X
- Spruit, J. P., van Bodegraven, K. S., Logtmeijer, R. A., & Parent, J. M. (2009). Survivable naval platform distribution systems and their automation.
- Sui, C., Stapersma, D., Visser, K., de Vos, P., & Ding, Y. (2019). Energy effectiveness of ocean-going cargo ship under various operating conditions. *Ocean Engineering*, *190*, 106473. doi: 10.1016/j.oceaneng.2019.106473
- Sydney, A., Scoglio, C., Schumm, P., & Kooij, R. (2008). Elasticity: Topological characterization of robustness in complex networks. *Bionetics*(08).
- Trajanovski, S., Martin-Hernandez, J., Winterbach, W., & Van Mieghem, P. (2013). Robustness envelopes of networks. *Journal of Complex Networks*, *1*(1), 44–62. doi: 10.1093/comnet/cnt004
- van Lent, J. (2021). *Coevolve: A design journey towards more inclusive and circular medical practices* (Unpublished doctoral dissertation). Delft University of Technology, Delft.
- Van Mieghem, P. (2018). Directed graphs and mysterious complex eigenvalues.
- Van Mieghem, P., Doerr, C., Wang, H., Martin Hernandez, J., Hutchison, D., Karaliopoulos, M., & Kooij, R. E. (2010). A framework for computing topological network robustness. Retrieved from [nas.ewi.tudelft.nl](http://nas.ewi.tudelft.nl)
- Van Mieghem, P., Ge, X., Schumm, P., Trajanovski, S., & Wang, H. (2010). Spectral graph analysis of modularity and assortativity. *Physical review. E, Statistical, nonlinear, and soft matter physics*, *82*(5 Pt 2), 056113. doi: 10.1103/PhysRevE.82.056113
- van Oers, B., & Van Ingens, G., Stapersma, D. (2012). An integrated approach for the design of resilient ship services systems. *INEC 2012: Engineering Naval Capability, Edinburgh, UK*.
- Wang, L., Liu, Q., Dong, S., & Guedes Soares, C. (2019). Effectiveness assessment of ship navigation safety countermeasures using fuzzy cognitive maps. *Safety Science*, *117*, 352–364. doi: 10.1016/j.ssci.2019.04.027
- West, D. B. (2001). *Introduction to graph theory* (2nd ed. ed.). Upper Saddle River, N.J. and London: Pearson Education.

Woud, H. K., & Stapersma, D. (2003). *Design of propulsion and electric generation system*. London: IMarEST - The Institute of Marine Engineering, Science and Technology.

# Appendices

# Appendix A

## Robustness Related Definitions

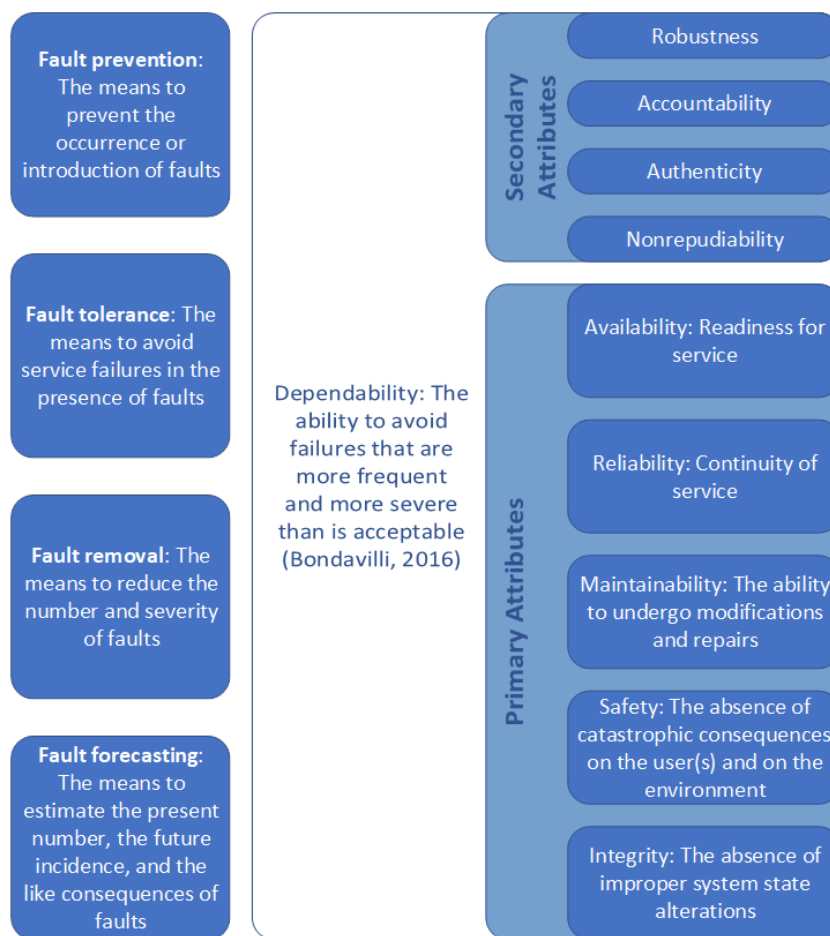


Figure A.1: Overview of Robustness Related Definitions by [Bondavilli et al. \(2016\)](#)

References Figure A.2: ([Habben Jansen et al., 2020](#)), ([Chalfant, 2015](#)), ([He, 2020](#)), ([de Vos & Stapersma, 2018](#)), ([Haimes, 2009](#)), ([Cats et al., 2017](#)), ([Cetinay et al., 2018](#)), ([Çetinay et al., 2019](#)), ([Cuadra et al., 2015](#)), ([Ellens & Kooij, 2013](#)), ([Koç et al., 2016](#)), ([Trajanovski et al., 2013](#)), ([Van Mieghem, Ge, et al., 2010](#)), ([Bondavilli et al., 2016](#))

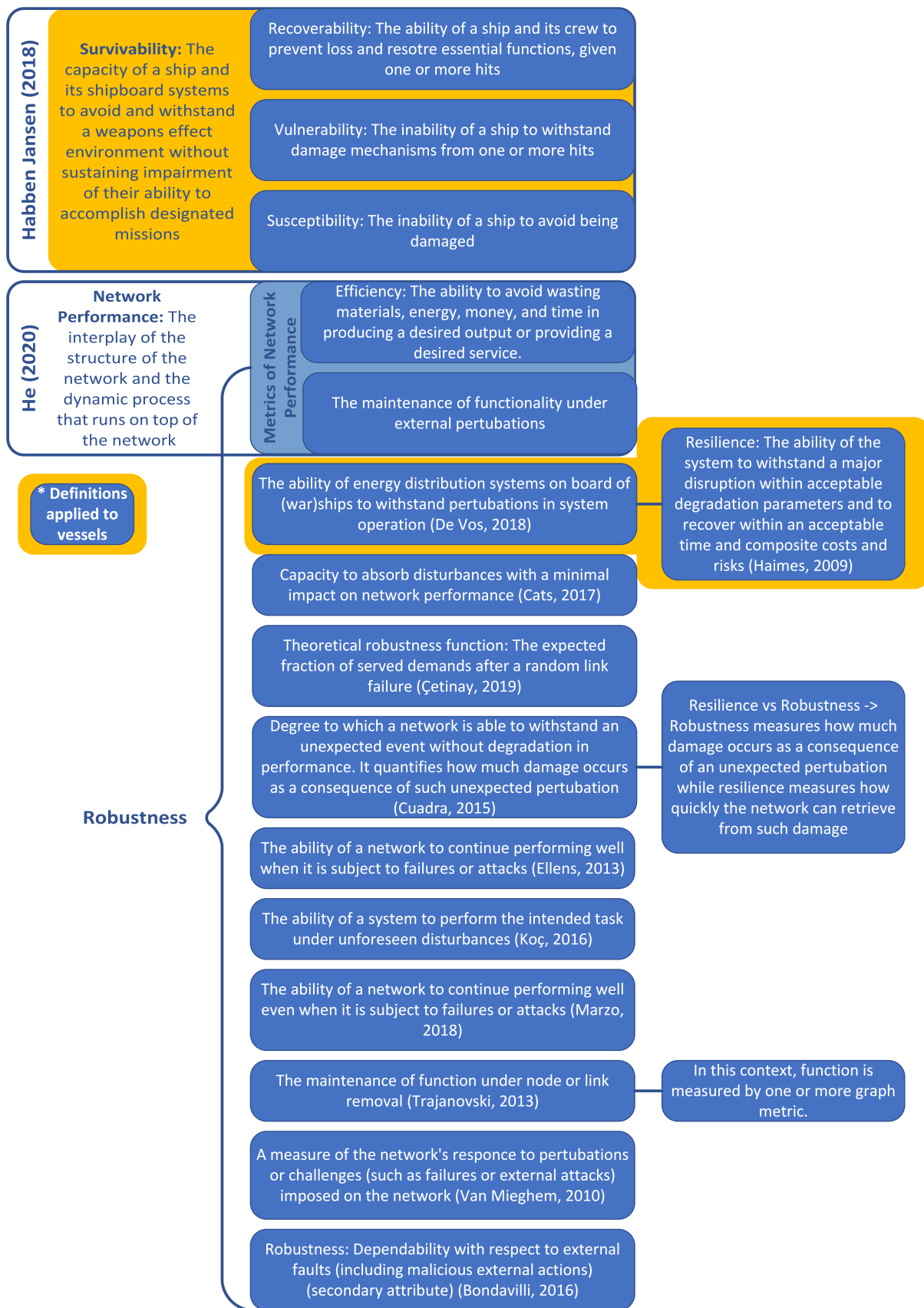


Figure A.2: Overview of Robustness Related Definitions in Literature

# Appendix B

## Verification Set: Robustness and Graph Measure

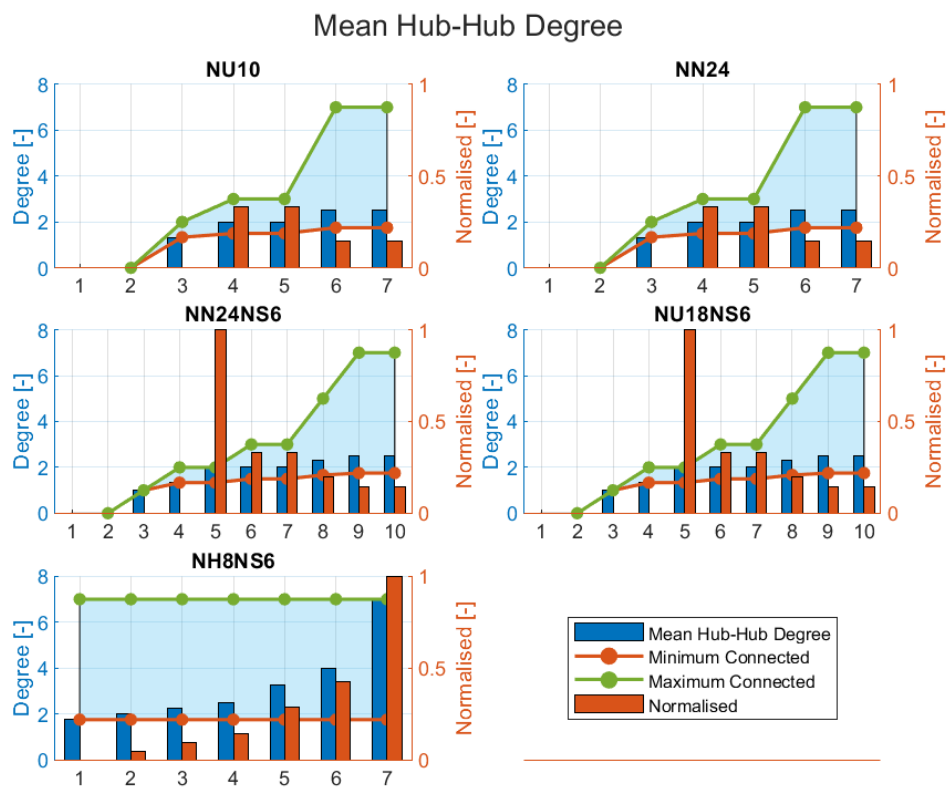


Figure B.1: Verification Study Mean Hub-Hub Degree

### Number of Cycles

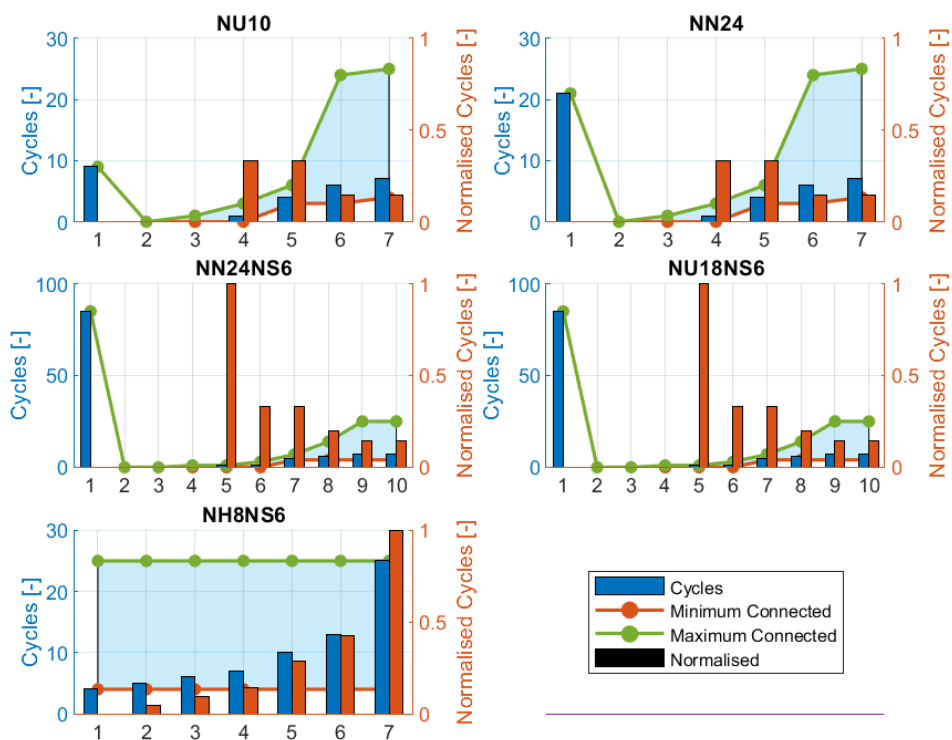


Figure B.2: Verification Study Number of Cycles

### Mean Node Eccentricity

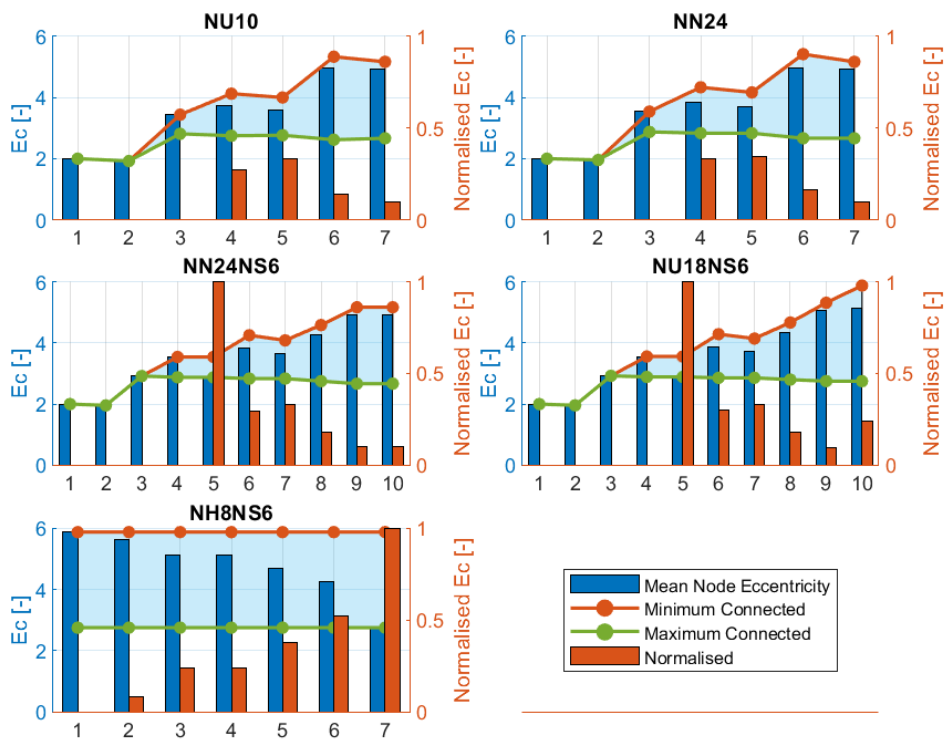


Figure B.3: Verification Study Mean Node Eccentricity

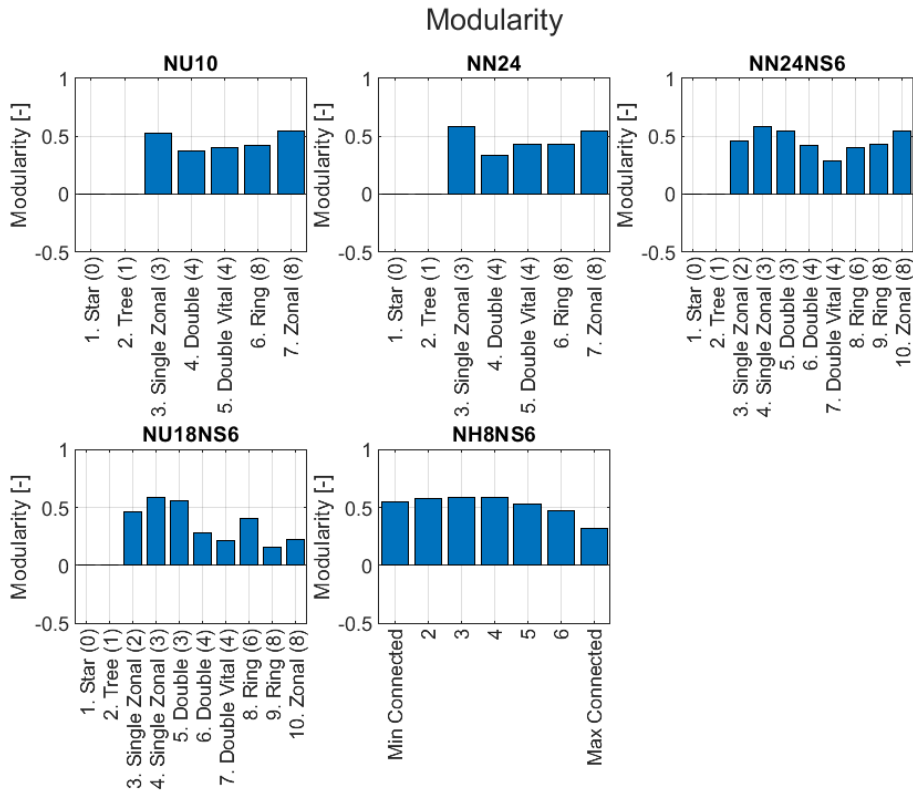


Figure B.4: Verification Study Modularity

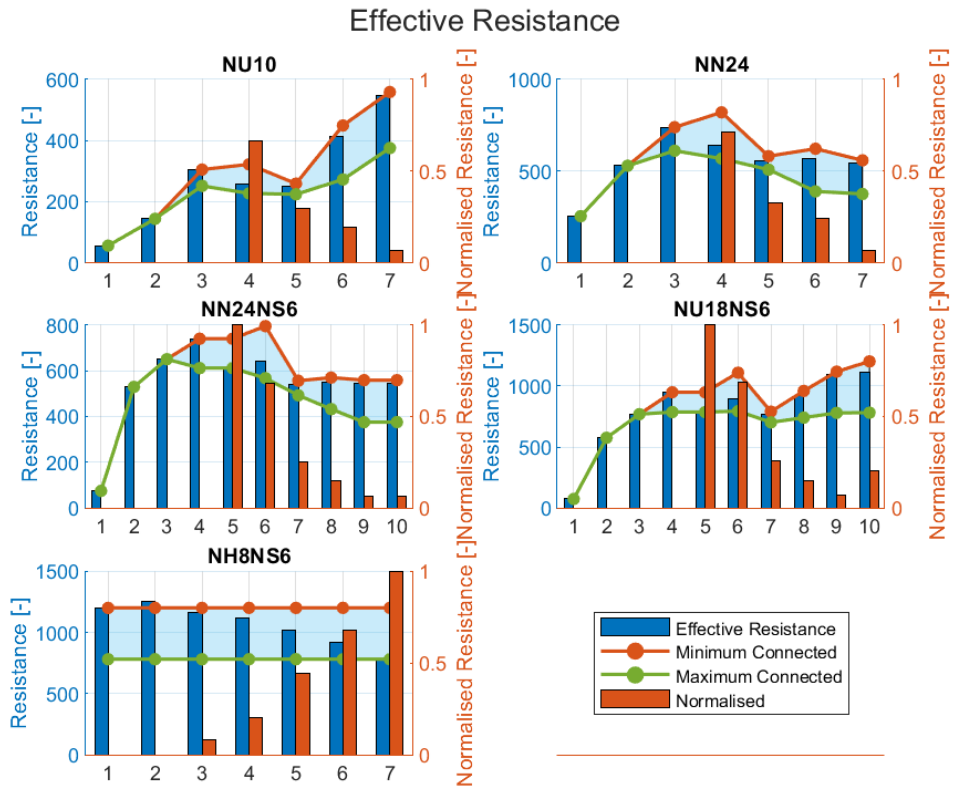


Figure B.5: Verification Study Effective Resistance

### Hub-Edge Connectivity

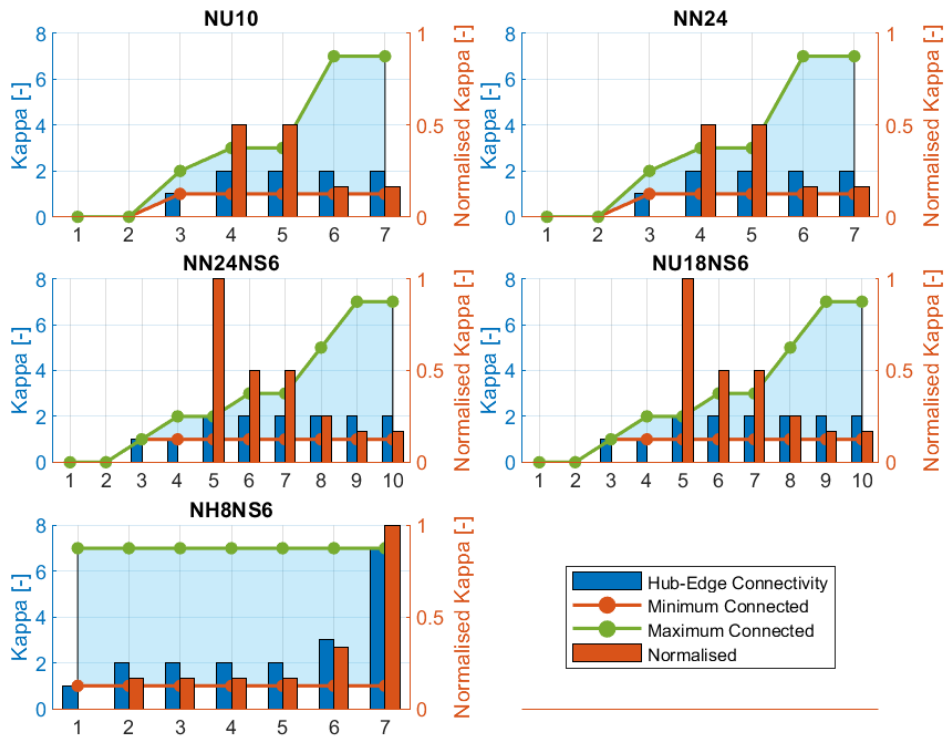


Figure B.6: Verification Study Mean Connectivity

### R-Value

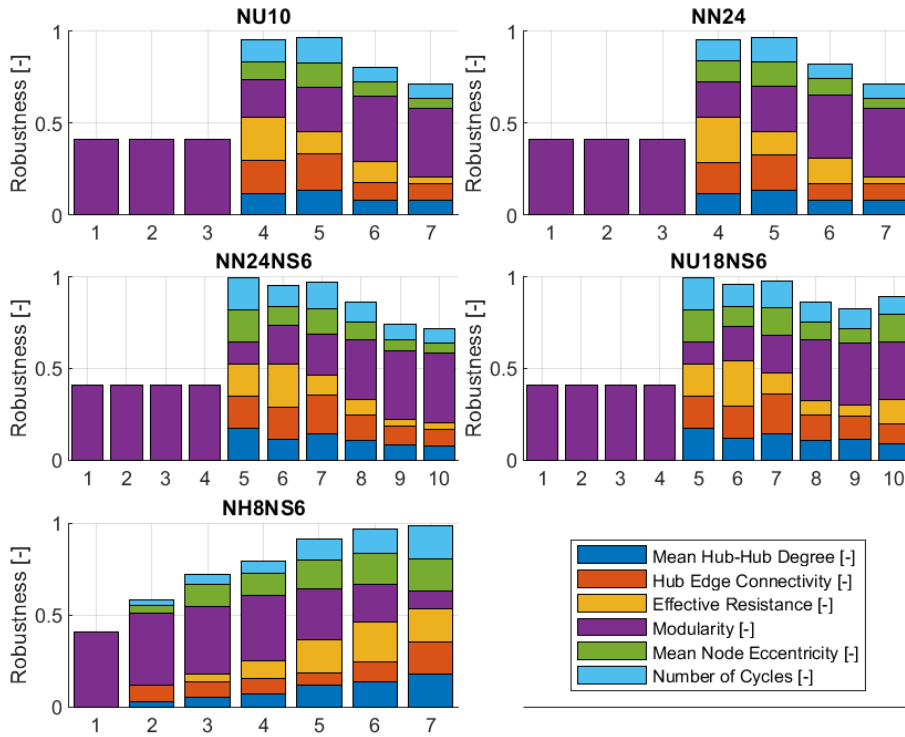


Figure B.7: Verification Study R-Value

# Appendix C

## Case Study Sample Set: Robustness and Graph Measures

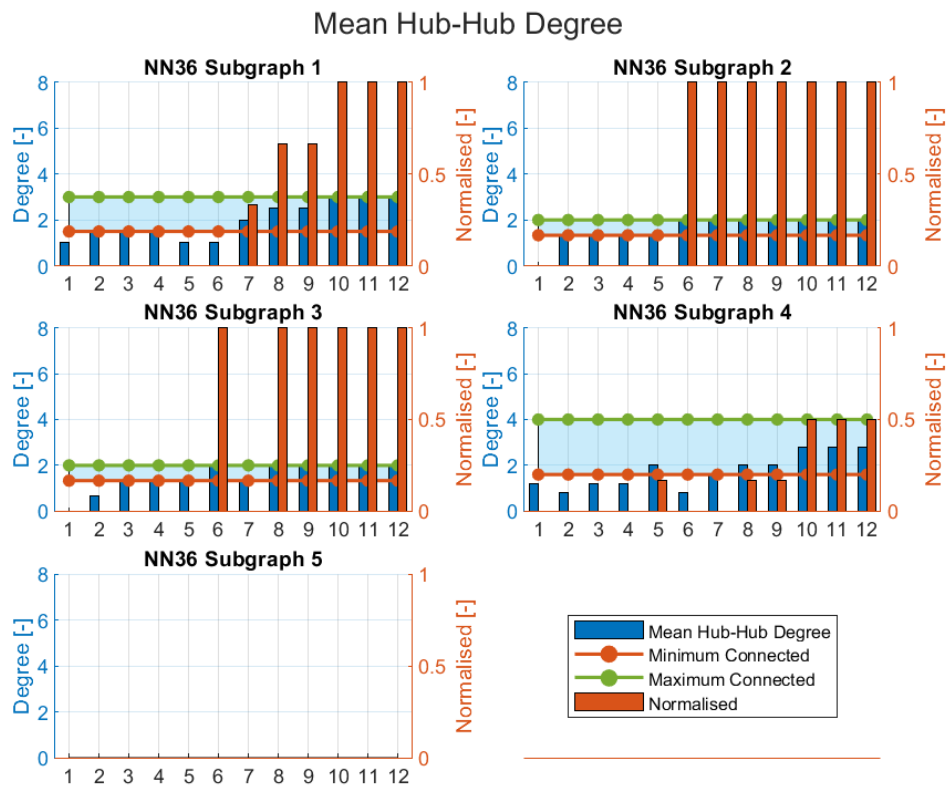


Figure C.1: Case Study Mean Hub-Hub Degree

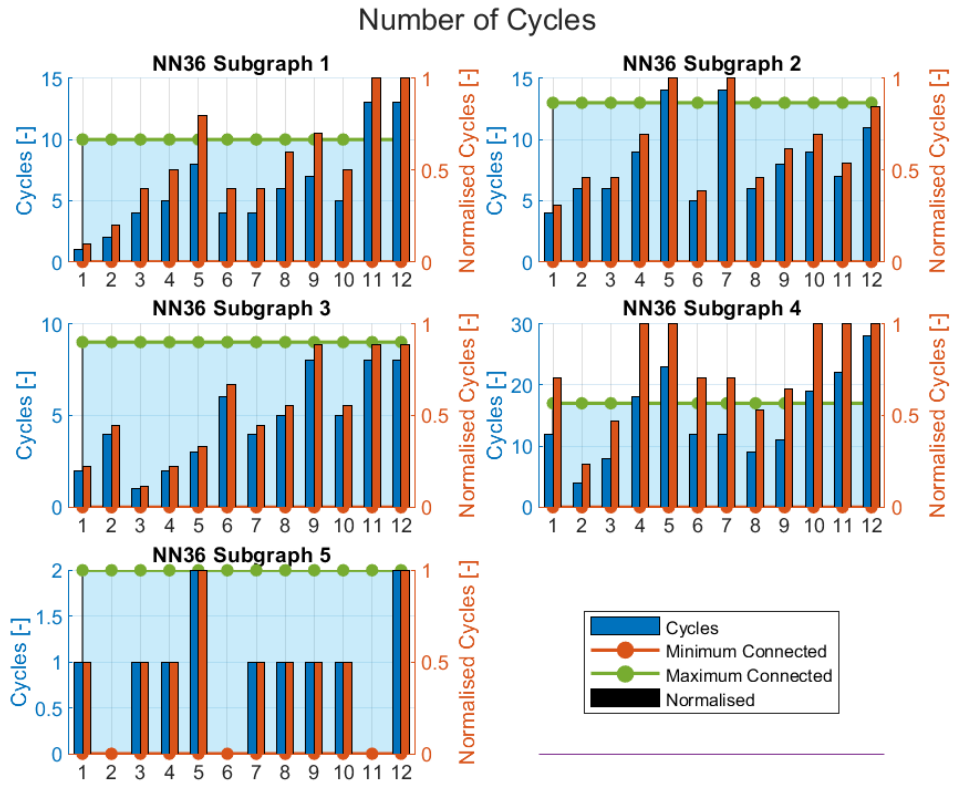


Figure C.2: Case Study Number of Cycles

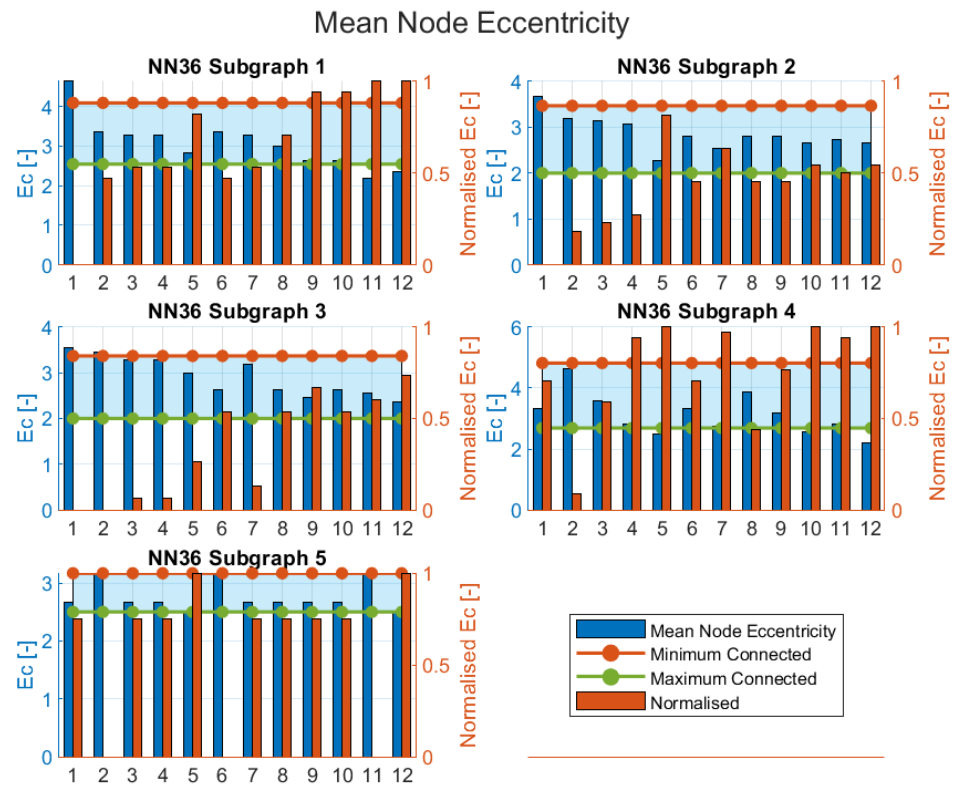


Figure C.3: Case Study Mean Node Eccentricity

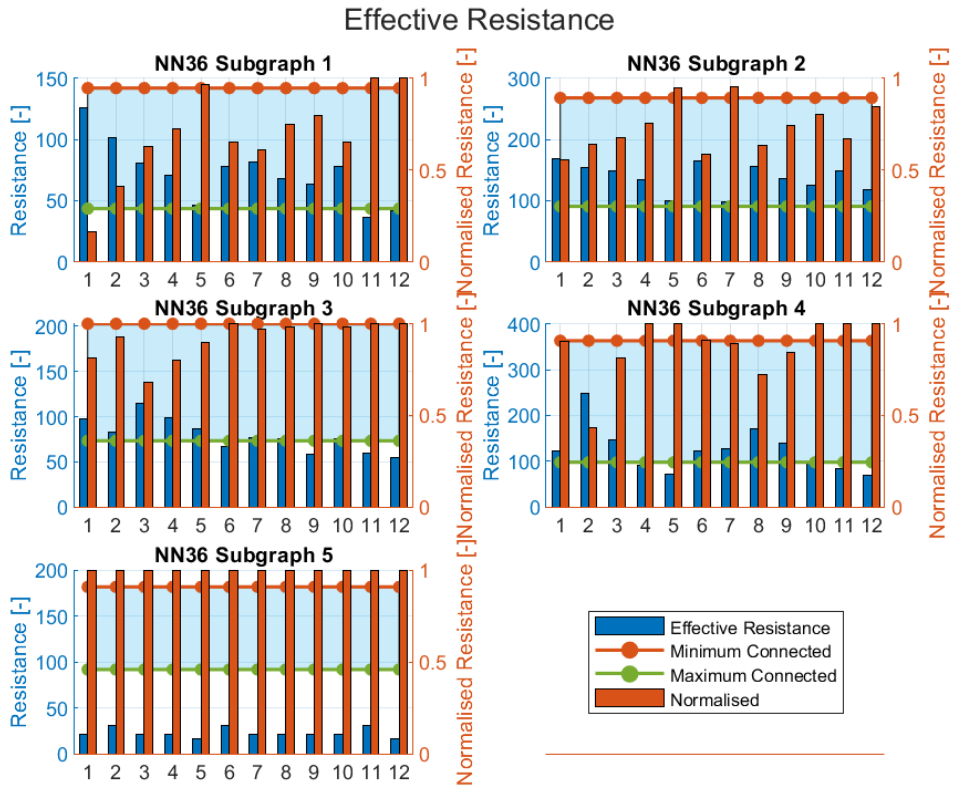


Figure C.4: Case Study Effective Resistance

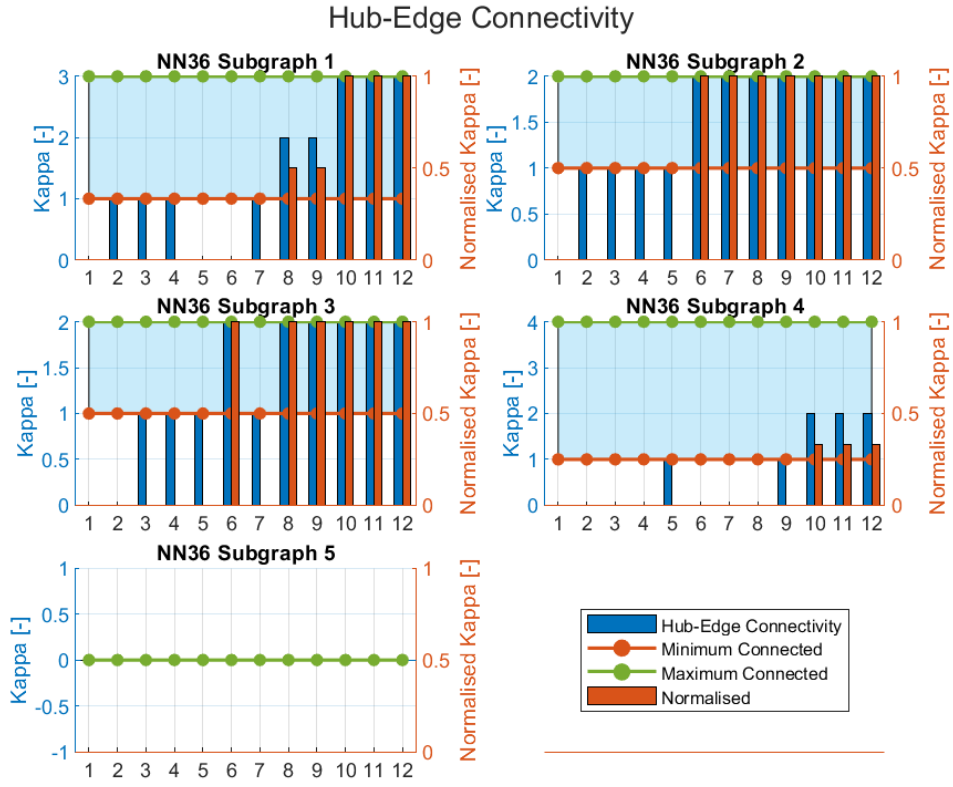


Figure C.5: Case Study Mean Connectivity

### R-Value

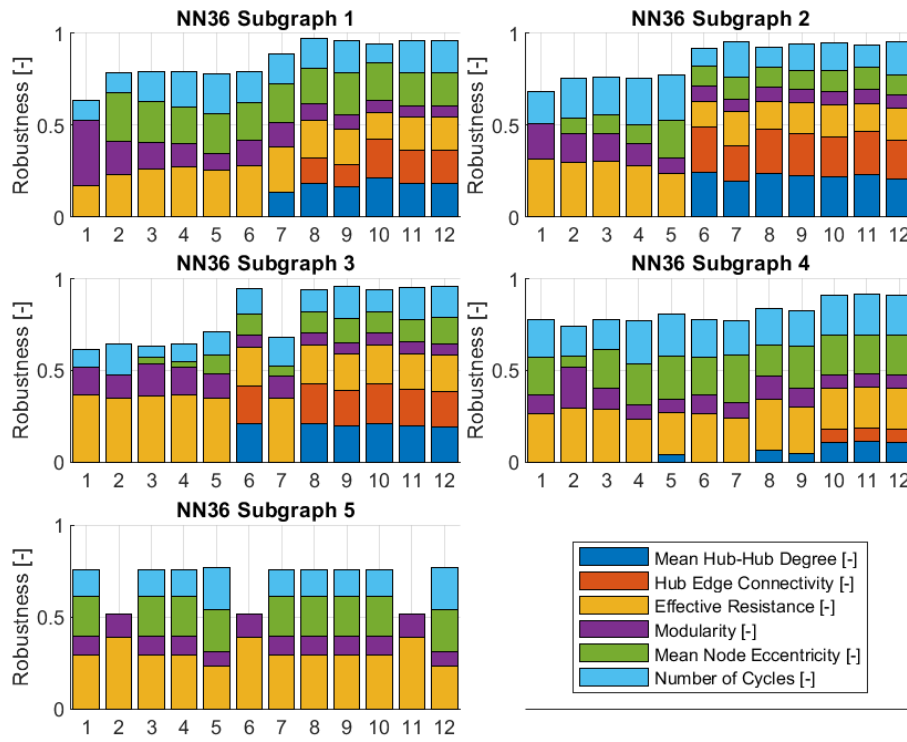


Figure C.6: Case Study R-Value

## Appendix D

# Schematic Representation MATLAB

The *MATLAB* files are available at request.

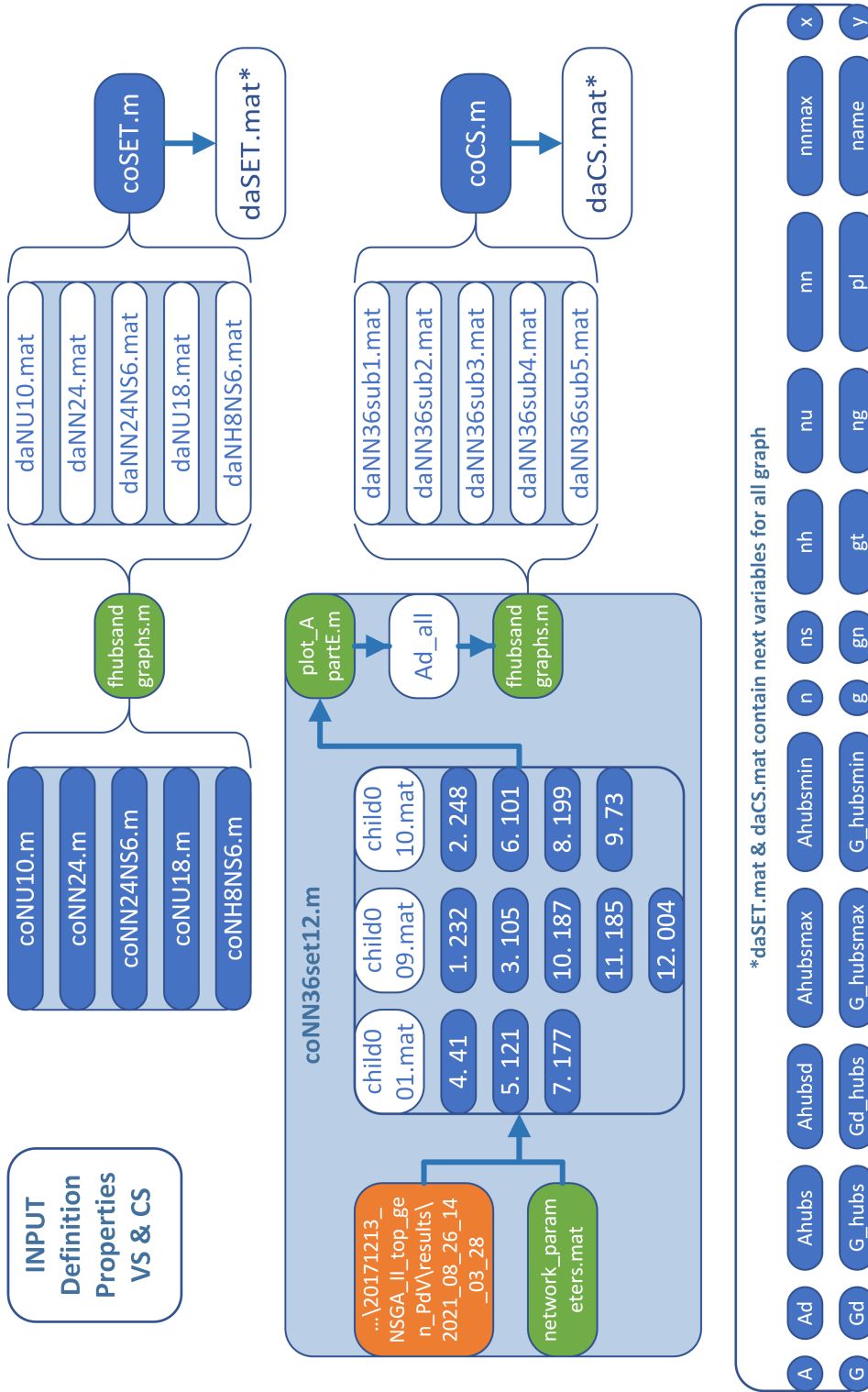


Figure D.1: Schematic Representation MATLAB Input

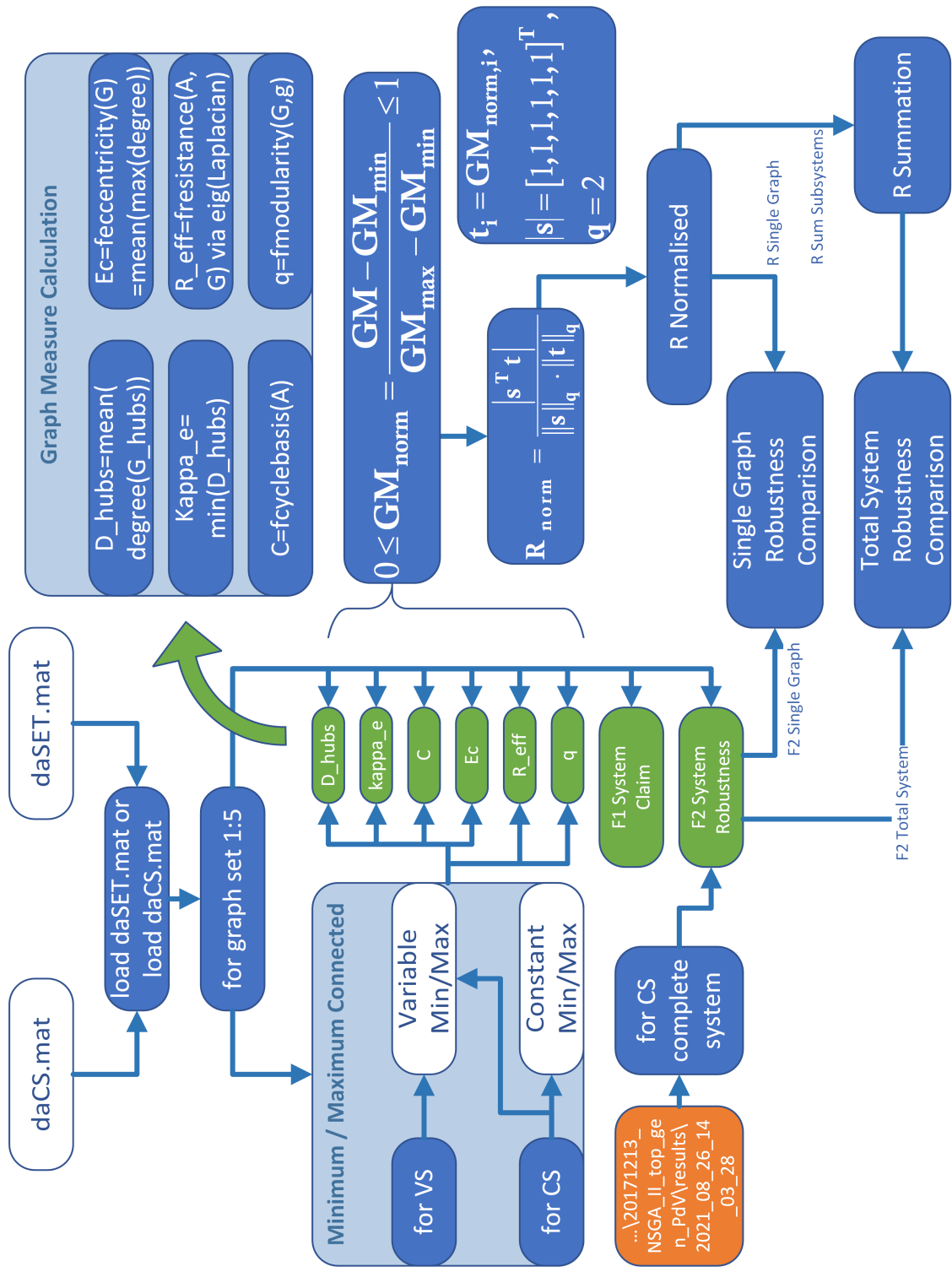


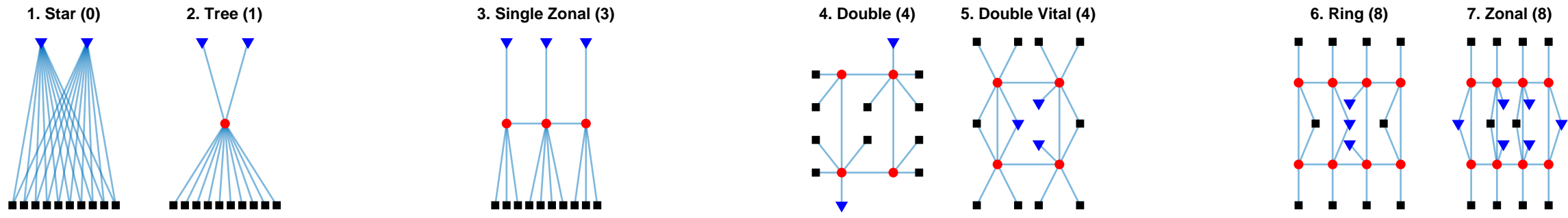
Figure D.2: Schematic Representation MATLAB R-Calculation

## Appendix E

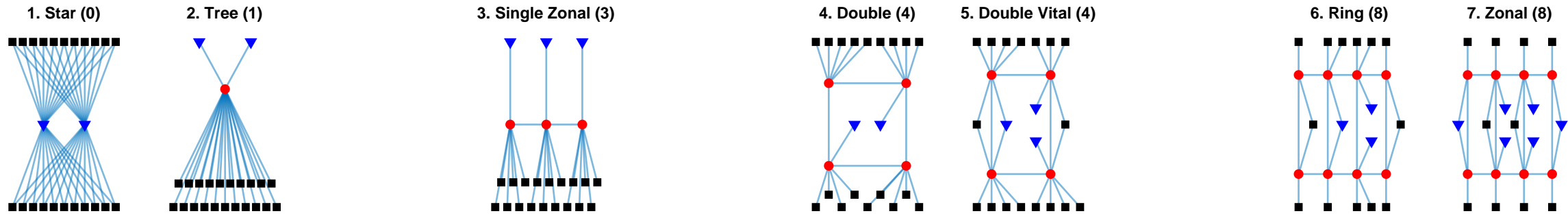
### Verification Set I-V

# Verification Set

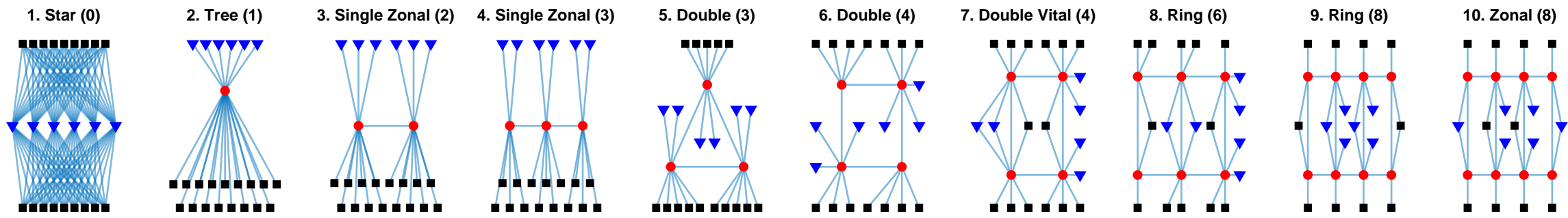
NU10



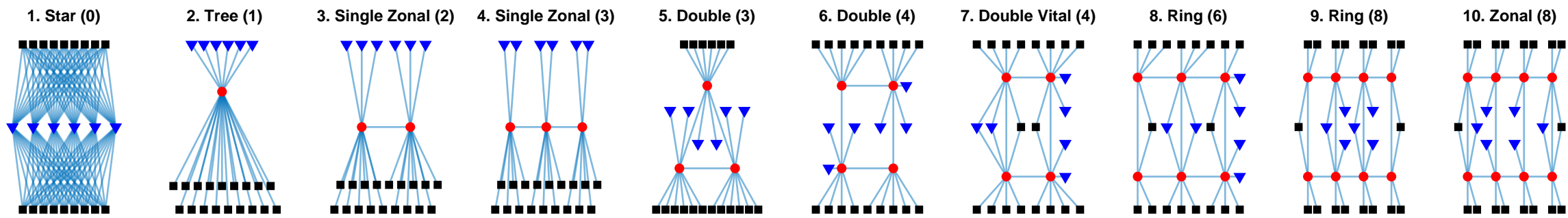
NN24



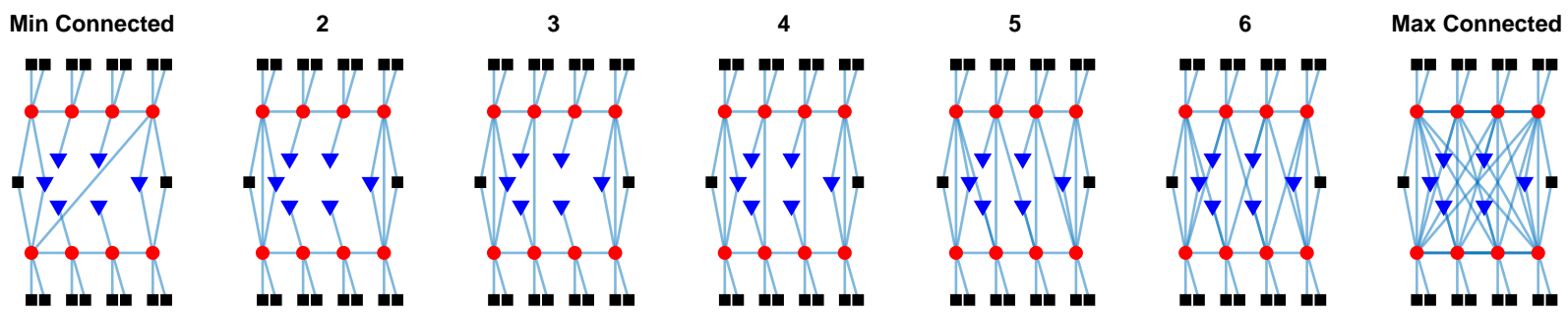
NN24NS6



NU18NS6



NH8NS6

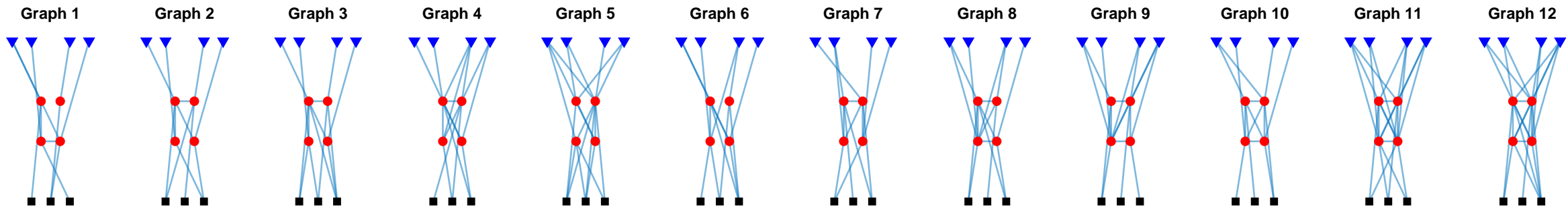


## Appendix F

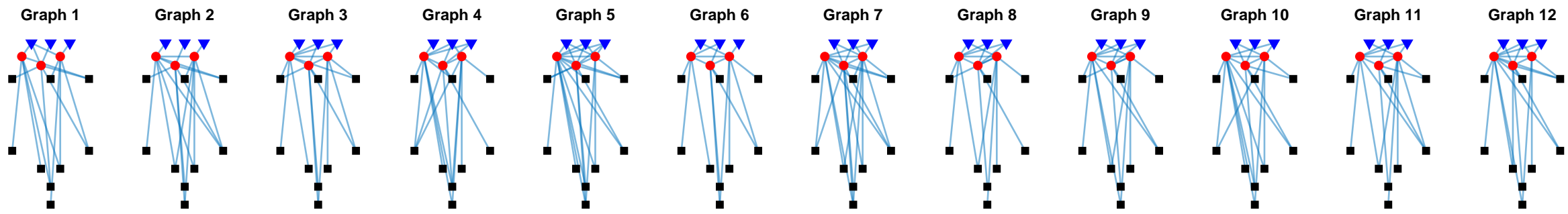
# Case Study Sample Set

# Case Study Sample Set

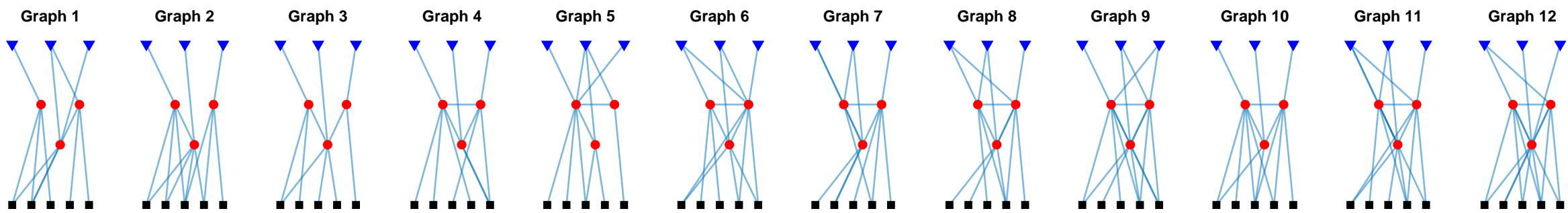
NN36 Subgraph 1



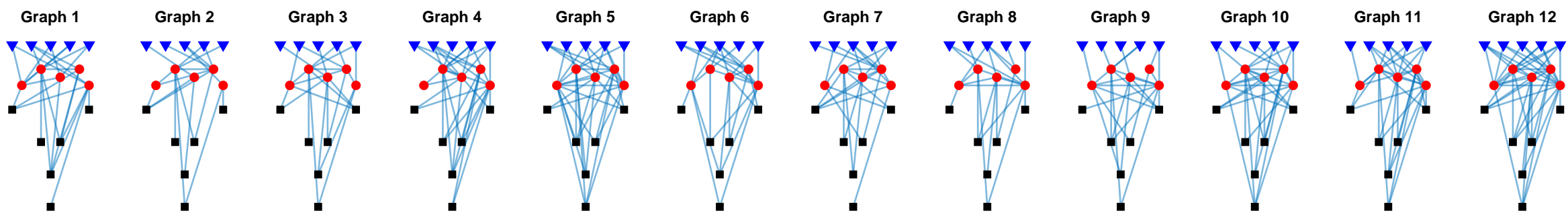
NN36 Subgraph 2



NN36 Subgraph 3



NN36 Subgraph 4



NN36 Subgraph 5

